March / April 2024
Volume 53, Number 2

AppliedRadiology®

The Journal of Practical Medical Imaging and Management

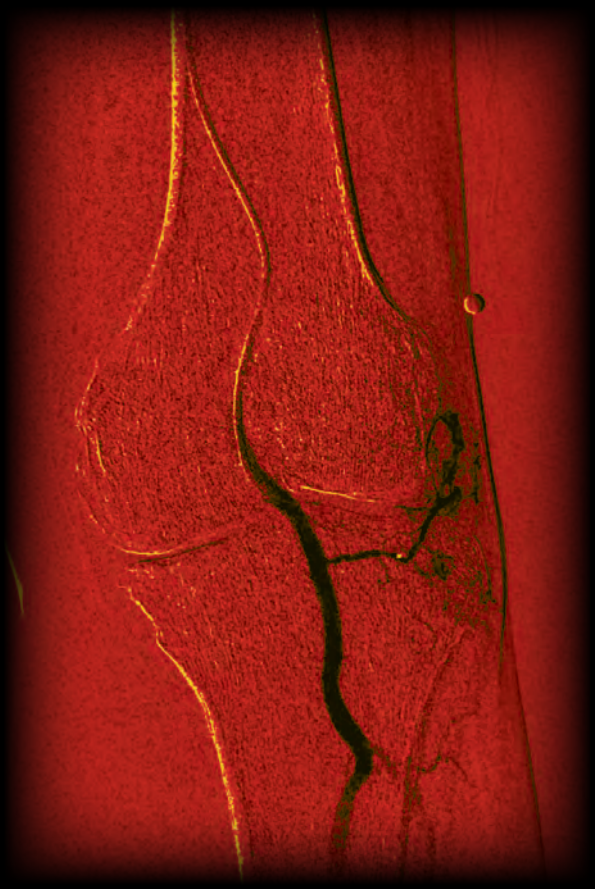

CME Genicular Artery Embolization for Symptomatic Knee Osteoarthritis

Chronic Mesenteric Ischemia: Mesenteric Artery Duplex Sonography and the Utility of Postprandial Imaging

Global Health Imaging Goes Beyond Radiology

Cyberattacks: Not a Matter of If, but When

Aortoenteric Fistula Following Aortobifemoral Grafting

www.appliedradiology.com

Applied Radiology
March / April 2024 Volume 53, Number 2

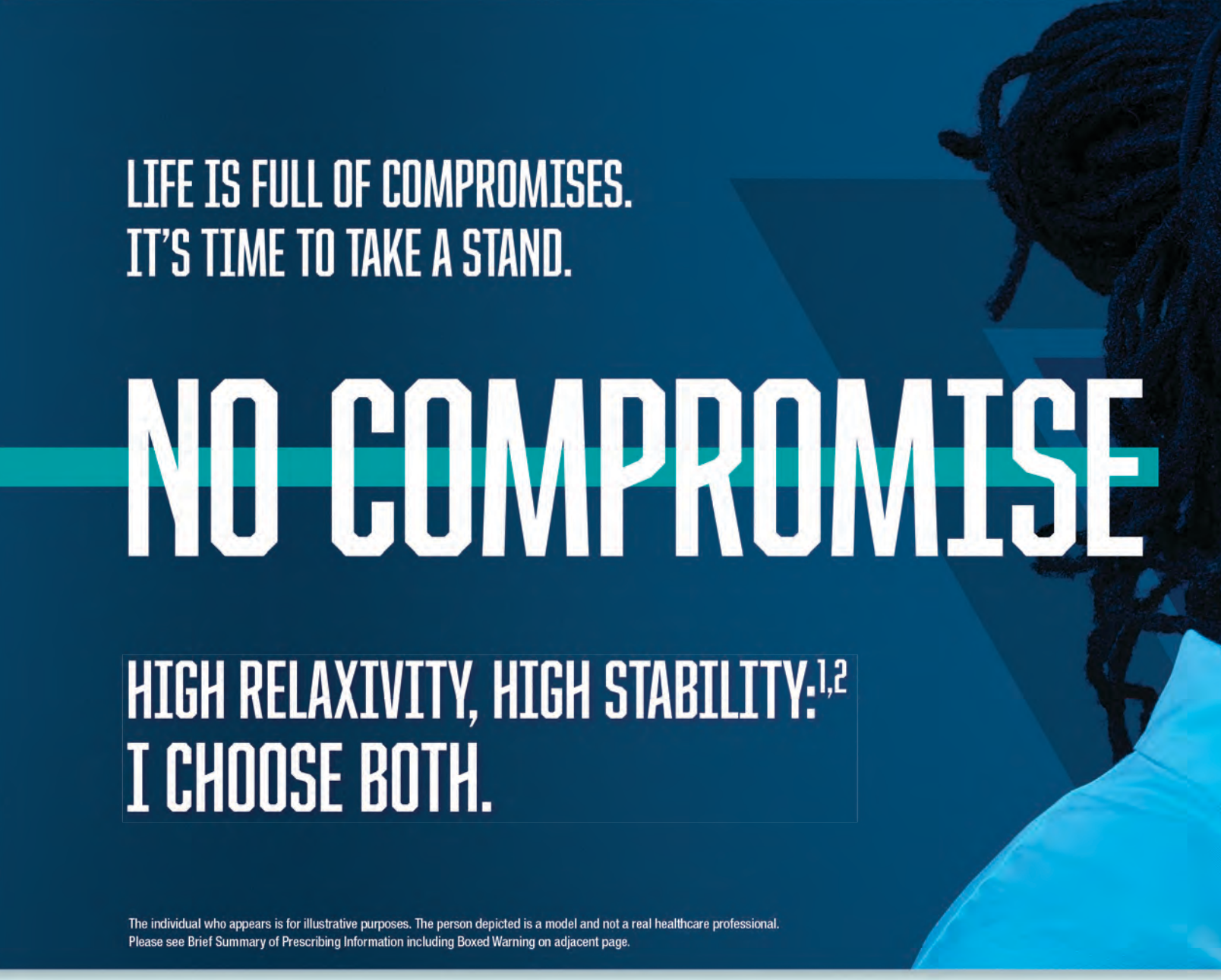

LIFE IS FULL OF COMPROMISES. IT'S TIME TO TAKE A STAND.

NO COMPROMISE

HIGH RELAXIVITY, HIGH STABILITY:[1,2] I CHOOSE BOTH.

The individual who appears is for illustrative purposes. The person depicted is a model and not a real healthcare professional.
Please see Brief Summary of Prescribing Information including Boxed Warning on adjacent page.

VUEWAY™ (gadopiclenol) solution for injection

Indications
VUEWAY injection is indicated in adults and children aged 2 years and older for use with magnetic resonance imaging (MRI) to detect and visualize lesions with abnormal vascularity in:

- the central nervous system (brain, spine and surrounding tissues),
- the body (head and neck, thorax, abdomen, pelvis, and musculoskeletal system).

IMPORTANT SAFETY INFORMATION

WARNING: NEPHROGENIC SYSTEMIC FIBROSIS (NSF)

Gadolinium-based contrast agents (GBCAs) increase the risk for NSF among patients with impaired elimination of the drugs. Avoid use of GBCAs in these patients unless the diagnostic information is essential and not available with non-contrasted MRI or other modalities. NSF may result in fatal or debilitating fibrosis affecting the skin, muscle and internal organs.

- **The risk for NSF appears highest among patients with:**
  - **Chronic, severe kidney disease (GFR <30 mL/min/1.73 m^2), or**
  - **Acute kidney injury.**
- **Screen patients for acute kidney injury and other conditions that may reduce renal function. For patients at risk for chronically reduced renal function (e.g. age >60 years, hypertension, diabetes), estimate the glomerular filtration rate (GFR) through laboratory testing.**
- **For patients at highest risk for NSF, do not exceed the recommended VUEWAY dose and allow a sufficient period of time for elimination of the drug from the body prior to any re-administration.**

Contraindications
VUEWAY injection is contraindicated in patients with history of hypersensitivity reactions to VUEWAY.

Warnings
Risk of **nephrogenic systemic fibrosis** is increased in patients using GBCA agents that have impaired elimination of the drugs, with the highest risk in patients chronic, severe kidney disease as well as patients with acute kidney injury. Avoid use of GBCAs among these patients unless the diagnostic information is essential and not available with non-contrast MRI or other modalities.

Hypersensitivity reactions, including serious hypersensitivity reactions, could occur during use or shortly following VUEWAY administration. Assess all patients for any history of a reaction to contrast media, bronchial asthma and/or allergic disorders, administer VUEWAY only in situations where trained personnel and therapies are promptly available for the treatment of hypersensitivity reactions, and observe patients for signs and symptoms of hypersensitivity reactions after administration.

INTRODUCING

Vueway™
(gadopiclenol) injection
485.1 mg/mL

HALF THE GADOLINIUM DOSE COMPARED TO OTHER MACROCYCLIC GBCAS IN APPROVED INDICATIONS.[1,3-6] FROM BRACCO, YOUR TRUSTED PARTNER IN MRI.

BRACCO
LIFE FROM INSIDE

Gadolinium retention can be for months or years in several organs after administration. The highest concentrations (nanomoles per gram of tissue) have been identified in the bone, followed by other organs (brain, skin, kidney, liver and spleen). Minimize repetitive GBCA imaging studies, particularly closely spaced studies, when possible.

Acute kidney injury requiring dialysis has occurred with the use of GBCAs in patients with chronically reduced renal function. The risk of acute kidney injury may increase with increasing dose of the contrast agent.

Ensure catheter and venous patency before injecting as **extravasation** may occur, and cause tissue irritation.

VUEWAY may **impair the visualization of lesions** seen on non-contrast MRI. Therefore, caution should be exercised when Vueway MRI scans are interpreted without a companion non-contrast MRI scan.

The most common adverse reactions (incidence ≥ 0.5%) are injection site pain (0.7%), and headache (0.7%).

You are encouraged to report negative side effects of prescription drugs to the FDA. Visit www.fda.gov/medwatch or call 1-800-FDA-1088.

Please see BRIEF SUMMARY of Prescribing Information for VUEWAY, including BOXED WARNING on Nephrogenic Systemic Fibrosis.

Manufactured for Bracco Diagnostics Inc. by Liebel-Flarsheim Company LLC - Raleigh, NC, USA 27616.

VUEWAY is a trademark of Bracco Imaging S.p.A.

References: 1. Vueway™ (gadopiclenol) Injection Full Prescribing Information. Monroe Twp., NJ: Bracco Diagnostics Inc.; September 2022. **2.** Robic C, Port M, Rousseaux O, et al. Physicochemical and Pharmacokinetic Profiles of Gadopiclenol: A New Macrocyclic Gadolinium Chelate With High T1 Relaxivity. *Invest Radiol.* 2019 Aug;54: 475–484. **3.** GADAVIST® (gadobutrol) Injection. Full Prescribing Information. Bayer HealthCare Pharmaceuticals Inc. Whippany, NJ; April 2022. **4.** DOTAREM® (gadoterate meglumine) Injection. Full Prescribing Information. Guerbet LLC. Princeton, NJ; April 2022. **5.** CLARISCAN™ (gadoterate meglumine) injection for intravenous use. Full Prescribing Information. GE Healthcare. Marlborough, MA; February 2020. **6.** ProHance® (Gadoteridol) Injection. Full Prescribing Information and Patient Medication Guide. Monroe Twp., NJ: Bracco Diagnostics Inc.; December 2020.

VISIT VUEWAY.COM FOR MORE INFORMATION

Bracco Diagnostics Inc.
259 Prospect Plains Road, Building H
Monroe Township, NJ 08831 USA
Phone: 609-514-2200
Toll Free: 1-877-272-2269 (U.S. only)
Fax: 609-514-2446

Bracco Diagnostics Inc.

Vueway™

(gadopiclenol) injection, for intravenous use

BRIEF SUMMARY: Please see package insert of full prescribing information.

WARNING: NEPHROGENIC SYSTEMIC FIBROSIS (NSF)

Gadolinium-based contrast agents (GBCAs) increase the risk for NSF among patients with impaired elimination of the drugs. Avoid use of GBCAs in these patients unless the diagnostic information is essential and not available with non-contrasted MRI or other modalities. NSF may result in fatal or debilitating fibrosis affecting the skin, muscle and internal organs.

- **The risk for NSF appears highest among patients with:**
  - **Chronic, severe kidney disease (GFR <30 mL/min/1.73 m²), or**
  - **Acute kidney injury.**
- **Screen patients for acute kidney injury and other conditions that may reduce renal function. For patients at risk for chronically reduced renal function (e.g. age >60 years, hypertension, diabetes), estimate the glomerular filtration rate (GFR) through laboratory testing.**
- **For patients at highest risk for NSF, do not exceed the recommended Vueway dose and allow a sufficient period of time for elimination of the drug from the body prior to any re-administration *[see Warnings and Precautions (5.1) in the full Prescribing Information]*.**

INDICATIONS AND USAGE

Vueway™ (gadopiclenol) is a gadolinium-based contrast agent indicated in adult and pediatric patients aged 2 years and older for use with magnetic resonance imaging (MRI) to detect and visualize lesions with abnormal vascularity in:

- the central nervous system (brain, spine, and associated tissues),
- the body (head and neck, thorax, abdomen, pelvis, and musculoskeletal system).

CONTRAINDICATIONS

Vueway is contraindicated in patients with history of hypersensitivity reactions to gadopiclenol.

WARNINGS AND PRECAUTIONS

Nephrogenic Systemic Fibrosis Gadolinium-based contrast agents (GBCAs) increase the risk for nephrogenic systemic fibrosis (NSF) among patients with impaired elimination of the drugs. Avoid use of GBCAs among these patients unless the diagnostic information is essential and not available with non-contrast MRI or other modalities. The GBCA-associated NSF risk appears highest for patients with chronic, severe kidney disease (GFR <30 mL/min/1.73 m²) as well as patients with acute kidney injury. The risk appears lower for patients with chronic, moderate kidney disease (GFR 30-59 mL/min/1.73 m²) and little, if any, for patients with chronic, mild kidney disease (GFR 60-89 mL/min/1.73 m²). NSF may result in fatal or debilitating fibrosis affecting the skin, muscle, and internal organs. Report any diagnosis of NSF following Vueway administration to Bracco Diagnostics Inc. (1-800-257-5181) or FDA (1-800-FDA-1088 or www.fda.gov/medwatch).

Screen patients for acute kidney injury and other conditions that may reduce renal function. Features of acute kidney injury consist of rapid (over hours to days) and usually reversible decrease in kidney function, commonly in the setting of surgery, severe infection, injury or drug-induced kidney toxicity. Serum creatinine levels and estimated GFR may not reliably assess renal function in the setting of acute kidney injury. For patients at risk for chronically reduced renal function (e.g., age >60 years, diabetes mellitus or chronic hypertension), estimate the GFR through laboratory testing.

Among the factors that may increase the risk for NSF are repeated or higher than recommended doses of a GBCA and the degree of renal impairment at the time of exposure. Record the specific GBCA and the dose administered to a patient. For patients at highest risk for NSF, do not exceed the recommended Vueway dose and allow a sufficient period of time for elimination of the drug prior to re-administration. For patients receiving hemodialysis, physicians may consider the prompt initiation of hemodialysis following the administration of a GBCA in order to enhance the contrast agent's elimination *[see Use in Specific Populations (8.6) and Clinical Pharmacology (12.3) in the full Prescribing Information]*. The usefulness of hemodialysis in the prevention of NSF is unknown.

Hypersensitivity Reactions With GBCAs, serious hypersensitivity reactions have occurred. In most cases, initial symptoms occurred within minutes of GBCA administration and resolved with prompt emergency treatment.

- Before Vueway administration, assess all patients for any history of a reaction to contrast media, bronchial asthma and/or allergic disorders. These patients may have an increased risk for a hypersensitivity reaction to Vueway.
- Vueway is contraindicated in patients with history of hypersensitivity reactions to Vueway *[see Contraindications (4) in the full Prescribing Information]*.
- Administer Vueway only in situations where trained personnel and therapies are promptly available for the treatment of hypersensitivity reactions, including personnel trained in resuscitation.
- During and following Vueway administration, observe patients for signs and symptoms of hypersensitivity reactions.

Gadolinium Retention Gadolinium is retained for months or years in several organs. The highest concentrations (nanomoles per gram of tissue) have been identified in the bone, followed by other organs (e.g. brain, skin, kidney, liver, and spleen). The duration of retention also varies by tissue and is longest in bone. Linear GBCAs cause more retention than macrocyclic GBCAs. At equivalent doses, gadolinium retention varies among the linear agents with gadodiamide causing greater retention than other linear agents such as gadoxetate disodium, and gadobenate dimeglumine. Retention is lowest and similar among the macrocyclic GBCAs such as gadoterate meglumine, gadobutrol, gadoteridol, and gadopiclenol.

Consequences of gadolinium retention in the brain have not been established. Pathologic and clinical consequences of GBCA administration and retention in skin and other organs have been established in patients with impaired renal function *[see Warnings and Precautions (5.1) in the full Prescribing Information]*. There are rare reports of pathologic skin changes in patients with normal renal function. Adverse events involving multiple organ systems have been reported in patients with normal renal function without an established causal link to gadolinium.

While clinical consequences of gadolinium retention have not been established in patients with normal renal function, certain patients might be at higher risk. These include patients requiring multiple lifetime doses, pregnant and pediatric patients, and patients with inflammatory conditions. Consider the retention characteristics of the agent when choosing a GBCA for these patients. Minimize repetitive GBCA imaging studies, particularly closely spaced studies, when possible.

Acute Kidney Injury In patients with chronically reduced renal function, acute kidney injury requiring dialysis has occurred with the use of GBCAs. The risk of acute kidney injury may increase with increasing dose of the contrast agent. Do not exceed the recommended dose.

Extravasation and Injection Site Reactions Injection site reactions such as injection site pain have been reported in the clinical studies with Vueway *[see Adverse Reactions (6.1) in the full Prescribing Information]*. Extravasation during Vueway administration may result in tissue irritation *[see Nonclinical Toxicology (13.2) in the full Prescribing Information]*. Ensure catheter and venous patency before the injection of Vueway.

Interference with Visualization of Lesions Visible with Non-Contrast MRI As with any GBCA, Vueway may impair the visualization of lesions seen on non-contrast MRI. Therefore, caution should be exercised when Vueway MRI scans are interpreted without a companion non-contrast MRI scan.

ADVERSE REACTIONS

The following serious adverse reactions are discussed elsewhere in labeling:

- Nephrogenic Systemic Fibrosis *[see Warnings and Precautions (5.1) in the full Prescribing Information]*
- Hypersensitivity Reactions *[see Contraindications (4) and Warnings and Precautions (5.2) in the full Prescribing Information]*

Clinical Trials Experience Because clinical trials are conducted under widely varying conditions, adverse reaction rates observed in the clinical trials of a drug cannot be directly compared to rates in the clinical trials of another drug and may not reflect the rates observed in clinical practice.

The safety of Vueway was evaluated in 1,047 patients who received Vueway at doses ranging from 0.025 mmol/kg (one half the recommended dose) to 0.3 mmol/kg (six times the recommended dose). A total of 708 patients received the recommended dose of 0.05 mmol/kg. Among patients who received the recommended dose, the average age was 51 years (range 2 years to 88 years) and 56% were female. The ethnic distribution was 79% White, 10% Asian, 7% American Indian or Alaska native, 2% Black, and 2% patients of other or unspecified ethnic groups.

Overall, approximately 4.7% of subjects receiving the labeled dose reported one or more adverse reactions.

Table 1 lists adverse reactions that occurred in >0.2% of patients who received 0.05 mmol/kg Vueway.

TABLE 1. ADVERSE REACTIONS REPORTED IN >0.2% OF PATIENTS RECEIVING VUEWAY IN CLINICAL TRIALS

Adverse Reaction	Vueway 0.05 mmol/kg (n=708) (%)
Injection site pain	0.7
Headache	0.7
Nausea	0.4
Injection site warmth	0.4
Injection site coldness	0.3
Dizziness	0.3
Local swelling	0.3

Adverse reactions that occurred with a frequency ≤ 0.2% in patients who received 0.05 mmol/kg Vueway included: maculopapular rash, vomiting, worsened renal impairment, feeling hot, pyrexia, oral paresthesia, dysgeusia, diarrhea, pruritus, allergic dermatitis, erythema, injection site paresthesia, Cystatin C increase, and blood creatinine increase.

Adverse Reactions in Pediatric Patients

One study with a single dose of Vueway (0.05 mmol/kg) was conducted in 80 pediatric patients aged 2 years to 17 years, including 60 patients who underwent a central nervous system (CNS) MRI and 20 patients who underwent a body MRI. One adverse reaction (maculopapular rash of moderate severity) in one patient (1.3%) was reported in the CNS cohort.

USE IN SPECIFIC POPULATIONS

Pregnancy Risk Summary There are no available data on Vueway use in pregnant women to evaluate for a drug-associated risk of major birth defects, miscarriage or other adverse maternal or fetal outcomes. GBCAs cross the human placenta and result in fetal exposure and gadolinium retention. The available human data on GBCA exposure during pregnancy and adverse fetal outcomes are limited and inconclusive *(see Data)*. In animal reproduction studies, there were no adverse developmental effects observed in rats or rabbits with intravenous administration of Vueway during organogenesis *(see Data)*. Because of the potential risks of gadolinium to the fetus, use Vueway only if imaging is essential during pregnancy and cannot be delayed. The estimated background risk of major birth defects and miscarriage for the indicated population(s) are unknown. All pregnancies have a background risk of birth defect, loss, or other adverse outcomes. In the U.S. general population, the estimated background risk of major birth defects and miscarriage in clinically recognized pregnancies is 2% to 4% and 15% to 20% respectively. Data *Human Data* Contrast enhancement is visualized in the placenta and fetal tissues after maternal GBCA administration. Cohort studies and case reports on exposure to GBCAs during pregnancy have not reported a clear association between GBCAs and adverse effects in the exposed neonates. However, a retrospective cohort study comparing pregnant women who had a GBCA MRI to pregnant women who did not have an MRI reported a higher occurrence of stillbirths and neonatal deaths in the group receiving GBCA MRI. Limitations of this study include a lack of comparison with non-contrast MRI and lack of information about the maternal indication for MRI. Overall, these data preclude a reliable evaluation of the potential risk of adverse fetal outcomes with the use of GBCAs in pregnancy.

Animal Data Gadolinium Retention: GBCAs administered to pregnant non-human primates (0.1 mmol/kg on gestational days 85 and 135) result in measurable gadolinium concentration in the offspring in bone, brain, skin, liver, kidney, and spleen for at least 7 months. GBCAs administered to pregnant mice (2 mmol/kg daily on gestational days 16 through 19) result in measurable gadolinium concentrations in the pups in bone, brain, kidney, liver, blood, muscle, and spleen at one-month postnatal age.

Reproductive Toxicology: Animal reproduction studies conducted with gadopiclenol showed some signs of maternal toxicity in rats at 10 mmol/kg and rabbits at 5 mmol/kg (corresponding to 52 times and 57 times the recommended human dose, respectively). This maternal toxicity was characterized in both species by swelling, decreased activity, and lower gestation weight gain and food consumption.

No effect on embryo-fetal development was observed in rats at 10 mmol/kg (corresponding to 52 times the recommended human dose). In rabbits, a lower mean fetal body weight was observed at 5 mmol/kg (corresponding to 57 times the recommended human dose) and this was attributed as a consequence of the lower gestation weight gain.

Lactation Risk Summary There are no data on the presence of gadopiclenol in human milk, the effects on the breastfed infant, or the effects on milk production. However, published lactation data on other GBCAs indicate that 0.01% to 0.04% of the maternal gadolinium dose is excreted in breast milk. Additionally, there is limited GBCA gastrointestinal absorption in the breast-fed infant. Gadopiclenol is present in rat milk. When a drug is present in animal milk, it is likely that the drug will be present in human milk *(see Data)*. The developmental and health benefits of breastfeeding should be considered along with the mother's clinical need for Vueway and any potential adverse effects on the breastfed infant from Vueway or from the underlying maternal condition. Data In lactating rats receiving single intravenous injection of [^{153}Gd]-gadopiclenol, 0.3% and 0.2% of the total administered radioactivity was transferred to the pups via maternal milk at 6 hours and 24 hours after administration, respectively. Furthermore, in nursing rat pups, oral absorption of gadopiclenol was 3.6%.

Pediatric Use The safety and effectiveness of Vueway for use with MRI to detect and visualize lesions with abnormal vascularity in the CNS (brain, spine, and associated tissues), and the body (head and neck, thorax, abdomen, pelvis, and musculoskeletal system) have been established in pediatric patients aged 2 years and older.

Use of Vueway in this age group is supported by evidence from adequate and well-controlled studies in adults with additional pharmacokinetic and safety data from an open-label, uncontrolled, multicenter, single dose study of Vueway (0.05 mmol/kg) in 80 pediatric patients aged 2 to 17 years. The 80 patients consisted of 60 patients who underwent a CNS MRI and 20 patients who underwent a body MRI *[see Adverse Reactions (6.1) and Clinical Pharmacology (12.3) in the full Prescribing Information]*.

The safety and effectiveness of Vueway have not been established in pediatric patients younger than 2 years of age.

Geriatric Use Of the total number of Vueway-treated patients in clinical studies, 270 (26%) patients were 65 years of age and over, while 62 (6%) patients were 75 years of age and over. No overall differences in safety or efficacy were observed between these subjects and younger subjects.

This drug is known to be substantially excreted by the kidney, and the risk of adverse reactions to this drug may be greater in patients with impaired renal function. Because elderly patients are more likely to have decreased renal function, it may be useful to monitor renal function.

Renal Impairment In patients with renal impairment, the exposure of gadopiclenol is increased compared to patients with normal renal function. This may increase the risk of adverse reactions such as nephrogenic systemic fibrosis (NSF). Avoid use of GBCAs among these patients unless the diagnostic information is essential and not available with non-contrast MRI or other modalities. No dose adjustment of Vueway is recommended for patients with renal impairment. Vueway can be removed from the body by hemodialysis *[see Warnings and Precautions (5.1, 5.3, 5.4) and Clinical Pharmacology (12.3) in the full Prescribing Information]*.

OVERDOSAGE

Among subjects who received a single 0.3 mmol/kg intravenous dose of gadopiclenol (6 times the recommended dose of Vueway), headache and nausea were the most frequently reported adverse reactions. Gadopiclenol can be removed from the body by hemodialysis *[see Clinical Pharmacology (12.3) in the full Prescribing Information]*.

PATIENT COUNSELING INFORMATION Advise the patient to read the FDA-approved patient labeling (Medication Guide).

Nephrogenic Systemic Fibrosis Inform the patient that Vueway may increase the risk for NSF among patients with impaired elimination of the drugs and that NSF may result in fatal or debilitating fibrosis affecting the skin, muscle and internal organs.

Instruct the patients to contact their physician if they develop signs or symptoms of NSF following Vueway administration, such as burning, itching, swelling, scaling, hardening and tightening of the skin; red or dark patches on the skin; stiffness in joints with trouble moving, bending or straightening the arms, hands, legs or feet; pain in the hip bones or ribs; or muscle weakness *[see Warnings and Precautions (5.1) in the full Prescribing Information]*.

Gadolinium Retention Advise patients that gadolinium is retained for months or years in brain, bone, skin, and other organs following Vueway administration even in patients with normal renal function. The clinical consequences of retention are unknown. Retention depends on multiple factors and is greater following administration of linear GBCAs than following administration of macrocyclic GBCAs *[see Warnings and Precautions (5.3) in the full Prescribing Information]*.

Injection Site Reactions Inform the patient that Vueway may cause reactions along the venous injection site, such as mild and transient burning or pain or feeling of warmth or coldness at the injection site *[see Warnings and Precautions (5.5) in the full Prescribing Information]*.

Pregnancy Advise pregnant women of the potential risk of fetal exposure to Vueway *[see Use in Specific Populations (8.1) in the full Prescribing Information]*.

Rx only

US Patent No. 10,973,934

Manufactured for Bracco Diagnostics Inc. by Liebel-Flarsheim Company LLC - Raleigh, NC, USA 27616.

Toll Free: 1-877-272-2269 (U.S. only)

Revised November 2022

US-VW-2200022 11/22

AppliedRadiology®

The Journal of Practical Medical Imaging and Management

Anderson Publishing, Ltd
180 Glenside Avenue,
Scotch Plains, NJ 07076
Tel: 908-301-1995
Fax: 908-301-1997
info@appliedradiology.com

Editorial Advisory Board

Applied Radiology®

The Journal of Practical Medical Imaging and Management

March / April 2024
Vol 53 No 2

ONLINE PEDIATRIC CASE SUPPLEMENT AT APPLIEDRADIOLOGY.COM

Applied Radiology (ISSN 0160-9963, USPS 943180) is published in print 6 times a year, January, March, May, July, September, and November, by Anderson Publishing Ltd at 180 Glenside Ave., Scotch Plains NJ 07076. Periodicals postage paid at Scotch Plains, NJ and additional mailing offices. Free subscriptions for US-based qualified radiology professionals. Subscriptions for the US and its territories and possessions: $115 per year, $225 for two years. Foreign and Canadian subscriptions $215 for one year payable in US funds, international money orders, or by credit card only. Postmaster: Please send address changes to Applied Radiology, PO Box 317, Lincolnshire, IL 60069-0317 (847-564-5942) or email AppliedRadiology@0meda.com.

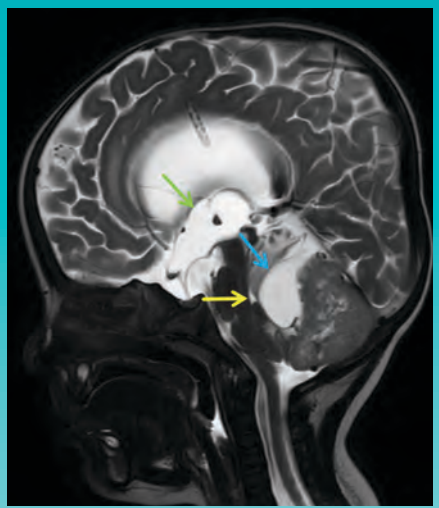

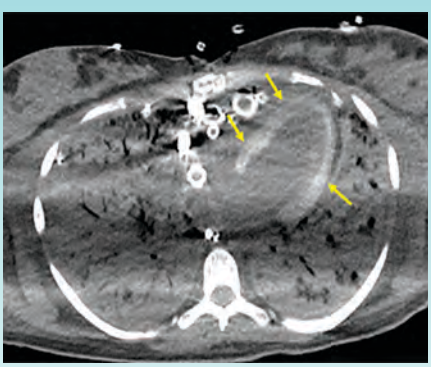

AppliedRadiology®

The Journal of Practical Medical Imaging and Management

Call for Cases

If you have an interesting case we want to know about it!

Sharing your case is a fantastic opportunity to gain recognition for your work and receive feedback from peers all over the world!

Author Guidelines* can be found at

https://appliedradiology.com/author-guidelines

- Abdominal
- Thoracic
- Genitourinary
- GI
- Emergency
- Interventional
- Vascular
- Peds
- Breast
- Neuro
- MSK
- Oncologic
- Cardiac
- Molecular Imaging
- Nuclear Medicine

* Cases undergo peer review before being accepted for publication.

PRINT / ONLINE

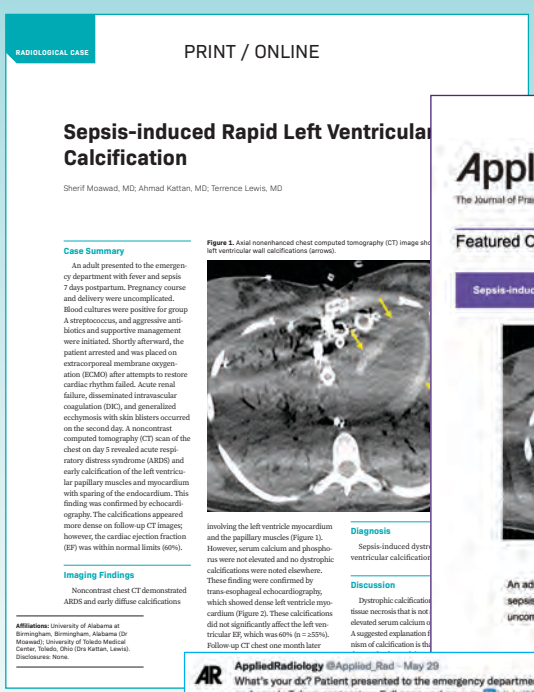
RADIOLOGICAL CASE

Sepsis-induced Rapid Left Ventricular Calcification

Sherif Moawad, MD; Ahmad Kattan, MD; Terrence Lewis, MD

Case Summary

An adult presented to the emergency department with fever and sepsis 7 days postpartum. Pregnancy course and delivery were uncomplicated. Blood cultures were positive for group A streptococcus, and aggressive antibiotics and supportive management were initiated. Shortly afterward, the patient arrested and was placed on extracorporeal membrane oxygenation (ECMO) after attempts to restore cardiac rhythm failed. Acute renal failure, disseminated intravascular coagulation (DIC), and generalized ecchymosis with skin blisters occurred on the second day. A noncontrast computed tomography (CT) scan of the chest on day 5 revealed acute respiratory distress syndrome (ARDS) and early calcification of the left ventricular papillary muscles and myocardium with sparing of the endocardium. This finding was confirmed by echocardiography. The calcifications appeared more dense on follow-up CT images; however, the cardiac ejection fraction (EF) was within normal limits (60%).

Imaging Findings

Noncontrast chest CT demonstrated ARDS and early diffuse calcifications involving the left ventricle myocardium and the papillary muscles (Figure 1). However, serum calcium and phosphorus were not elevated and no dystrophic calcifications were noted elsewhere. These finding were confirmed by trans-esophageal echocardiography, which showed dense left ventricle myocardium (Figure 2). These calcifications did not significantly affect the left ventricular EF, which was 60% (n = ≥55%). Follow-up CT chest one month later

Figure 1. Axial nonenhanced chest computed tomography (CT) image sho left ventricular wall calcifications (arrows).

Diagnosis

Discussion

Affiliations: University of Alabama at Birmingham, Birmingham, Alabama (Dr Moawad); University of Toledo Medical Center, Toledo, Ohio (Drs Kattan, Lewis).
Disclosures: None.

EMAIL ANNOUNCEMENT

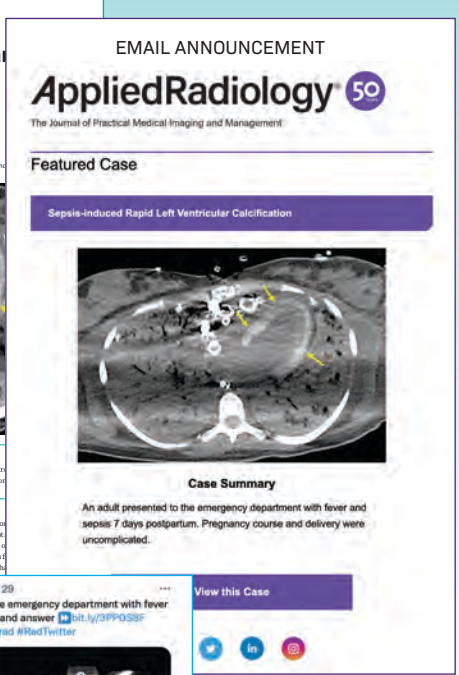
AppliedRadiology 50

The Journal of Practical Medical Imaging and Management

Featured Case

Sepsis-induced Rapid Left Ventricular Calcification

Case Summary

An adult presented to the emergency department with fever and sepsis 7 days postpartum. Pregnancy course and delivery were uncomplicated.

View this Case

SOCIAL MEDIA


AppliedRadiology @Applied_Rad · May 29

What's your dx? Patient presented to the emergency department with fever and sepsis 7 days postpartum Full case and answer bit.ly/3PP0S3F #radiology #RadRes #FOAMed #FOAMrad #RadTwitter

Global Health Imaging Goes Beyond Radiology

Pradnya Mhatre, MD, MRMD (MRSC); Reed A. Omary, MD, MS

Dr Mhatre is an assistant professor of Radiology and Imaging Sciences at Emory University School of Medicine, Atlanta, Georgia. She is also program manager, Radiology Safety/Quality Assurance, RAD-AID International.

Dr Omary is the Carol D. & Henry P. Pendergrass Professor of Radiology and Radiological Sciences, and a professor of Biomedical Engineering at Vanderbilt University Medical Center and School of Medicine, Nashville, Tennessee.

Three years ago, *Applied Radiology* introduced a new department, "Global Health Imaging," dedicated to highlighting radiological issues of worldwide importance. Your enthusiastic and sustained engagement with this topic has encouraged us to create an entirely new section of our Editorial Advisory Board focused solely on global imaging.

This section will be based on the same mission that has guided the department since its inception; ie, to bring the international medical imaging community together to share ideas on a multitude of issues affecting imaging professionals and patients worldwide.

Applied Radiology will serve as a dedicated platform for healthcare workers engaged in this important endeavor. Our expansion emphasizes the rising importance of medical imaging around the world, especially at a time when we find ourselves navigating numerous geopolitical conflicts.

We will include global health projects undertaken by a broad array of radiology organizations and individuals working in low- and middle-income countries (LMICs). By sharing our insights and experiences, we can collectively learn how to generate greater long-term impact on healthcare and radiology throughout the world.

We will also highlight such diverse facets of radiology as health equity, an important aspect worthy of greater attention as dozens of LMICs rise from centuries of colonialism. We will be mindful of how colonialism intersects with health projects in LMICs, as well as how tools such as global information systems can be used to distribute healthcare resources equitably in these regions.

As it has done so here in the US, artificial intelligence (AI) has emerged as a powerful approach to advance access to radiology in many other countries. Indeed, innovative AI applications can address the shortage of skilled healthcare workers, including imaging professionals, in remote settings.

However, our goal will also be to highlight the need to tailor AI use across different LMICs, in recognition of the fact that no one solution is equally effective in all settings. We will also delve more deeply into the ethical considerations surrounding AI and the data it generates from these regions.

We will also strive to include environmental impacts on medical imaging, and vice versa, in the discussion within these pages. The World Health Organization has identified climate change as the greatest health threat to humanity. We humans are just one of over two million interconnected species on our planet.

The emerging concept of "planetary health" recognizes the links among human health, that of all other living organisms, and the overall condition of Earth. As radiologists, we can play a crucial role in addressing healthcare issues related to climate change. Indeed, we can teach medicine and society that climate care is healthcare.

Ultimately, we believe this new section can play an important role in fostering greater collaboration among policymakers, public-private partnerships, industry, governments, and non-governmental organizations to improve access to high-quality healthcare overall, and to high-quality medical imaging, in particular.

Thank you for helping us achieve this important milestone at *Applied Radiology*. We look forward to working with all of you to help improve the health of our patients, our communities, and our planet. As radiologists, we believe this is more than just an opportunity.

It is also our responsibility.

Genicular Artery Embolization for Symptomatic Knee Osteoarthritis

Description

Genicular artery embolization (GAE), previously used to manage recurrent hemarthrosis after total knee arthroplasty (TKA), is now being actively investigated for managing symptomatic moderate to severe osteoarthritis (OA) in patients resistant to medical/conservative treatment and not eligible for TKA.

This activity is designed to educate radiologists about the pathophysiology of OA, mechanism of action of GAE on alleviating the symptoms, GAE's procedural technique, safety profile, and recent advances.

Learning Objectives

Upon completing this activity, the reader should be able to:

- Describe the pathophysiology of OA.
- Explain how embolization helps improve patient symptoms.
- Explain the patient's procedural candidacy.
- Explain the vessel pruning technique employed in this embolization procedure.

Target Audience

- Radiologists
- Related Imaging Professionals

Authors

Ali Husnain, MD; Shah Jamal Wali, MBBS; Wali Badar, MD; Osman Ahmed, MD.

Affiliations: Department of Radiology, Section of Interventional Radiology, Northwestern University, Chicago, IL (Dr Husnain); Department of Radiology, King Edward Medical University, Lahore, Pakistan (Dr Wali); Department of Radiology, Section of Interventional Radiology, University of Illinois at Chicago, Chicago, IL (Dr Badar); Department of Radiology, Section of Interventional Radiology, University of Chicago, Chicago, IL (Dr Ahmed). Dr Ahmed is also a member of the Editorial Advisory Board of Applied Radiology.

Commercial Support

None

Accreditation/ Designation Statement

This activity has been planned and implemented in accordance with the accreditation requirements and policies of the Accreditation Council for Continuing Medical Education (ACCME) through the joint providership of IAME and Anderson Publishing.

IAME is accredited by the ACCME to provide continuing medical education for physicians. IAME designates this enduring material for a maximum of 1 AMA PRA Category 1 Credits™. Physicians should claim only the credit commensurate with the extent of their participation in the activity.

Instructions

This activity is designed to be completed within the designated time period. To successfully earn credit, participants must complete the activity during the valid credit period. To receive CME credit, you must:

1. Review this article in its entirety.
2. Visit *appliedradiology.org/SAM2*.
3. Log into your account or create an account (new users).
4. Complete the post-test and review the discussion and references.
5. Complete the evaluation.
6. Print your certificate.

Estimated time for completion: 1 hour

Date of release and review: March 1, 2024

Expiration date: February 28, 2025

Disclosures

Planner: Erin Simon Schwartz, MD, discloses no relevant financial relationships with any ineligible companies.

Authors: Ali Husnain, MD, discloses no relevant financial relationships with ineligible companies. Shah Jamal Wali, MBBS, discloses no relevant financial relationships with ineligible companies. Wali Badar, MD, discloses no relevant financial relationships with ineligible companies. Osman Ahmed, MD, discloses no relevant financial relationships with ineligible companies.

IAME has assessed conflict of interest with its faculty, authors, editors, and any individuals who were in a position to control the content of this CME activity. Any identified relevant conflicts of interest have been mitigated. IAME's planners, content reviewers, and editorial staff disclose no relationships with ineligible entities.

Genicular Artery Embolization for Symptomatic Knee Osteoarthritis

Ali Husnain, MD; Shah Jamal Wali, MBBS; Wali Badar, MD; Osman Ahmed, MD

Knee osteoarthritis (OA) is one of the leading causes of chronic disability in adults, affecting more than 9.3 million Americans.[1] Many options for managing OA-associated symptoms exist, ranging from conservative therapy to invasive total knee replacement. Conservative treatment includes weight loss, aerobic and muscle-strengthening exercises, NSAIDs, and tramadol.[2] Intra-articular steroid injections are an accepted therapy, but hyaluronic acid use remains controversial, as studies have reported no significant benefit compared to other conservative therapies.[3,4] Further, intra-articular steroids may accelerate the progression of OA. [5]

Total knee arthroplasty (TKA) is a well-established treatment for osteoarthritis; however, not every patient is an ideal candidate for TKA, owing to underlying comorbidities.[6] Elderly patients with comorbidities, moreover, may be at increased risk of periprosthetic bone fracture. Additionally, the daunting postoperative recovery period serves as a deterrent for patients considering TKA.[6,7]

Genicular artery embolization (GAE) is a minimally invasive procedure that has shown benefit for managing recurrent hemarthroses post-TKA.[8] Recently, GAE has been used to treat medically refractory OA-related pain in patients who are not eligible for or who do not desire to undergo surgery. Multiple clinical trials have demonstrated the efficacy of GAE in controlling pain with an acceptable safety profile.[9–16] In this review, we will discuss the pathophysiology of OA, along with procedural details and recent advances regarding GAE.

Pathophysiology of Osteoarthritis

Osteoarthritis once was considered a degenerative process from progressive wear and tear of the joint. However, recent research has demonstrated that OA is mediated by an inflammatory cascade and represents a key clinical phenotype of the disease.[17,18]

When the intraarticular tissues are exposed to excessive or abnormal stress, they generate inflammatory mediators (chemokines and cytokines) and proteases (matrix metalloproteinases), which lead to an inflammatory cascade and alteration of the normal balance between cartilage breakdown and restoration. Chronic bone and synovial inflammation stimulate vascular endothelial cells to form aberrant neovasculature in response to an imbalance between pro-angiogenic and anti-angiogenic factors. Pro-angiogenic factors consist of prostaglandin E2, histamine, vascular endothelial growth factor, interleukin-1, platelet-derived growth factor, and nitric oxide.[19] In addition, unmyelinated sensory nerves grow around the neovasculature, resulting in pain-related symptoms.[20] It is proposed that embolization of the hyperemic knee vasculature curtails this inflammation, inhibiting angiogenesis and proliferation of unmyelinated nerve fibers. Significant reduction in nerve growth factor, a pain and cartilage destruction mediator in OA, have been demonstrated after GAE.[21]

Animal Models

The synovial changes in OA and the effects of GAE have been evaluated in animal studies. Korchi et al confirmed the presence of synovial inflammation and hypervascularization in knee OA of a canine model

Affiliations: Department of Radiology, Section of Interventional Radiology, Northwestern University, Chicago, Illinois (Dr Husnain); Department of Radiology, King Edward Medical University, Lahore, Pakistan (Dr Wali); Department of Radiology, Section of Interventional Radiology, University of Illinois at Chicago, Chicago, Illinois (Dr Badar); Department of Radiology, Section of Interventional Radiology, University of Chicago, Chicago, Illinois (Dr Ahmed). Dr Ahmed is also a member of the Editorial Advisory Board of *Applied Radiology.*

Figure 1. Lateral compartment pain in an adult with bilateral knee osteoarthritis. (A) Anterior-posterior projection DSA following left SFA injection demonstrates genicular arterial anatomy (arrows) including the descending genicular artery (DGA, blue), lateral superior genicular artery (LSGA, black), lateral inferior genicular artery (LIGA, red), anterior tibial recurrent artery (ATRA, yellow). (B) Selective catheterization of the LIGA (blue arrow; parent vessel) demonstrates significant hyperemia and neo-angiogenesis along the lateral compartment (green arrow; target vessel). This vessel was subsequently embolized with 0.4cc of 200-micron microspheres. (C) Postembolization demonstrates successful embolization and pruning of the hyperemic target vessels (green arrow) with preserved flow within the parent genicular artery (blue arrow). (D) Selective catheterization of the LSGA (blue arrow; parent vessel) demonstrates additional hyperemia and neo-angiogenesis along the superior-lateral aspect of the joint (green arrow; target vessel).

Note the BB markers placed at the sites of the patient's focal pain. (E) Post embolization with 0.5cc of 200-micron microspheres demonstrates pruning of hyperemic target vessels (green arrow) with preserved flow within the parent LSGA (blue arrow).

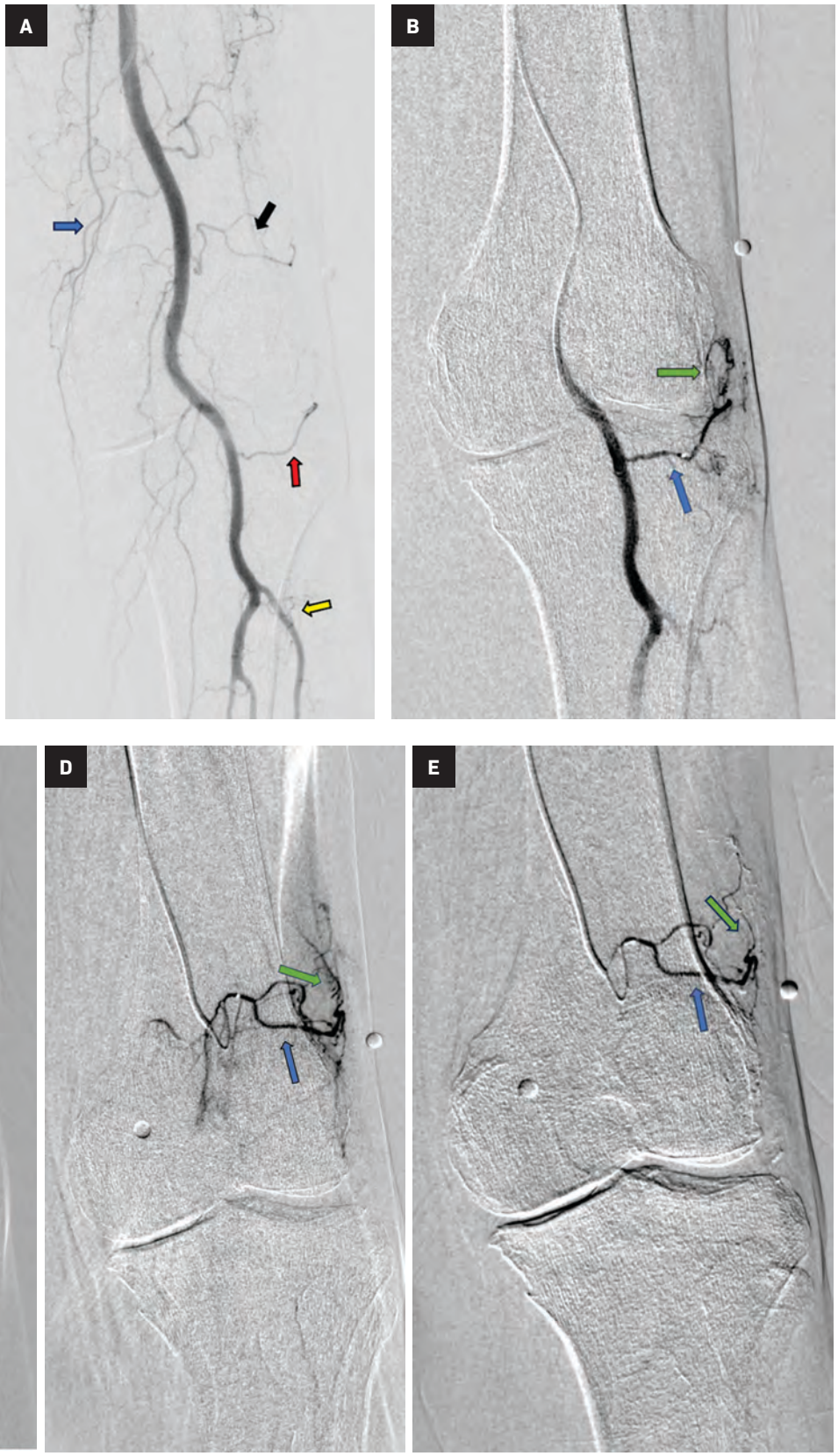

using a comprehensive imaging approach and reported a positive correlation of image findings with histopathological analysis. Imaging included conventional MRI, dynamic contrast-enhanced MRI, contrast-enhanced MRI, and quantitative digital subtraction angiography (Q-DSA). The study also underscored the role of early imaging in diagnosis and monitoring disease progression.[22] Ro et al evaluated the efficacy of GAE by randomly assigning rabbit knee OA models to GAE or sham interventions.[23] A significant decrease in synovial inflammation and CD3+ cell infiltration was reported among the GAE group, indicating the procedure's potential to mitigate OA-related symptoms.

Workup and Selection Criteria

Osteoarthritis severity is graded according to the Kellgren-Lawrence (KL) classification model based on radiographic findings such as presence of osteophytes, joint space narrowing and sclerosis.[24] Subjective scoring methods for assessing symptom severity include the Western Ontario and McMaster Universities Osteoarthritis index (WOMAC), the Knee Injury and Osteoarthritis Outcome Score (KOOS), and the visual analog scale (VAS). WOMAC (total score range: 0-96; pain sub-scale score range: 0-20) and KOOS (range: 0-100) involve parameters such as pain, stiffness, physical function, activities of daily living, sport and recreation function, and related quality of life. The VAS considers only one parameter: pain (range: 1-10). Imaging metrics are also sometimes used to quantify symptom severity, known as whole-organ magnetic resonance scoring (WORMS). This approach utilizes conventional MR images and comprises fourteen articular features, focusing on articular cartilage loss and osteophytes, which are recognized as central to OA pathophysiology.[25]

The GAE selection criteria typically involve patients with radiography-proven, moderate-to-severe OA (within 3 months), who are experiencing moderate to severe pain (VAS > 3), that persists despite conservative treatments (for at least 6 months), and who are ineligible for (or not desiring not to undergo) TKA. Generally accepted contraindications include rheumatoid or other inflammatory arthritis, irreversible coagulopathy, acute knee trauma mandating surgery, prior partial or total knee replacement in the ipsilateral knee, lower-extremity arterial or venous insufficiency, severe iodinated contrast allergy or eGFR < 45. Preprocedural MRI is often performed to rule out other underlying sources of pain and poor treatment response, such as structural abnormalities or malignancy. A thorough history and physical examination are performed and symptom severity is assessed using the subjective scoring methods described above, with majority of the current studies using WOMAC as the scoring tool.[26,27]

Procedural Technique/ Vascular Pruning Technique

Preparation and Setup

GAE is generally performed under moderate sedation on an outpatient basis. Routine prerequisites such as performing basic lab investigations, discontinuing oral anticoagulants, and securing informed consent are completed, and pain sites are identified with radiopaque markers for precision.[27]

Access and Catheterization

Three approaches can be used to access the femoral artery: Ipsilateral antegrade, contralateral retrograde, and retrograde pedal.[28] Access is obtained under local anesthesia and ultrasound guidance, then an angiographic catheter is advanced to the distal superficial femoral artery, a critical step in identifying the genicular branches responsible for the hyperemic regions near the radiopaque markers. Further refinement is achieved by introducing and advancing a microcatheter, often 1.7–2.4-French in size, super-selectively into the genicular arteries for precise targeting. Lower-profile microcatheters (≤ 2 -French) may be considered to enhance navigational ease in complex anatomy.[28]

Contrast and Embolization

Contrast is administered from the distal superficial femoral artery above the origin of the descending genicular artery. Both early and delayed phase DSA are deployed to facilitate the identification of genicular arteries or any anatomical variants and target hyperemic areas (Figure 1). Additionally, cone-beam CT and angio-CT can be used to map the feeding vessels and to determine vessel obliquity.[27] Once the target vessel is reached, the "pruning" method is employed to inject embolic material (miniscule aliquots ranging 0.1-0.4 mL) to achieve sub-stasis.

This technique effectively clears hyperemic vessels while simultaneously ensuring sustained flow within the parent genicular artery and thereby mitigating the risk of ischemic complications.[28] This was validated in a pilot study by Badar et al, who reported favorable clinical outcomes and significant perfusion reduction in the target vessels with preserved flow in the parent vessel.[29] For enhanced precision, microspheres can be diluted with the appropriate ratio of contrast and saline and injected under fluoroscopic guidance.[27,28] The six main target vessels are the descending genicular artery (DGA), the superior medial genicular artery (SMGA), the inferior medial genicular artery (IMGA), the superior lateral genicular artery (SLGA), the inferior lateral genicular artery (ILGA), and the anterior tibial (ATRA) artery.[10]

Table 1. Clinical outcomes of genicular artery embolization studies*

STUDY	YEAR PUBLISHED (DESIGN)	NO. OF PATIENTS	AGE (MEAN)	K-L GRADE	EMBOLIC USED	CHANGE IN VAS AT 6 MONTHS	CHANGE IN WOMAC AT 6 MONTHS
Okuno et al.[9]	2015 (Pros)	14	65.2	0-2	IPM/CS, Embozene	-	-
Okuno et al.[10]	2017 (Pros)	72	64.4	1-3	IPM/CS, Embozene	-73.6%	-69.4%
Lee et al.[11]	2019 (Retro)	41	67.2	1-3	IPM/CS	-65.4%	-
Lander et al.[12]	2020 (Pros)	10	62.2	1-3	PVA, IPM/CS	-	-
Bagla et al.[13]	2020 (Pros)	20	59.4	1-3	Embozene	-59.2%	-49.18%
Little et al.[14]	2021 (Pros)	38	60	1-3	Embosphere	-	-
Padia et al.[15]	2021 (Pros)	40	69	2-4	Embozene	-62.5%	-62.5%
Bagla et al.[16]	2022 (RSC)	21	63.5	1-3	Optisphere	-75%	-54.8%
Sapoval et al.[32]	2023 (Pros)	22	66	≥2	Ioversol/ Ethiodized oil	-	-

Abbreviations: Pros: Prospective; Retro: Retrospective; RSC: Randomized Sham-Controlled; KL: Kellgren-Lawrence; IPM/CS: Imipenem/Cilastatin sodium; PVA: polyvinyl alcohol; VAS: visual pain analog; WOMAC: Western Ontario McMaster Universities Osteoarthritis Index
*For the sake of simplicity, only the 6-month follow-up outcomes were included for this table.

Assessment, Additional Treatment, and Postprocedure Care

The resolution of distal hypervascularity while keeping the parent genicular artery and its branches patent marks the technical success of the procedure. Patients are advised to remain supine and maintain their access leg straight in the recovery area for four hours. A steroid taper, such as post-procedure methylprednisolone, and 500 mg naproxen twice a day for five days, can be prescribed to manage short-term postprocedure inflammation and pain.[27]

Follow-up

Clinical success is determined by amelioration of symptoms at 1, 3, 6, and 12-month follow-up and based on the scoring methods. Physical exams are also performed to rule out any potential adverse events. In the majority of cases, patients with mild to moderate OA report significant improvement within 1-3 months, which may last for years.[10] For severe OA, studies have reported initial symptom improvement with relapse on long-term.[11–13] In cases of persistent symptoms, repeat intervention has been described.[12] For patients who remain non-responsive to treatment, TKA remains a viable option.[12,14,15]

Types of Embolic Agents

The particulate embolics can be categorized into temporary and permanent. Effective temporary embolics encompass imipenem/cilastatin sodium (IPM/CS).[9–11] IPM/CS represents a combination of antibiotic crystals that generate transient embolic effects when blended with a contrast medium, resulting in particle sizes between 10 and 70 µm.[30] Permanent embolics ranging in size from 70-300 µm have also been used in certain studies that prove their efficacies. These include Embozene (75-100 µm; Varian Medical Systems, Palo Alto, CA), Embospheres (100-300 µm; Merit Medical Systems, South Jordan, UT), Optisphere (100-300 µm; Medtronic, Minneapolis, MN), and polyvinyl alcohol (10-70 µm; Contour, Boston Scientific, Marlborough, MA).[10,11,31,32] More recently, ethiodized oil-based emulsion (ioversol/ethiodized oil) (Optiray/Lipiodol; Guerbet, Villepinte, France) has been evaluated in a prospective study with significant results.[33] Still, the choice of ideal embolic remains a matter of debate.

Adverse Events

The most common adverse events (Society of Interventional Radiology class A and B, Cardiovascular, and Interventional Radiological Society of Europe grade 1 and 2) associated with GAE are skin changes, including but not limited to transient erythema,

discoloration, and ulceration resulting from non-targeted embolization of cutaneous arteries; puncture site hematoma; paresthesia; and fever. No serious adverse event has been reported.[32]

A systematic review by Casadaban et al reported transient skin erythema in 11% (21/186) of patients across three included studies. Embozene exhibited a higher rate (63%) and longer duration (1-3 months) compared to IPM/CS (2.5% and 3 weeks, respectively). The plausible reason for this disparity may be the permanent nature of embozene compared to IPM/CS. Puncture site hematoma was reported in 10% (18/186) patients, with resolution within 1-3 weeks.[20] Bagla et al reported paresthesia in the great toe and plantar region in two cases, which ultimately resolved within two weeks.[13] Lee et al reported a sole instance of fever that subsided within a day, with a prevalence of 0.5% among 186 cases.[11] Padia et al reported hematoma formation at the femoral puncture site, which resolved without any sequelae. Skin ulceration was reported in 18% (7/40) of patients and did not require any treatment. Two small, asymptomatic bone infarcts in non-weight bearing areas were identified on a 3-month follow-up MRI. One case of fat necrosis was found in the lower thigh.[15]

The risk of cutaneous ischemia can be alleviated by applying ice packs to the affected knee skin to induce vasoconstriction before embolization. Padia et al reported a reduction from 18% to 0% by utilizing this technique.[15] Furthermore, higher microsphere volumes (≥ 3 mL) in one setting were reported to be associated with increased risk of cutaneous adverse events.[29] However, this volume cutoff pertains to a specific embolic type (200 µm Hydropearl microspheres) and dilution method (1:3) which limits generalizability to other embolics. More studies are needed to consolidate this volume threshold.

Anatomical Variants of the Geniculate Arteries

The popliteal artery is the continuation of the superficial femoral artery. At the knee joint level, the popliteal artery gives the DGA that supplies the anterior portion of the knee joint. Below the origin of the DGA are the SLGA and the SMGA, which supply the lateral and medial portions of the knee joint, respectively. More distally, arising from the popliteal artery, are the ILGA and IMGA. Finally, the ATRA, which arises from the anterior tibial artery, is the most inferior artery supplying the knee. Bagla et al proposed a classification system for the arteries of the knee joint by analyzing the angiographic findings from 41 GAE procedures. The following branching patterns were observed: M1 (presence of all three medial branches: DGA, SMGA, IMGA), M2 (presence of two of the three medial branches: either DGA and SMGA, or DGA and IMGA), L1 (presence of all three lateral branches: SLGA, ILGA, ATRA) and L2 (presence of two or three lateral branches: either ATRA and SLGA, or ATRA and ILGA). Understanding these variants is crucial as it may help decrease the risk of non-target embolization and prolonged radiation exposure.

Outcomes of GAE

Since 2015, the efficacy of GAE in reducing VAS, WOMAC, and KOOS scores has been demonstrated in multiple studies. These include:

- A 2015 prospective pilot study of 11 patients that found significant improvement in WOMAC scores at 12 months compared to baseline.[9]
- A 2017 prospective study of 72 patients demonstrated significant improvement in WOMAC scores at 12 months, as well as WORMS scores at baseline and 2 years postprocedure showing significant improvement in synovitis.[10]
- A 2019 retrospective study of 41 patients with severe and mild-to-moderate knee OA demonstrated significant improvement through 10 months. In the severe OA group, the VAS score returned to baseline at the 3-month follow-up.[11]A detailed breakdown of these and five other studies showing the impact of GAE on knee OA is provided in Table 1.

Future Steps and Possible Limitations in Implementation

These studies have included only patients with mild-to-moderate (KL 1-3) OA. Less is known about the outcomes of GAE in severe OA with KL 4. Moreover, studies comparing TKA or intra-articular steroids with GAE and different types of embolic agents could provide more explicit evidence. Results from the *MOTION* [34] (GAE vs intra-articular steroids) and *GAUCHO* (IPM/CS vs microspheres) trials, for example, are expected in the near future.

Current literature comprises single-arm and small, randomized studies. In addition, some studies have also reported positive placebo effects with sham procedures. Therefore, the ongoing *GENESIS 2* (double-blinded randomized sham-controlled) trial with large sample size could provide robust results. Outcomes in most of the studies have been reported based on subjective scoring methods. For instance, pre- and postprocedure WORMS was evaluated in only one study.[10]

Furthermore, new objective measures identified by Taslakian et al[21] and Badar et al[29] are paving the way to better understanding of treatment effects and warrant further research. Studies involving patients from different geographical areas and ethnicities would also be helpful, as studies performed thus far have focused on only a few geographical regions.

References

1) Dillon CF, Rasch EK, Gu Q, Hirsch R. Prevalence of knee osteoarthritis in the United States: arthritis data from the Third National Health and Nutrition Examination Survey 1991-94. *J Rheumatol*. 2006;33(11):2271-2279.

2) Brown GA. AAOS clinical practice guideline: treatment of osteoarthritis of the knee: evidence-based guideline, 2nd edition. *J Am Acad Orthop Surg*. 2013;21(9):577-579. doi:10.5435/JAAOS-21-09-577

3) Deyle GD, Allen CS, Allison SC, et al. Physical Therapy versus Glucocorticoid Injection for Osteoarthritis of the Knee. *N Engl J Med*. 2020;382(15):1420-1429. doi:10.1056/NEJMoa1905877

4) Jevsevar D, Donnelly P, Brown GA, Cummins DS. Viscosupplementation for Osteoarthritis of the Knee: A Systematic Review of the Evidence. *J Bone Joint Surg Am*. 2015;97(24):2047-2060. doi:10.2106/JBJS.N.00743

5) Kompel AJ, Roemer FW, Murakami AM, Diaz LE, Crema MD, Guermazi A. Intra-articular Corticosteroid Injections in the Hip and Knee: Perhaps Not as Safe as We Thought? *Radiology*. 2019;293(3):656-663. doi:10.1148/radiol.2019190341

6) Mathis DT, Lohrer L, Amsler F, Hirschmann MT. Reasons for failure in primary total knee arthroplasty - An analysis of prospectively collected registry data. *J Orthop*. 2021;23:60-66. doi:10.1016/j.jor.2020.12.008

7) Sharkey PF, Lichstein PM, Shen C, Tokarski AT, Parvizi J. Why are total knee arthroplasties failing today--has anything changed after 10 years? *J Arthroplasty*. 2014;29(9):1774-1778. doi:10.1016/j.arth.2013.07.024

8) Cornman-Homonoff J, Kishore SA, Waddell BS, et al. Genicular Artery Embolization for Refractory Hemarthrosis following Total Knee Arthroplasty: Technique, Safety, Efficacy, and Patient-Reported Outcomes. *J Vasc Interv Radiol JVIR*. 2021;32(8):1128-1135. doi:10.1016/j.jvir.2021.04.020

9) Okuno Y, Korchi AM, Shinjo T, Kato S. Transcatheter arterial embolization as a treatment for medial knee pain in patients with mild to moderate osteoarthritis. *Cardiovasc Intervent Radiol*. 2015;38(2):336-343. doi:10.1007/s00270-014-0944-8

10) Okuno Y, Korchi AM, Shinjo T, Kato S, Kaneko T. Midterm Clinical Outcomes and MR Imaging Changes after Transcatheter Arterial Embolization as a Treatment for Mild to Moderate Radiographic Knee Osteoarthritis Resistant to Conservative Treatment. *J Vasc Interv Radiol JVIR*. 2017;28(7):995-1002. doi:10.1016/j.jvir.2017.02.033

11) Lee SH, Hwang JH, Kim DH, et al. Clinical Outcomes of Transcatheter Arterial Embolisation for Chronic Knee Pain: Mild-to-Moderate Versus Severe Knee Osteoarthritis. *Cardiovasc Intervent Radiol*. 2019;42(11):1530-1536. doi:10.1007/s00270-019-02289-4

12) Landers S, Hely R, Page R, et al. Genicular Artery Embolization to Improve Pain and Function in Early-Stage Knee Osteoarthritis-24-Month Pilot Study Results. *J Vasc Interv Radiol JVIR*. 2020;31(9):1453-1458. doi:10.1016/j.jvir.2020.05.007

13) Bagla S, Piechowiak R, Hartman T, Orlando J, Del Gaizo D, Isaacson A. Genicular Artery Embolization for the Treatment of Knee Pain Secondary to Osteoarthritis. *J Vasc Interv Radiol JVIR*. 2020;31(7):1096-1102. doi:10.1016/j.jvir.2019.09.018

14) Little MW, Gibson M, Briggs J, et al. Genicular artery embolization in patients with osteoarthritis of the knee (GENESIS) Using Permanent Microspheres: Interim Analysis. *Cardiovasc Intervent Radiol*. 2021;44(6):931-940. doi:10.1007/s00270-020-02764-3

15) Padia SA, Genshaft S, Blumstein G, et al. Genicular Artery Embolization for the Treatment of Symptomatic Knee Osteoarthritis. *JB JS Open Access*. 2021;6(4):e21.00085. doi:10.2106/JBJS.OA.21.00085

16) Bagla S, Piechowiak R, Sajan A, Orlando J, Hartman T, Isaacson A. Multicenter Randomized Sham Controlled Study of Genicular Artery Embolization for Knee Pain Secondary to Osteoarthritis. *J Vasc Interv Radiol*. 2022;33(1):2-10.e2. doi:10.1016/j.jvir.2021.09.019

17) van den Bosch MHJ, van Lent PLEM, van der Kraan PM. Identifying effector molecules, cells, and cytokines of innate immunity in OA. *Osteoarthritis Cartilage*. 2020;28(5):532-543. doi:10.1016/j.joca.2020.01.016

18) Lane NE, Brandt K, Hawker G, et al. OARSI-FDA initiative: defining the disease state of osteoarthritis. *Osteoarthritis Cartilage*. 2011;19(5):478-482. doi:10.1016/j.joca.2010.09.013

19) Bonnet CS, Walsh DA. Osteoarthritis, angiogenesis and inflammation. *Rheumatol Oxf Engl*. 2005;44(1):7-16. doi:10.1093/rheumatology/keh344

20) Casadaban LC, Mandell JC, Epelboym Y. Genicular Artery Embolization for Osteoarthritis Related Knee Pain: A Systematic Review and Qualitative Analysis of Clinical Outcomes. *Cardiovasc Intervent Radiol*. 2021;44(1):1-9. doi:10.1007/s00270-020-02687-z

21) Taslakian B, Swilling D, Attur M, et al. Genicular Artery Embolization for Treatment of Knee Osteoarthritis: Interim Analysis of a Prospective Pilot Trial Including Effect on Serum Osteoarthritis-Associated Biomarkers. *J Vasc Interv Radiol JVIR*. 2023;34(12):2180-2189.e3. doi:10.1016/j.jvir.2023.08.029

22) Korchi AM, Cengarle-Samak A, Okuno Y, et al. Inflammation and Hypervascularization in a Large Animal Model of Knee Osteoarthritis: Imaging with Pathohistologic Correlation. *J Vasc Interv Radiol*. 2019;30(7):1116-1127. doi:10.1016/j.jvir.2018.09.031

23) Ro DH, Jang MJ, Koh J, et al. Mechanism of action of genicular artery embolization in a rabbit model of knee osteoarthritis. *Eur Radiol*. 2023;33(1):125-134. doi:10.1007/s00330-022-09006-9

24) Katz JN, Arant KR, Loeser RF. Diagnosis and Treatment of Hip and Knee Osteoarthritis: A Review. *JAMA*. 2021;325(6):568-578. doi:10.1001/jama.2020.22171

25) Peterfy CG, Guermazi A, Zaim S, et al. Whole-Organ Magnetic Resonance Imaging Score (WORMS) of the knee in osteoarthritis. *Osteoarthritis Cartilage*. 2004;12(3):177-190. doi:10.1016/j.joca.2003.11.003

26) hoi JW, Ro DH, Chae HD, et al. The Value of Preprocedural MR Imaging in Genicular Artery Embolization for Patients with Osteoarthritic Knee Pain. *J Vasc Interv Radiol JVIR*. 2020;31(12):2043-2050. doi:10.1016/j.jvir.2020.08.012

27) Sterbis E, Casadaban L. Genicular Artery Embolization Technique. *Tech Vasc Interv Radiol*. 2023;26(1):100878. doi:10.1016/j.tvir.2022.100878

28) Heller DB, Beggin AE, Lam AH, Kohi MP, Heller MB. Geniculate Artery Embolization: Role in Knee Hemarthrosis and Osteoarthritis. *RadioGraphics*. 2022;42(1):289-301. doi:10.1148/rg.210159

29) Badar W, Anitescu M, Ross B, Wallace S, Uy-Palmer R, Ahmed O. Quantifying Change in Perfusion after Genicular Artery Embolization with Parametric Analysis of Intraprocedural Digital Subtraction Angiograms. *J Vasc Interv Radiol JVIR*. 2023;34(12):2190-2196. doi:10.1016/j.jvir.2023.08.041

30) Woodhams R, Nishimaki H, Ogasawara G, et al. Imipenem/cilastatin sodium (IPM/CS) as an embolic agent for transcatheter arterial embolisation: a preliminary clinical study of gastrointestinal bleeding from neoplasms. *SpringerPlus*. 2013;2:344. doi:10.1186/2193-1801-2-344

31) Bagla S, Piechowiak R, Sajan A, Orlando J, Canario DAH, Isaacson A. Angiographic Analysis of the Anatomical Variants in Genicular Artery Embolization. *J Clin Interv Radiol ISVIR*. 2022;6(01):18-22. doi:10.1055/s-0041-1729464

32) Torkian P, Golzarian J, Chalian M, et al. Osteoarthritis-Related Knee Pain Treated With Genicular Artery Embolization: A Systematic Review and Meta-analysis. *Orthop J Sports Med*. 2021;9(7):23259671211021356. doi:10.1177/23259671211021356

33) Sapoval M, Querub C, Pereira H, et al. Genicular artery embolization for knee osteoarthritis: Results of the LipioJoint-1 trial. *Diagn Interv Imaging*. Published online December 14, 2023:S2211-5684(23)00239-5. doi:10.1016/j.diii.2023.12.003

34) Merit Medical Systems, Inc. *Multicenter, PrOspective, Randomized, Controlled Trial Comparing GenIcular Artery EmbOlization Using Embosphere Microspheres to Corticosteroid iNjections for the Treatment of Symptomatic Knee Osteoarthritis: MOTION Study*. clinicaltrials.gov; 2024. Accessed December 31, 2023. https://clinicaltrials.gov/study/NCT05818150

REVIEW

Chronic Mesenteric Ischemia: Mesenteric Artery Duplex Sonography and the Utility of Postprandial Imaging

Kaitlin M. Zaki-Metias, MD; Rajbir S. Pannu, MD; Nicholas Mills, MD; Tima F. Tawil, MD; Bilal Turfe, MD; Stephen M. Seedial, MD, RPVI; Kevin K. Hannawa, MD

Chronic mesenteric ischemia (CMI), also referred to as abdominal angina, is characterized by gradually worsening perfusion of the bowel as a consequence of narrowing of the celiac artery (CA), superior mesenteric artery (SMA), and/or inferior mesenteric artery (IMA).[1] The majority of the small and large bowel is supplied by branches of the SMA; however, owing to the significant collateral blood supply of the mesentery, typically more than one mesenteric artery must be compromised to manifest symptoms of CMI. Most often the result of atherosclerosis, CMI also may sometimes be caused by fibromuscular dysplasia and vasculitis.[1] Risk factors include increased age, female gender, and comorbidities that predispose to atherosclerosis, such as smoking and diabetes. Patients often present with postprandial pain, weight loss, and food aversion.[2]

The American College of Radiology (ACR) Appropriateness Criteria® states that abdominal duplex sonography "may be appropriate" as initial imaging in symptomatic patients with suspected CMI.[3] However, the potential drawbacks of ultrasonography of the mesenteric vasculature, such as technical difficulty in visualization due to bowel gas, are considered in the ACR's recommendations. Computed tomographic angiography (CTA) or magnetic resonance angiography (MRA) of the abdomen and pelvis are considered "usually appropriate" per the ACR Appropriateness Criteria®, although CTA has proven to be most accurate, with the highest inter-reader agreement relative to MRA and ultrasound.[3]

Ultrasonography is a cost-effective and noninvasive way to evaluate for CMI in symptomatic patients. The examination consists of grayscale and color Doppler imaging of the aorta, CA, SMA, and IMA, in addition to spectral Doppler evaluation with measurement of the peak systolic velocity (PSV) at the proximal portion of each artery (Figure 1). End-diastolic velocity (EDV) and PSV ratios relative to the aorta may also be obtained based on institutional protocol. Ultrasound may provide additional information regarding functional flow limitations that will not be evident on nondynamic CTA or MRA imaging.

Ultrasound Evaluation of Chronic Mesenteric Ischemia in the Fasting State

Sonographic examination is best performed in the fasting state to reduce artifact and interference from bowel gas.[2] Although no universally

Affiliations: Department of Radiology, Trinity Health Oakland Hospital, Pontiac, Michigan (Drs Zaki-Metias, Pannu, Mills, Tawil, Turfe, Seedial, Hannawa); Wayne State University School of Medicine, Detroit, Michigan (Drs Zaki-Metias, Pannu, Mills, Tawil, Turfe); Huron Valley Radiology, Ypsilanti, Michigan (Dr Hannawa).
Disclosures: Dr Zaki-Metias serves on the Early Career Section of the *Applied Radiology* Editorial Advisory Board. The authors have no relevant disclosures or conflicts of interest.
Prior publication/presentation: Some of the contents of this manuscript have been previously presented, as follows:
Zaki-Metias, KM, et al. Chronic Mesenteric Ischemia: Mesenteric Artery Duplex Sonography and the Utility of Postprandial Imaging. Radiological Society of North America 109th Scientific Assembly and Annual Meeting; November 26-30, 2023; Chicago, Illinois.
Zaki-Metias, KM, et al. Utility of postprandial duplex ultrasound in the evaluation of chronic mesenteric ischemia: experience at a community hospital. Canadian Association of Radiologists Annual Scientific Meeting; April 27-30, 2023; Montréal, Québec, Canada.
Zaki-Metias, KM, et al. Utility of postprandial duplex ultrasound in the evaluation of chronic mesenteric ischemia: experience at a community hospital. 7th Annual Michigan Summit on Quality Improvement and Patient Safety; May 18, 2022; Detroit, Michigan.
Keywords: chronic mesenteric ischemia; mesenteric artery ultrasound; postprandial ultrasound; Doppler ultrasound

Table 1. Recommended criteria for PSV and EDV with the highest accuracy suggestive of CMI.[3-6]

All velocities expressed as cm/s.

	NORMAL PSV	PSV SUGGESTING >50% STENOSIS	PSV SUGGESTING >70% STENOSIS	NORMAL EDV	EDV SUGGESTING >50% STENOSIS	EDV SUGGESTING >70% STENOSIS
CA	80-200	240	320	19-74	40	100
SMA	50-160	295	400	10-63	45	70
IMA	93-189	250	270	<20	90	100

Figure 1. Fasting duplex sonography of the SMA showing normal waveforms with continuous forward flow and a normal PSV of 183 cm/s measured at the origin of the SMA (cursor overlies the ostium/proximal SMA).

accepted criteria or standards exist for diagnosing CMI based on fasting PSV, multiple studies recommend a cutoff ranging from 200-320 cm/s in the CA and 275-400 cm/s in the SMA to be suggestive of at least 70% stenosis in these vessels (Table 1).[3,4]

A 2012 study by AbuRahma et al found PSV values to be more accurate in discerning hemodynamically significant arterial stenosis of greater than 50% and greater than 70% compared to EDV and SMA or CA/aorta PSV ratios.[4] Cutoff PSV values of 295 cm/s and 400 cm/s in the SMA correspond to >50% (sensitivity 87%, specificity 89%, accuracy 88%) and >70% stenosis (sensitivity 72%, specificity 93%, accuracy 85%), respectively (Table 1).[4] Slightly lower PSV measurements are used as the cutoff in the CA, with PSV of 240 cm/s and 320 cm/s correlating with >50% (sensitivity 87%, specificity 83%, accuracy 86%) and >70% stenosis (sensitivity 80%, specificity 89%, accuracy 85%), respectively (Table 1).[4] End-diastolic velocities have been found to have markedly lower sensitivity for hemodynamically significant stenosis, ranging from 58-84%, although some institutions continue to obtain these measurements as part of their imaging protocol.[4]

Peak systolic velocity ratios of the interrogated vessel and aorta can also be utilized to assess for functional flow limitations secondary to stenosis relative to the aorta. Superior mesenteric artery/aorta PSV ratios of 3.5 and 4.5 in the SMA correspond to >50% (sensitivity 69%, specificity 78%, accuracy 73%) and >70% stenosis (sensitivity 67%, specificity 83%, accuracy 78%), respectively.[4]

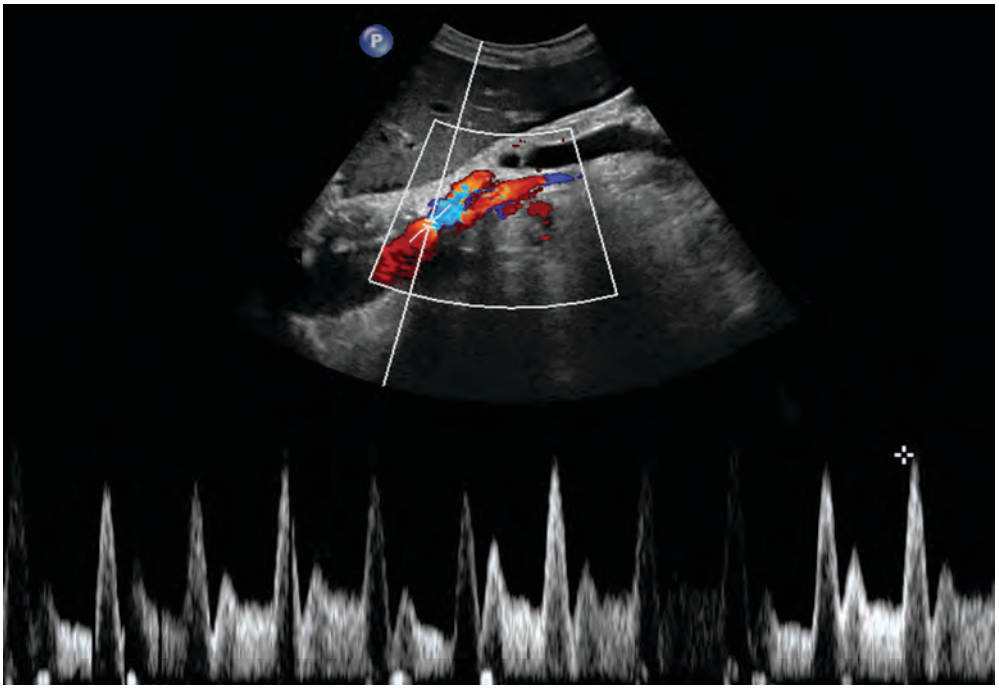

Figure 2. Fasting duplex sonography of the CA showing normal waveforms with continuous forward flow and a normal PSV of 139 cm/s.

Figure 3. Fasting (A) and postprandial (B) duplex sonography of the CA showing normal waveforms with continuous forward flow and a PSV of 225 cm/s in the fasting state and 298 cm/s in the postprandial state. This constitutes a normal postprandial rise in PSV (32%).

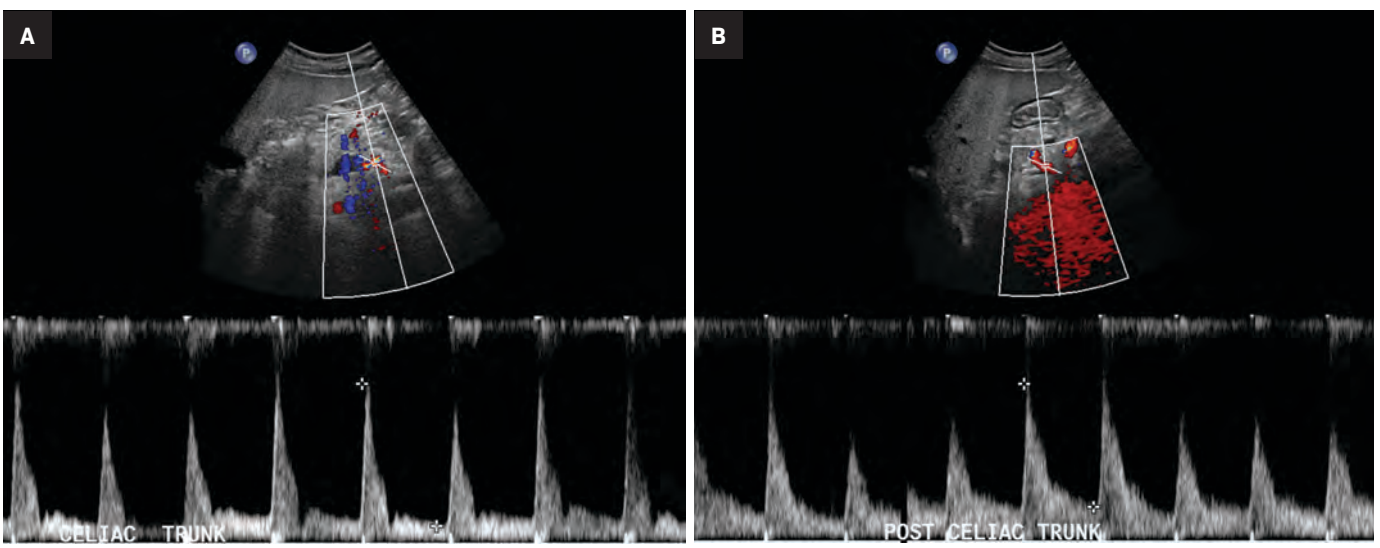

Conversely, CA/aorta PSV ratios of 2.75 and 4.5 in the SMA correspond to >50% (sensitivity 81%, specificity 71%, accuracy 78%) and >70% stenosis (sensitivity 75%, specificity 87%, accuracy 82%), respectively.[4] Although renal/aorta PSV ratios are commonly used for assessing renal artery stenosis, they are generally not as accurate as the PSV in detecting ≥50% and ≥70% stenosis of the SMA and ≥50% stenosis of the CA.[4]

Postprandial Ultrasound in the Assessment of Chronic Mesenteric Ischemia

The role of postprandial sonography remains controversial, although several studies have documented its potential utility. Fasting sonogram findings are typically sufficient to suggest a diagnosis of CMI, although postprandial imaging may be performed as a sort of "stress test," analogous to a cardiac stress test to evaluate for coronary artery disease. Typically, a standard 250-calorie, mixed liquid meal (240 mL) is rapidly ingested by the patient prior to postprandial imaging.[6,7]

However, imaging performed in the postprandial state often results in fluctuations in PSV measurements, which may lead to lack of reproducibility and variations in interpretation.[7] For instance, a 1995 study by

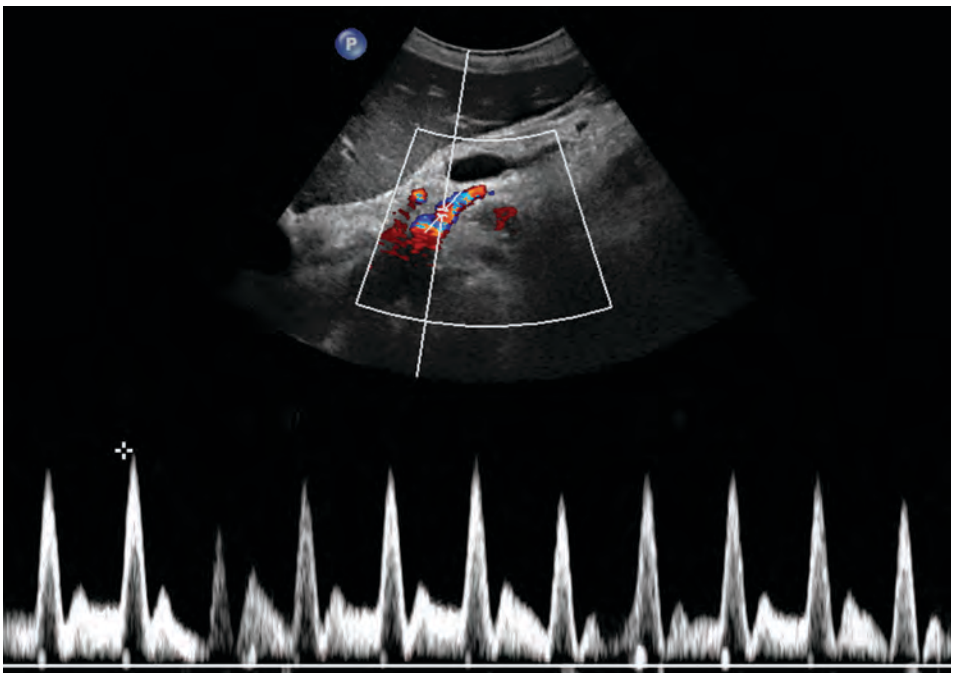

Figure 4. Fasting duplex sonography of the SMA showing normal waveforms with continuous forward flow and a normal PSV of 98.9 cm/s.

Figure 5. Fasting (A) and postprandial (B) duplex sonography of the SMA showing normal waveforms with continuous forward flow and a normal PSV of 225 cm/s in the fasting state and 315 cm/s in the postprandial state. This constitutes a normal postprandial rise in PSV (40%).

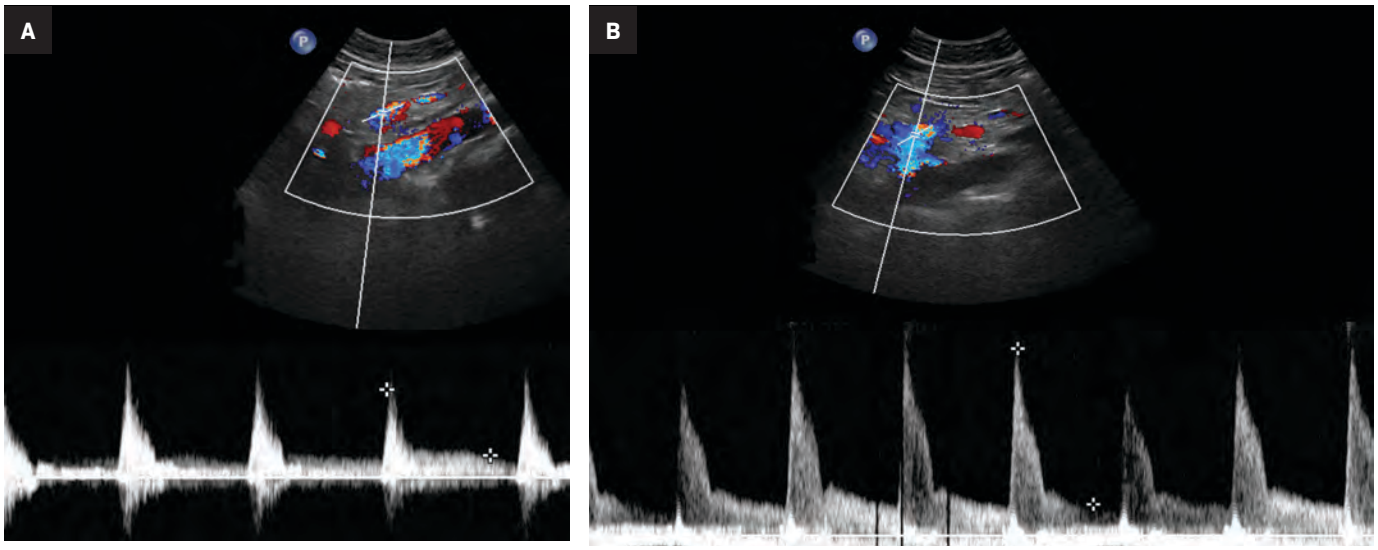

Gentile et al found that the combination of fasting and postprandial duplex ultrasound was less sensitive than fasting mesenteric duplex ultrasound alone.[8] Furthermore, the literature on postprandial mesenteric arterial sonography is limited and its utility has not been clearly demonstrated.[8,9]

The CA demonstrates a low-resistance pattern with EDV and continuous forward flow during both systole and diastole with blood flow pattern independent of food intake (Figures 2,3).[7] The SMA and IMA demonstrate a high-resistance pattern with low diastolic velocities in the fasting state (Figures 4,5). The normal physiological response to a meal is vasodilation of the mesenteric arteries to allow for increased blood flow during digestion, resulting in elevation of PSV and EDV of the mesenteric arteries.[7] Some studies have found that both velocities increase after a meal, with at least a doubling of the SMA EDV, while others suggest a modest physiological increase in PSV of 20%-30%.[8,10] Overall, increased postprandial velocities are suggestive of patency of the mesenteric arteries. In cases of mesenteric arterial stenosis, the normal postprandial velocity increase would be blunted, resulting in insufficient circulation to the bowel. The failure of PSV to increase

at least 20%-30% between fasting and postprandial states is indicative of greater than 70% hemodynamically significant stenosis (Figure 6).[8,9]

Previous studies have demonstrated that postprandial imaging provides useful information regarding functional flow limitation in symptomatic patients with otherwise normal fasting imaging; the hemodynamic stress of feeding has been proposed as a source of additional information in symptomatic patients.[11] A 2013 study by Zachrisson et al found that, in patients with postprandial pain, PSV did not significantly increase after feeding when compared to those without postprandial pain, although mesenteric stenosis was not confirmed by CT or catheter angiography, suggesting that postprandial imaging may provide information about collateral reserve flow capacity.[12]

In theory, postprandial imaging may provide additional information on functional flow to the bowel after caloric stress, given that the criteria used to diagnose stenosis on postprandial images does not include collateral vasculature. However, the potential exists for a high rate of false positives. Collateral vessels, such those of the pancreaticoduodenal arcade, allow for adequate perfusion of the bowel despite hemodynamically significant stenosis in the primary feeder artery.[8,12] Therefore, if bowel perfusion results primarily from compensatory flow through collateral vessels, flow velocity in the primary artery may not increase after the caloric bolus, resulting in a false positive finding.

Reliance on postprandial PSV elevation as a measure of vessel patency may be skewed, as compensatory collateral circulation, such as via the pancreaticoduodenal arcade, may allow for adequate perfusion and an increase in postprandial PSV despite critical proximal stenosis.[12] Additionally, including postprandial sonography in the

Figure 6. Fasting (A) and postprandial (B) duplex sonography of the SMA showing abnormal waveforms with aliasing and an elevated PSV of 391 cm/s in the fasting state, indicating at least 50% stenosis. The postprandial PSV is also elevated at 433 cm/s, which constitutes only a 10% rise between the fasting and postprandial states, less than the expected 20-30% rise. While supporting the diagnosis of SMA stenosis, the postprandial PSV does not add much more information.

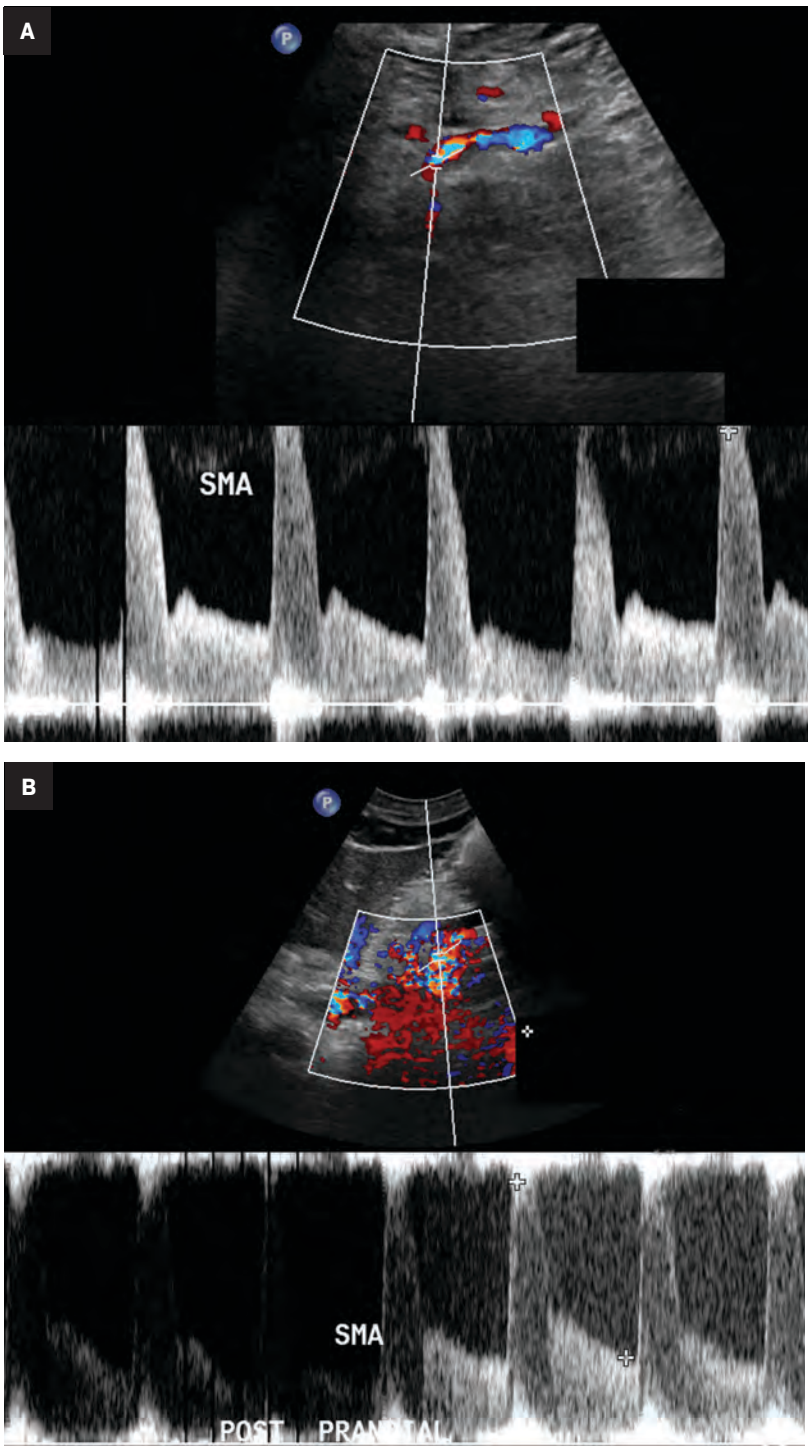

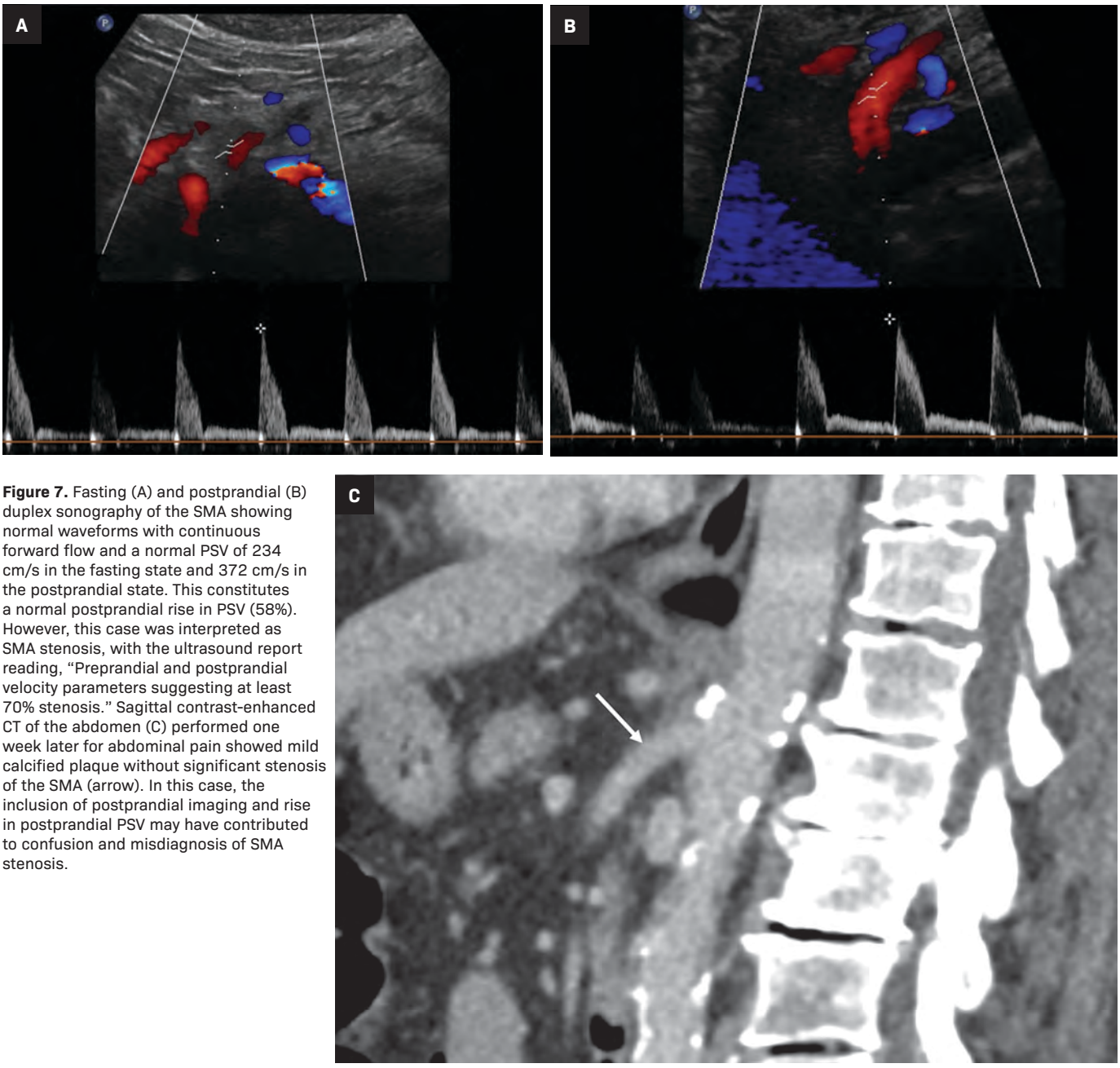

Figure 7. Fasting (A) and postprandial (B) duplex sonography of the SMA showing normal waveforms with continuous forward flow and a normal PSV of 234 cm/s in the fasting state and 372 cm/s in the postprandial state. This constitutes a normal postprandial rise in PSV (58%). However, this case was interpreted as SMA stenosis, with the ultrasound report reading, "Preprandial and postprandial velocity parameters suggesting at least 70% stenosis." Sagittal contrast-enhanced CT of the abdomen (C) performed one week later for abdominal pain showed mild calcified plaque without significant stenosis of the SMA (arrow). In this case, the inclusion of postprandial imaging and rise in postprandial PSV may have contributed to confusion and misdiagnosis of SMA stenosis.

protocol prolongs examination and risks increasing nondiagnostic images due to increased bowel gas. Despite its demonstrated potential utility, postprandial imaging of the mesenteric arteries is not routinely recommended given the aforementioned potential confounding factors and limited additional useful information, especially considering the availability of more advanced imaging techniques.[9]

Limitations of Mesenteric Artery Ultrasound

Sonographic evaluation of the mesenteric vessels has significant limitations regardless of fasting or postprandial state. These include patient body habitus, bowel gas, and anatomic variations, as well as variability between sonographers and interpreting radiologists. Overestimation of stenosis may occur secondary to variant anatomy, vessel tortuosity, and the presence of dense calcifications without significant luminal narrowing due to alterations in blood flow (Figure 7).[1,3,13] Furthermore, the importance of clarity on the sonographer worksheet cannot be overstated to avoid confusion surrounding the interpretation of fasting and postprandial PSV, which may inadvertently lead to overdiagnosis of SMA stenosis (Figure 8).

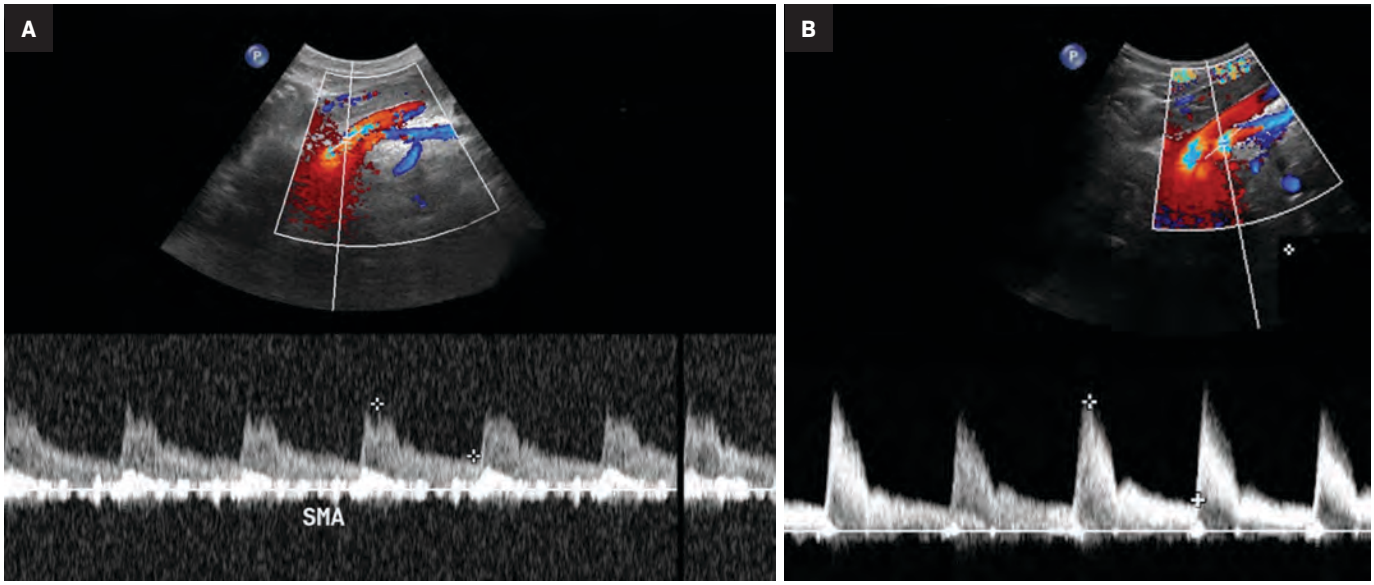

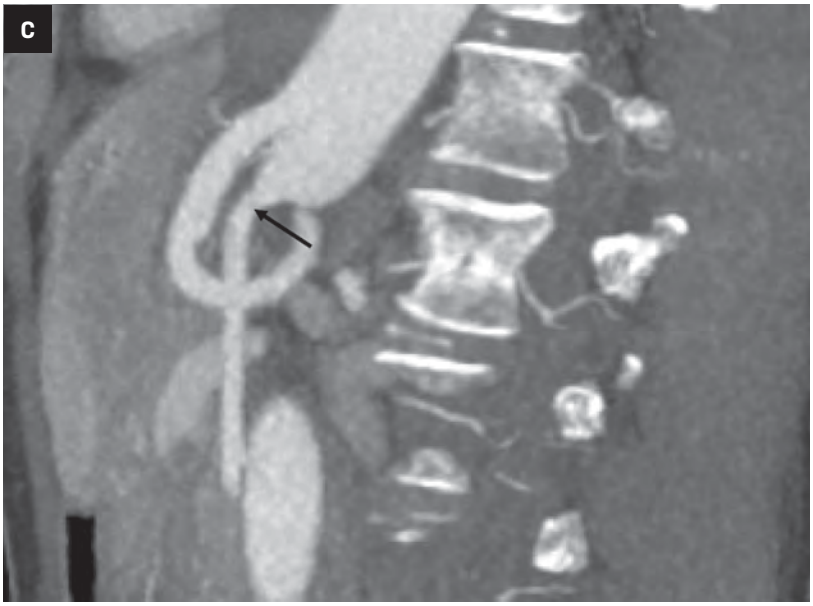

Figure 8. Fasting (A) and postprandial (B) duplex sonography of the SMA showing normal waveforms with continuous forward flow and a normal PSV of 160 cm/s in the fasting state and 328 cm/s in the postprandial state. This constitutes a normal postprandial rise in PSV (105%). However, this case was interpreted as SMA stenosis, with the impression of the ultrasound report reading, "Findings consistent with chronic mesenteric ischemia (greater than 70% stenosis)." Sagittal maximum intensity projection CT angiogram of the abdomen with intravenous contrast (C) performed for further assessment showed a widely patent SMA (arrow). Note the tortuous course of the abdominal aorta. The inclusion of postprandial imaging and rise in postprandial PSV resulted in confusion and misdiagnosis of SMA stenosis.

Management of Chronic Mesenteric Ischemia

In cases of CMI diagnosed at sonography, the next step in management may consist of CTA for further characterization of the stenosis or catheter angiography for definitive diagnosis and treatment. Abdominopelvic CTA has been demonstrated superior to ultrasound at detecting high-grade stenosis of the celiac and mesenteric arteries.[13] In fact, CTA and catheter angiography are now considered the gold standard in assessing CMI.[14] The treatments of choice for CMI include endovascular interventions, such as balloon angioplasty and stent placement, and open surgical interventions such as endarterectomy and bypass.[13,14] The latter interventions are typically reserved for symptomatic patients who are otherwise in relatively good health with a focal lesion.[13,14] A meta-analysis of several published series evaluating the outcome of endovascular treatment of CMI found high clinical success rates (80-100%).[1] Follow-up ultrasound and/or CTA is typically performed to assess for vessel and/or stent patency.[3,13,14] Conservative management is usually pursued in patients with multiple medical comorbidities and generally consists of antiplatelet therapy, anticoagulation, and/or nitrate therapy.[13,14]

Conclusion

While postprandial duplex sonography of the mesenteric vessels may provide additional information regarding the functional reserve and collateral flow in patients with CMI,

postprandial imaging in the mesenteric artery ultrasound protocol may result in confusion and overdiagnosis. This potential for overdiagnosis based on expected elevated postprandial PSV values may lead to unnecessary imaging and unnecessary interventions. Fasting duplex sonography has proven useful for CMI screening, although there are pitfalls pertaining to operator dependency and patient-related factors such as bowel gas, body habitus, variant anatomy, and vessel tortuosity.

References

1) Hohenwalter EJ. Chronic mesenteric ischemia: diagnosis and treatment. *Semin Intervent Radiol*. 2009;26(4):345-351. doi:10.1055/s-0029-1242198

2) Nichols S, Windeler H. Duplex scanning in diagnosis of mesenteric insufficiency. *J Diagn Med Sonogr.* 1995;11(3):120-126. doi: 10.1177/875647939501100302

3) Expert Panels on Vascular Imaging and Gastrointestinal Imaging: Ginsburg M, Obara P, Lambert DL, et al. ACR Appropriateness Criteria® Imaging of Mesenteric Ischemia. *J Am Coll Radiol.* 2018;15(11S):S332-S340. doi: 10.1016/j.jacr.2018.09.018. PMID: 30392602

4) AbuRahma AF, Stone PA, Srivastava M, et al. Mesenteric/celiac duplex ultrasound interpretation criteria revisited. *J Vasc Surg*, 2012;55(2):428-436.e6; discussion 435-436. doi: 10.1016/j.jvs.2011.08.052. PMID: 22195765.

5) AbuRahma AF, Scott Dean L. Duplex ultrasound interpretation criteria for inferior mesenteric arteries. *Vascular*. 2012; 20(3):145-149. doi:10.1258/vasc.2011.oa0349

6) Flinn WR, Rizzo RJ, Park JS, Sandager GP. Duplex scanning for assessment of mesenteric ischemia. *Surg Clin North Am*. 1990;70(1):99-107. doi:10.1016/s0039-6109(16)45036-x

7) Revzin MV, Pellerito JS, Nezami N, Moshiri M. The radiologist's guide to duplex ultrasound assessment of chronic mesenteric ischemia. *Abdom Radiol.* 2020;45(10):2960-2979. doi: 10.1007/s00261-019-02165-2. PMID: 31410506.

8) Gentile AT, Moneta GL, Lee RW, et al. Usefulness of fasting and postprandial duplex ultrasound examinations for predicting high-grade superior mesenteric artery stenosis. *Am J Surg*, 1995;169(5):476-9. doi: 10.1016/S0002-9610(99)80198-6. PMID: 7747822.

9) Nicoloff AD, Williamson WK, Moneta GL, Taylor LM, Porter JM. Duplex ultrasonography in evaluation of splanchnic artery stenosis. *Surg Clin North Am*. 1997 Apr;77(2):339-355. doi: 10.1016/s0039-6109(05)70553-3. PMID: 9146717.

10) Moneta GL, Yeager RA, Dalman R, Antonovic R, Hall LD, Porter JM. Duplex ultrasound criteria for diagnosis of splanchnic artery stenosis or occlusion. *J Vasc Surg*. 1991; 14(4):511-8; discussion 518-20. PMID: 1920649.

11) Muller AF. Role of duplex Doppler ultrasound in the assessment of patients with postprandial abdominal pain. *Gut.* 1992;33(4):460-465. doi: 10.1136/gut.33.4.460. PMID: 1582587.

12) Zachrisson H, Svensson C, Forssell C, Lassvik C. Postprandial evaluation of possible collateral pathways in chronic mesenteric ischemia with duplex ultrasound. *J Med Diagn Meth.* 201;3:2. doi: 10.4172/2168-9784.1000154

13) Cognet F, Ben Salem D, Dranssart M, et al. Chronic mesenteric ischemia: imaging and percutaneous treatment. *Radiographics*. 2002;22(4):863-879; discussion 879-80. doi: 10.1148/radiographics.22.4.g02jl07863. PMID: 12110715.

14) Terlouw LG, Moelker A, Abrahamsen J, et al. European guidelines on chronic mesenteric ischaemia - joint United European Gastroenterology, European Association for Gastroenterology, Endoscopy and Nutrition, European Society of Gastrointestinal and Abdominal Radiology, Netherlands Association of Hepatogastroenterologists, Hellenic Society of Gastroenterology, Cardiovascular and Interventional Radiological Society of Europe, and Dutch Mesenteric Ischemia Study group clinical guidelines on the diagnosis and treatment of patients with chronic mesenteric ischaemia. *United European Gastroenterol J*. 2020; 8(4):371-395. doi:10.1177/2050640620916681

Telix
SPONSORED REVIEW ARTICLE

Not All Prostate-Specific Membrane Antigen Imaging Agents Are Created Equal: Diagnostic Accuracy of Ga-68 PSMA-11 PET/CT for Initial and Recurrent Prostate Cancer

Andrei S. Purysko, MD,[1,2]; Andre L. Abreu, MD,[3]; Daniel W. Lin, MD,[4]; and Sanoj Punnen, MD, MAS[5]

Abstract

Positron emission tomography (PET) radiotracers that target prostate-specific membrane antigen (PSMA), a transmembrane protein overexpressed in prostate cancer (PCa) cells, are highly sensitive and specific for the detection of metastatic PCa. The radioactive PET imaging agent Ga-68 PSMA-11 has demonstrated higher PCa detection rates compared with conventional imaging techniques, leading to its increased use in the diagnosis of PCa. In this review of literature published between February 2015 and December 2022, of 76 studies in >5000 men with PCa, we examined the accuracy and clinical use of Ga-68 PSMA-11 PET for the initial staging of PCa, assessment of biochemical recurrence (BCR), and how this technique may affect the clinical management of PCa. The majority of studies evaluating Ga-68 PSMA-11 PET for primary staging and for BCR demonstrated a sensitivity ≥80% and a specificity ≥90%. Ga-68 PSMA-11 PET led to a change in clinical management in 19% to 52% and 16% to 75% of patients with primary PCa and BCR, respectively. Variations in diagnostic accuracy parameters were observed among studies but were anticipated given differences in patient characteristics (eg, PSA, lesion sizes) and study designs. No serious adverse events were noted with Ga-68 PSMA-11 PET. Overall, Ga-68 PSMA-11 offers high sensitivity, is well tolerated, and can result in clinical management changes for patients with primary PCa and BCR.

Affiliations: [1]Imaging Institute, Cleveland Clinic, Cleveland, Ohio, USA; [2]Glickman Urological and Kidney Institute, Cleveland Clinic, Cleveland, Ohio, USA; [3]USC Institute of Urology, Center for Image-Guided Surgery, Focal Therapy and Artificial Intelligence for Prostate Cancer, University of Southern California, Los Angeles, California; [4]University of Washington, Seattle, Washington; [5]Desai Sethi Urology Institute, University of Miami, and Sylvester Comprehensive Cancer Center, Miami, Florida.
Corresponding author: Sanoj Punnen, MD, MAS, 1120 NW 14th Street, Suite 1560, Miami, FL 33136, USA. Telephone: 305-243-6596; E-mail: s.punnen@med.miami.edu
Declaration of competing interest: Andre L. Abreu has received honoraria for Koelis. Andrei S. Purysko has received grants from Blue Earth Diagnostics and American College of Radiology, consulting fees from Blue Earth Diagnostics and Koelis, and honoraria from Blue Earth Diagnostics. Daniel W. Lin has no conflicts to disclose. Sanoj Punnen has been a speaker for Telix Pharmaceuticals.
Disclaimer: Collation of publicly available data. Cross-trial comparisons not based on head-to-head studies should be interpreted with caution.
Acknowledgments: The views are those of the authors. Medical writing and editorial support were provided by David Gibson, PhD, CMPP, and Ricky Sidhu, PharmD (ApotheCom, San Francisco, California), and funded by Telix Pharmaceuticals. We are grateful for the editorial assistance of Megan M. Griffiths, scientific writer for the Imaging Institute, Cleveland Clinic, Cleveland, Ohio.
Author contributions: All authors were involved in the conceptualization, data curation, and writing, review, and editing of the manuscript. All authors approved the final version of the manuscript to be published and agreed to be accountable for all aspects of the work in ensuring that questions related to the accuracy or integrity of any part of the work are appropriately investigated and resolved.

Keywords: Prostate-specific membrane antigen, Prostate cancer, Imaging, Positron emission tomography

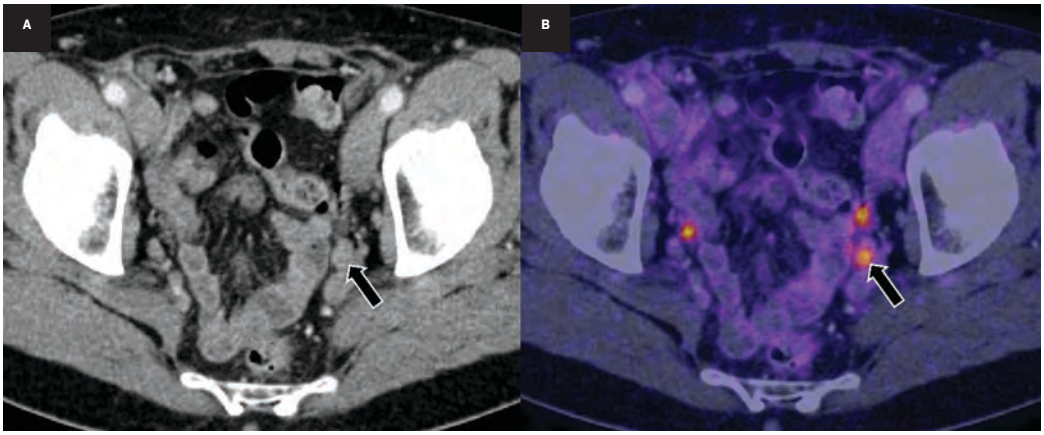

Figure 1. An adult with a history of grade group 2 prostate cancer presented with biochemical recurrence (prostate-specific antigen [PSA] 0.75 ng/mL) 18 months after radical prostatectomy. Contrast-enhanced computed tomography (CT) image (A) and Ga-68 prostate-specific membrane antigen (PSMA) positron emission tomography (PET)/CT image (B) show a 0.8 x 0.7 cm left internal iliac node (arrow) with increased tracer uptake (SUVmax 7.2). *(Image provided by Dr. Andrei Purysko, Imaging Institute, Cleveland Clinic, Cleveland, Ohio.)*

Introduction

Prostate cancer (PCa) is diagnosed in approximately 1.3 million men each year and represents the second most common cancer in men worldwide.[1] The American Cancer Society estimated 288,300 new cases and 34,700 deaths from PCa in the United States in 2023.[2] The 5-year survival rate is 99% for patients with localized/regional PCa, but only 32% for patients with distant metastasis.[3]

PCa recurrence, defined as an increase in prostate-specific antigen (PSA) levels after treatment, occurs in up to 90% of cases, depending on initial risk categorization and definitive therapy. Biochemical recurrence (BCR) is defined as a PSA level of 0.2 ng/mL followed by a confirmatory PSA level of ≥0.2 ng/mL after radical prostatectomy (RP) and nadir PSA level + 2.0 ng/mL after radiotherapy.[4] Patients with preoperative PSA levels of <2.6 ng/mL, 2.6 to 10 ng/mL, and >10 ng/mL are expected to have recurrence rates of 10%, 20%, and 50%, respectively.[5] Approximately 40% to 90% of patients with high-risk features develop BCR following prostatectomy[3, 6] and 30% to 50% experience BCR following radiation therapy.[7] However, multinomial nomograms based on other clinical factors, such as Gleason grade group and clinical stage, provide more accurate estimates of BCR.[8]

Figure 2. Results of literature searches to identify studies evaluating Ga-68 prostate-specific membrane antigen 11 (PSMA-11) for staging primary prostate cancer (PCa) and detecting biochemical recurrence (BCR). *Irrelevant articles included studies of radiotracers that were not Ga-68 PSMA-11, review articles, opinion articles, studies of laboratory results, studies of drug manufacturing process, studies regarding the use of Ga-68 PSMA-11 in other cancers, studies with no comparator or standard of truth, case reports, and nonclinical evaluations. †One study identified from second PubMed search from November 2021 to December 2022. ††Three studies identified from second PubMed search from November 2021 to December 2022.

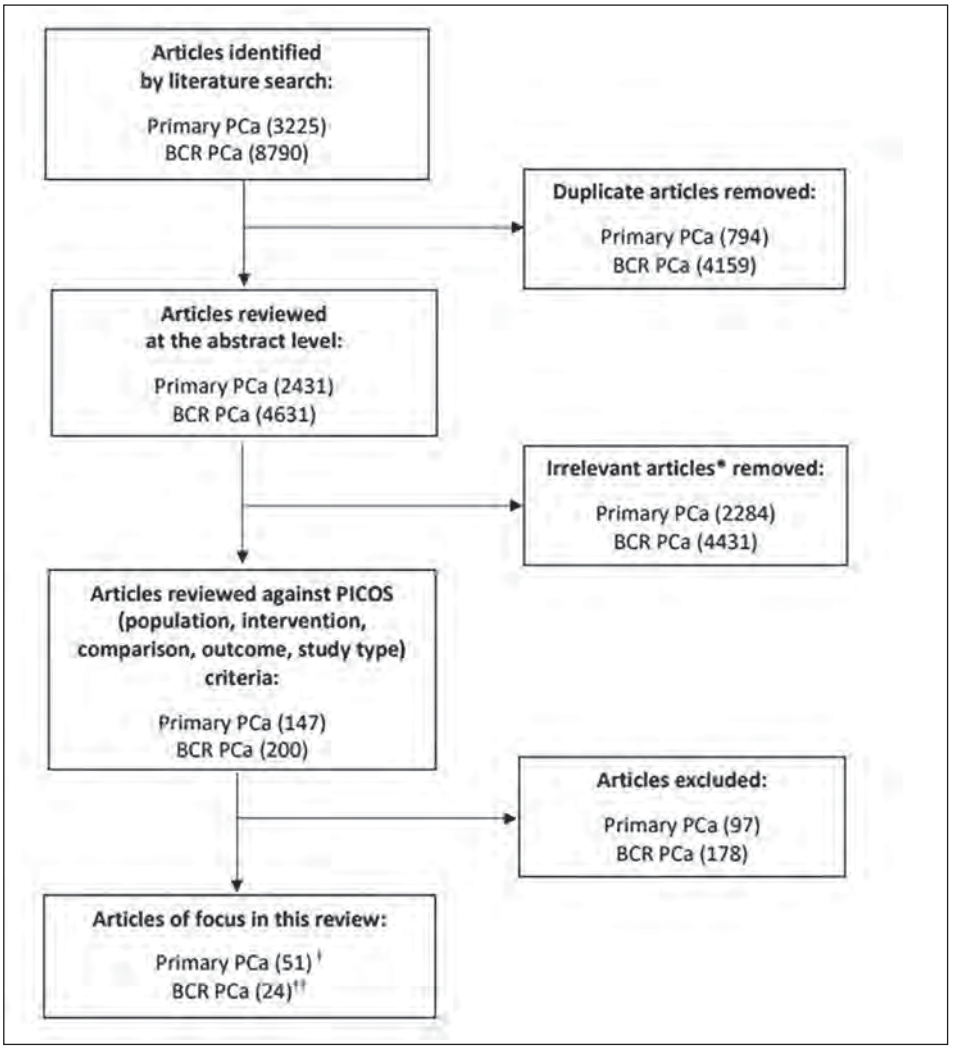

Table 1. Efficacy of Ga-68 PSMA-11 imaging in detecting primary PCa.

STUDY*	N	MODALITY	REGION	SENSITIVITY (%)	SPECIFICITY (%)	PPV (%)	NPV (%)	CHANGE IN CLINICAL MANAGEMENT (%)
Al-Bayati et al, 2018[17]	22	PET, PET/MRI	Prostate	M-1 PET: 81, PET/MRI: 88 M-2 PET: 91, PET/MRI: 94				
Basha et al, 2019[18]	173	PET/CT	Prostate	96				
Berger et al, 2018[19]	48	PET/CT	Prostate	81 (p) 100 (lesion-based)	85 (p)	89 (p)	74 (p)	
Budaus et al, 2016[20]	30	PET/CT	ln	33 (ln)	100	100	69	
Chen et al, 2019[21]	51	PET/CT	Prostate	90	94			
Chen et al, 2020[22]	54	PET/CT/MRI	Prostate	78 (ece) 75 (svi)	94 (ece) 95 (svi)	97 (ece) 82 (svi)	67 (ece) 93 (svi)	19
Demirci et al, 2019[23]	141	PET/CT	Prostate	78	81			
Donato et al, 2019[25]	58	PET/CT	Prostate	93				
Donato et al, 2020[24]	144	PET/CT	Prostate	90	94			
El Hajj et al, 2019[26]	23	PET/CT	Prostate	42	89	74	67	
Fendler et al, 2016[27]	21	PET/CT	Prostate	67 73 (svi)	92 100 (svi)	97 100 (svi)	42 77 (svi)	
Fendler et al, 2017[28]	10	PET/CT	Prostate, ln	93[a]	85[a]			
Ferraro et al, 2020[29]	60	PET/CT	ln	58	98	88	90	
Gao et al, 2019[30]	49	PET/CT	Prostate	76 (pp) 77 (pl)	86 (pp) 88 (pl)			
Gupta et al, 2017[31]	12	PET/CT	ln	67	99	86	96	
Gupta et al, 2018[32]	23	PET/CT	Prostate, ln	63 (epe) 55 (svi) 66 (lnm)	100 (epe) 100 (svi) 99 (lnm)	100 (epe) 100 (svi) 88 (lnm)	36 (epe) 25 (svi) 98 (lnm)	
Herlemann et al, 2016[33]	20	PET/CT	ln	84	82	84	82	
Hicks et al, 2018[12]	32	PET/MRI	Prostate, ln	73[b]	88[b]			
Hinsenveld et al, 2020[34]	53	PET/CT	ln	100	86			
Hirmas et al, 2019[35]	21	PET/CT	Prostate, ln, bone	86 (pro) 92 (pln) 100 (eln) 100 (bm)	100 (pln) 100 (eln) 92 (bm)	100 (pro) 100 (pln) 100 (eln 90 (bm))	89 (pln) 100 (eln) 100 (bm)	52
Hoffman et al, 2017[36]	25	PET/CT	Prostate, ln, bone, lung	84[c]	100[c]	67[c]	100[c]	
Hofman et al, 2020[37]	150	PET/CT	Prostate, ln	85	98			28
Hope et al, 2021[63]	277	PET/CT, PET/MRI	ln	40	95	75	81	
Jena et al, 2018[38]	82	PET/MRI	Prostate, ln	78	86			
Kalapara et al, 2020[39]	205	PET/CT	Prostate	94				
Kopp et al, 2020[40]	90	PET/CT	ln	44	96	70	89	
Liu et al, 2020[41]	31	PET/CT	Prostate	100 (csPCa) 93 (PCa)	68 (csPCa) 75 (PCa)	67 (csPCa)	100 (csPCa)	
Lopci et al, 2018[43]	45	PET	Prostate	82	72			
Lopci et al, 2021[42]	97	PET/CT	Prostate	60	97	92	81	24
Maurer et al, 2016[44]	130	PET/CT, PET/MRI	ln	74	99	95	95	

Table 1 (cont). Efficacy of Ga-68 PSMA-11 imaging in detecting primary PCa.

STUDY*	N	MODALITY	REGION	SENSITIVITY (%)	SPECIFICITY (%)	PPV (%)	NPV (%)	CHANGE IN CLINICAL MANAGEMENT (%)
Muehlematter et al, 2019[45]	40	PET/MRI	Prostate	69 (ece) 55 (svi)	67 (ece) 94 (svi)			
Nandurkar et al, 2019[46]	101	PET/CT	Prostate, ln	47 (svi)	87 (svi)			
Obek et al, 2017[47]	51	PET/CT	Prostate	53	86	62	81	
Pallavi et al, 2020[48]	29	PET/CT	Prostate, ln	86 71 (lnm) 75 (ppe) 60 (svi) 50 (bni)	95			
Park et al, 2018[49]	33	PET/MRI	Prostate	100 (pp) 86 (pl) 50 (pn)	88 (pl) 98 (pn)			
Petersen et al, 2020[50]	20	PET/CT	ln	39	100	100	47	
Rahbar et al, 2016[51]	6	PET/CT	Prostate	92	92	96	85	
Rahman et al, 2019[52]	28	PET/CT	Lymph node				100	
Sahlmann et al, 2016[53]	12	PET/CT	Prostate, lymph node	99a	89a	100a		
Thalgott et al, 2018[54]	73	PET/MRI	Prostate, ln	60 (lnm) 94 (ece) 82 (svi)	100 (lnm) 45 (ece) 80 (svi)	100 (lnm) 82 (ece) 77 (svi)	83 (lnm) 75 (ece) 84 (svi)	
Tulsyan et al, 2017[55]	36	PET/CT	Prostate, ln	49	95	85	88	
van Leeuwen et al, 2017[56]	30	PET/CT	ln	54	99	92	94	
van Leeuwen et al, 2019[57]	140	PET/CT	ln, SVI	53 (lnm) 46 (svi)	88 (lnm) 93 (svi)	71 (lnm) 74 (svi)	76 (lnm) 80 (svi)	
von Klot et al, 2017[58]	21	PET/CT	Prostate	95	75	97	60	
Wong et al, 2018[68]	131	PET/CT	Prostate, ln	66	99			28
Yaxley et al, 2019[64]	208	PET/CT	ln	38 (pb) 24 (ln)	94 (pb) 100 (ln)	68 (pb) 75 (ln)	81 (pb) 96 (ln)	
Yilmaz et al, 2019[59]	24	PET/CT	Prostate, ln	30 (epe) 75 (svi) 33 (bni) 100 (lnm)	93 (epe) 90 (svi) 100 (bni) 100 (lnm)	75 (epe) 60 (svi) 100 (bni) 100 (lnm)	65 (epe) 95 (svi) 82 (bni) 100 (lnm)	
Zang et al, 2017[60]	22	PET/CT	ln	97	100			43
Zhang et al, 2017[61]	42	PET/CT	ln	93	96	93	96	
Zhang et al, 2019[62]	58	PET/CT	Prostate	92	82	89	86	

*Klingenberg et al 2022 is not included in this table, as endpoints recorded in this table were not reported in the study.
Abbreviations: bm, bone metastases; bni, bladder neck invasion; csPCa, clinically significant prostate cancer; CT, computed tomography; ece, extracapsular extension; eln, extrapelvic lymph nodes; epe, extraprostatic extension; ln, lymph node; lnm, lymph node metastasis; M-1, method-1; M-2, method-2; MRI, magnetic resonance imaging; NPV, negative predictive value; p, primary/index localization; pb, patient based; PCa, prostate cancer; pl, per lobe; pln, pelvic lymph node; pn, per node; pp, per patient; ppe, periprostatic lesions; pro, prostate, PET, positron emission tomography; PPV, positive predictive value; PSMA, prostate-specific membrane antigen; svi, seminal vesicle invasion.
[a]N staging results pooled data over patients with primary PCa and biochemical recurrence of PCa.
[b]Median.
[c]Comparison between Gleason scores based on a receiver operating characteristic curve analysis cutoff score.
Collation of publicly available data. Cross-trial comparisons not based on head-to-head studies should be interpreted with caution.

PCa is diagnosed via biopsy of the prostate, with imaging playing an important role in its diagnosis and management. However, staging for higher-risk disease is often performed using conventional imaging with computed tomography (CT) and bone scintigraphy, which have suboptimal sensitivities for detecting metastases for initial staging.[9] CT and Tc-99m methyl diphosphonate bone scintigraphy are routinely used to stage disease in patients with confirmed PCa and to assess suspected PCa recurrence. These methods, however, have limited sensitivity in detecting metastatic disease, particularly when patients have smaller lesions and lower PSA levels.[10]

Recent advances in diagnostic imaging have overcome these limitations. Positron emission

Table 2. Efficacy of Ga-68 PSMA-11 imaging in detecting BCR of PCa.

STUDY	N	POST-RADIATION OR POST-RP	BCR DEFINITION	MODALITY	REGION	SENSITIVITY (%)	SPECIFICITY (%)	PPV (%)	NPV (%)	CHANGE IN CLINICAL MANAGEMENT (%)	MEAN SUV_{MAX}
Abghari-Gerst et al, 2022 [122]	2005	Both	Not defined	PET/CT	Full body			82 (lb) 83 (pb) 72 (ln)			
Abufaraj et al, 2019[69]	65	Post-RP	2 consecutive increases in PSA above 0.2 ng/mL	PET/CT, PET/MRI	Lymph node	72–100	96–100	95–100	93–100		
Afshar-Oromieh et al, 2015[83]	42	Both	Not defined	PET/CT	Prostate, lymph node	77	100	100	91		13.3 ± 14.6
Calais et al, 2019[70]	15	Post-RP	Not defined	PET/CT	Prostate, lymph node	67		100			8.21 ± 4.1
15	Post-RP	Not defined	PET/CT	Prostate, lymph node	67		100			8.21 ± 4.1	
Cerci et al[88]	1004	Either	PSA >0.2 ng/mL after RP, or absolute increase in PSA of 2 ng/mL above nadir after RT	PET/CT	Full body or prostate					57	
Deandreis et al, 2020[89]	17	Both	Not defined	PET/CT	Prostate					35	
Emmett et al, 2019[71]	11	Post-RP	Not defined	PET/CT	Prostate, lymph node	67	100	50	100	46	
Farolfi et al, 2019[90]	119	Post-RP	Not defined	PET/CT	Prostate, lymph node					30	
Fendler et al, 2017[28]	25	Both	Not defined	PET/CT	Prostate, lymph node	93 (ln)	85 (ln)				
Fendler et al, 2019[72]	87	Both	PSA ≥0.2 ng/mL more than 6 weeks after prostatectomy or PSA rise of ≥0.2 above nadir after RT	PET/CT	Prostate, lymph node	92 (pb) 90 (lb)		84 (pb) 84 (lb)			5.1
Fourquet et al, 2021[73]	294	Both	2 consecutive rising PSA values >0.2 ng/mL or PSA rise of ≥0.2 above nadir after RT	PET/CT	Prostate, lymph node	70	70			68	5.3 (p) 5.9 (ln)

tomography (PET) radiotracers that target prostate-specific membrane antigen (PSMA), a transmembrane protein overexpressed in PCa cells, are highly sensitive and specific, with a high detection rate for metastatic PCa lesions. Thus, PSMA radiotracers are recommended for PET imaging of PCa without the prerequisite use of conventional imaging.[11] Ga-68 PSMA-11 is one such radioactive PET imaging agent that has demonstrated higher PCa detection rates compared with conventional imaging techniques, leading to its increased use along with other PET imaging agents.[12] Figure 1 shows an example of a pelvic node in the setting of BCR that was positive on Ga-68 PSMA-11 PET/CT, but negative on CT.

Ga-68, a β+ emitting radionuclide, is one of the most common radioisotopes used in PET scans worldwide.[13] PET imaging using Ga-68 PSMA-11[14] was approved by the US Food and Drug Administration (FDA) as the first PSMA-targeted imaging agent on December 1, 2020, followed by approval of a kit for the preparation of Ga-68 PSMA-11 (TLX591-CDx) on December 17, 2021 for widespread commercial use.[15]

Ga-68 PSMA-11 is approved for the detection of suspected metastasis in the initial staging of patients with PCa and the identification of suspected PCa BCR after treatment.[14] Ga-68 PSMA-11 is also approved in the US to identify and select patients who are candidates for FDA-approved PSMA-directed radioligand therapy. A recent study also reported a significant effect of Ga-68 PSMA-11 on the staging and management of PCa across all relevant clinical scenarios,

Table 2 (cont). Efficacy of Ga-68 PSMA-11 imaging in detecting BCR of PCa.

STUDY	N	POST-RADIATION OR POST-RP	BCR DEFINITION	MODALITY	REGION	SENSITIVITY (%)	SPECIFICITY (%)	PPV (%)	NPV (%)	CHANGE IN CLINICAL MANAGEMENT (%)	MEAN SUV_{MAX}
Grubmuller et al, 2018[82]	117	Post-RP	Not defined	PET/CT, PET/MRI	Prostate, lymph node					75	
Hamed et al, 2019[74]	151	Both	Rising PSA >0.2 ng/mL	PET/CT	Prostate, lymph node	99	100	100	91		
Herlemann et al, 2016[33]	14	Post-RP	Not defined	PET/CT	Lymph node	83	63	86	56		
Jilg et al, 2017[75]	28	Both	Not defined	PET/CT	Lymph node	93 (mr) 81 (sr)	100 (mr) 100 (sr)	100 (mr) 99 (sr)	89 (mr) 93 (sr)		
Kunikowska et al, 2022[91]	108	Either	PSA ≥2 ng/mL after RT	PET/CT	Prostate, torso					16	
Lawhn-Heath et al, 2019[76]	72	Both	Not defined	PET/CT, PET/MRI	Prostate, lymph node	89	31	91	21		
Mandel et al, 2020[77]	23	Post-RP	Not defined	PET/CT, PET/MRI	Lymph node	90 (sb) 76 (fb)	74 (sb) 88 (fb)	71 (sb) 69 (fb)	91 (sb) 91 (fb)		
Morigi et al, 2015[92]	9	Both	Not defined	PET/CT, PET/MRI	Prostate, lymph node					54	
Pfister et al, 2016[78]	28	Both	Not defined	PET/CT	Prostate, lymph node	87	93	76	97		
Radzina et al, 2020[79]	8	Both	Not defined	PET/CT	Prostate, lymph node, bone	64 (lr) 83 (ln) 83 (bm)	74 (lr) 80 (ln) 92 (bm)	58 (lr) 80 (ln) 71 (bm)	78 (lr) 100 (ln) 96 (bm)		
Rauscher et al, 2016[80]	48	Both	PSA >0.2 ng/mL	PET/CT, PET/MRI	Lymph node	78 (lb) 100 (pb)	97 (lb) 50 (pb)	95 (lb) 93 (pb)	88 (lb) 100 (pb)		12.7±10.8
Rousseau et al, 2019[93]	8	Post-RP	Not defined	PET/CT	Prostate					73	
Sahlmann et al, 2016[53]	23	Both	Not defined	PET/CT	Prostate, lymph node	94[a]	99[a]	89[a]	100a		
Zacho et al, 2018[81]	10	Both	Not defined	PET/CT	Prostate	80[b]	98[b]	89[b]	97[b]	44	

Abbreviations: BCR, biochemical recurrence; bm, bone metastasis; CT, computed tomography; fb, field based; lb, lesion based; ln, lymph node; lr, local recurrence; M1, bone metastasis present; mr, main region; MRI, magnetic resonance imaging; NPV, negative predictive value; p, prostate; pb, patient based; PCa, prostate cancer; PET, positron emission tomography; PPV, positive predictive value; PSA, prostate-specific antigen; PSMA, prostate-specific membrane antigen; RP, radical prostatectomy; sb, side based; sr, subregion.
[a]Results pooled data over patients with primary PCa and BCR of PCa.
[b]Pessimistic analysis considered equivocal as M1.
Collation of publicly available data. Cross-trial comparisons not based on head-to-head studies should be interpreted with caution.

including patients with PSA below the threshold for BCR, those with known metastatic or advanced castration-resistant disease, and those who have undergone primary treatments other than surgery or radiotherapy.[16]

Herein we review the available literature to assess the sensitivity and specificity of Ga-68 PSMA-11 PET for PCa imaging along with its safety and clinical use for PCa management. Literature searches were conducted using PubMed to identify published studies relevant to the use of Ga-68 PSMA-11 PET for the detection and staging of primary PCa and to detect and localize BCR. Search terms included "primary prostate cancer," "prostate cancer," "PSMA," "PET," "staging," and "biochemically recurrent." The initial search was limited to studies published in English from February 2015 to November 2021. A second search was conducted to identify articles from November 2021 to December 2022 using the same search terms. Overall, 75 studies in >5000 men with PCa were identified that examined the accuracy and clinical use of Ga-68 PSMA-11 PET for the initial staging of PCa and assessing BCR (Figure 2).

Primary staging of PCa using Ga-68 PSMA-11

Table 1 summarizes the results of studies that assessed Ga-68 PSMA-11 for the primary staging of PCa. The majority of studies demonstrated a sensitivity ≥80% and a specificity ≥90%. Sensitivity of Ga-68 PSMA-11 ranged from 30% to 100% for detecting PCa, 24% to 100% for detecting cancer in the lymph nodes, and 84% to 100% for detecting bone metastases; its specificity ranged from 45% to 100% for the prostate, 82% to 100% for the lymph nodes, and 92% to 100% for bone metastases. The positive

predictive value (PPV) ranged from 60% to 100%, and the negative predictive value (NPV) ranged from 25% to 100% in both localized and metastatic PCa, with the majority of these studies reporting values in the upper range.[12, 17-64] Additionally, a prospective study highlighted the prognostic value of 68-Ga PSMA-11 PET/CT versus conventional imaging with 99mTc bone scintigraphy and CT for primary staging in 247 high-risk patients with PCa treated with RP. Primary staging with 68-Ga PSMA-11 PET/CT resulted in a significantly lower biochemical recurrence risk after RP vs conventional imaging, likely due to improved selection of patients for RP.[65]

Initial PCa detection and T staging

In a study evaluating 144 patients (median PSA 8.6 ng/mL), Ga-68 PSMA-11 PET/CT was compared with multiparametric MRI (mpMRI) for the detection of localized PCa, with biopsy histopathology used as a reference standard for the full cohort and RP specimen used as the reference standard in a subset of patients.[24] Ga-68 PSMA-11 showed a higher sensitivity for detecting index lesions (90.1%) compared with mpMRI (83.1%), although this difference was not significant ($p = 0.267$). The median size of index tumor foci missed by mpMRI (1.66 cm^3; interquartile range [IQR], 0.79–2.53 cm^3) was significantly larger than that of tumor foci missed by Ga-68 PSMA-11 PET/CT (0.72 cm^3; IQR, 0.36–1.0 cm^3; $p = 0.034$). Among the 136 patients who had clinically significant PCa detected on biopsy (defined as Gleason score of ≥7), Ga-68 PSMA-11 was significantly more sensitive than mpMRI in detecting cancer within the prostate (95% vs. 86%, respectively; $p = 0.017$), but both imaging methods had high specificities (93% vs. 94%, respectively). Overall, Ga-68 PSMA-11 PET/CT detected significantly more cancer than mpMRI for the entire cohort based on both biopsy ($p = 0.004$) and RP histopathology ($p = 0.020$).

In another study evaluating 54 patients with PCa with a median PSA level of 13.30 ng/mL, Ga-68 PSMA-11 PET/CT and PET/MRI were more sensitive in detecting extracapsular extension (PET/CT, 78%; PET/MRI, 83%) compared with mpMRI (mpMRI, 54%; $p < 0.05$).[22] Ga-68 PSMA-11 PET/CT and PET/MRI also tended to have higher sensitivity for detecting seminal vesicle invasion (75%) compared with mpMRI (67%), but the difference was not statistically significant. The specificity, PPV, and NPV were also not significantly different among these modalities. The timing of biopsy (before vs after Ga-68 PSMA-617 PET/CT) did not seem to affect the outcomes of Ga-68 PSMA PET/CT imaging in high-risk patients with PCa.[66]

Initial PCa N and M staging

In the multicenter proPSMA study, 302 patients were randomly assigned to undergo Ga-68 PSMA-11 PET/CT or conventional imaging (combination of CT and bone scan) for the evaluation of pelvic nodal and distant metastatic disease.[37] Patients were included in the study if they had untreated, biopsy-proven PCa; were being considered for curative-intent treatment; and had ≥1 high-risk criterion (PSA ≥20 ng/mL, International Society of Uropathology grade group 3–5, or clinical stage ≥T3). In these patients, Ga-68 PSMA-11 PET/CT demonstrated a 27% (95% confidence interval [CI], 23%–31%; $p < 0.0001$) absolute greater area under the curve (AUC) for accuracy than conventional imaging (92% vs. 65%, respectively). Conventional imaging, when compared with Ga-68 PSMA-11 PET/CT, had lower sensitivity (38% vs. 85%) and specificity (91% vs. 98%).

In another multicenter trial evaluating 764 patients, Ga-68 PSMA-11 PET/CT or PET/MRI was assessed for its accuracy in detecting pelvic nodal metastases compared with histopathology at the time of RP and pelvic lymph node dissection.[63] Patients were included if they had histopathology-proven PCa, were planning to undergo RP, and had intermediate- to high-risk disease (PSA level >10 ng/mL, T-state ≥T2b, Gleason score >6, or other risk factors). The sensitivity and specificity of Ga-68 PSMA-11 PET for pelvic nodal metastases were 40% and 95%, respectively. The sensitivities from this study were lower than the 59% weighted sensitivity reported in a systematic review, although the sensitivities in the systematic review did range from 23% to 100%.[67] This large variance in sensitivity and specificity for Ga-68 PSMA-11 across studies is likely explained by differences in study design such as the reference standard used, whether data were collected prospectively or retrospectively, and whether patients were recruited consecutively or nonconsecutively.

Effect of Ga-68 PSMA-11 PET On the initial management of PCa

Six studies ($n = 493$) reported a change in clinical management with Ga-68 PSMA-11 PET in 19% to 52% of patients with primary PCa.[22,35,37,42,60,68] Hofman and colleagues[37] reported a significant change in treatment plan in 28% of patients undergoing Ga-68 PSMA-11 PET/CT compared with 15% of patients undergoing conventional imaging ($p = 0.0076$). Similarly, Wong and colleagues[68] evaluated the effect of Ga-68 PSMA-11 PET on disease staging in 131 patients with biopsy-proven PCa. Ga-68 PSMA-11 PET led to a change in PCa stage in 28% of patients, with disease being upstaged in 13% of patients and downstaged in 15% of patients ($p < 0.001$) when compared with the stage assigned using conventional imaging. These findings suggest that Ga-68 PSMA-11 has the potential to provide more accurate staging for metastatic disease, thereby allowing for more risk-appropriate management through the selection of local vs systemic management. Patients may, therefore, receive more appropriate treatment, although the effects of these changes on cancer-specific and overall survival are yet to be determined.

Detection of BCR

Table 2 summarizes studies that evaluated Ga-68 PSMA-11 PET to assess BCR. The majority of studies demonstrate a sensitivity ≥80% and a specificity ≥90%. Sensitivity values ranged from 64% to 99% for the prostate, 72% to 100% for the lymph nodes, and one study reported a sensitivity of 83% for bone metastases. Specificity values ranged from 31% to 100% for the prostate, 50% to 100% for the lymph nodes, and one study reported a specificity of 92% for bone metastases.[28,33,53,69-83] The large variance in sensitivity and specificity can be explained by varying factors across studies, such as areas examined (prostate vs lymph nodes) and the reference standard used (Table 2).

In comparison with conventional imaging, Ga-68 PSMA-11 PET/CT has higher sensitivity, specificity, and accuracy for detecting local recurrence and lymph node metastases, as well as higher detection rates in patients with low PSA levels (≤0.5 ng/mL). In a study of patients who had BCR after definitive PCa treatment with RP (n = 24), radiotherapy (n = 117), or combined treatment (n = 47), patients underwent Ga-68 PSMA-11 PET/CT for the detection of PCa recurrence, with either histologic examination of biopsy sections or 12 months of clinical and imaging follow-up used as the reference standard.[74] Ga-68 PSMA-11 PET/CT was found to have a sensitivity of 99% and a specificity of 100% for detecting PCa recurrence. Receiver operating characteristic analysis yielded an ideal PSA cutoff value of >0.65 ng/mL (AUC = 0.964; 95% CI, 0.736–1.000; $p < 0.0001$), which was associated with a sensitivity of 93% and a specificity of 100% for detecting PCa recurrence with Ga-68 PSMA-11 PET/CT. In patients with lower PSA values (0 to <0.5 ng/mL), the detection rate was 54.2%.

In a study evaluating 66 patients (median PSA 0.23 ng/mL), Ga-68 PSMA-11 PET/MRI was 55% effective in detecting BCR after RP at low PSA levels (≤0.5 ng/mL), including in patients who had previously undergone or were currently undergoing androgen deprivation therapy (ADT).[84] Subgroup analysis of patients with a very low (0 to 0.2 ng/mL) and low PSA (0.2 to 0.5 ng/mL) demonstrated detection rates of 39% and 65%, respectively. Ga-68 PSMA-11 PET/MRI also detected PSMA-positive lesions outside a standard radiotherapy target volume in 39% of patients.

Another study evaluated the accuracy of Ga-68 PSMA-11 PET in detecting lymph node metastases in 65 patients with BCR after RP who were scheduled to undergo salvage lymph node dissection.[69] The salvage lymph node dissection templates included lymph nodes from the right and left pelvis, presacral region, and retroperitoneal region. The median diameter of lymph nodes detected on Ga-68 PSMA-11 PET was 7.2 mm (IQR, 5.3–9 mm), whereas the median diameter of false-negative lymph nodes was 3.4 mm (IQR, 2.1–5.4 mm; $p = 0.01$). Diagnostic accuracy was 99% in the left pelvic region and 95% in the right pelvic, presacral, and retroperitoneal regions. Specificity values were >96% in all regions; sensitivity values were >90% in all but the retroperitoneal region (73%), perhaps because of less dissection of the retroperitoneum during salvage lymph node dissection.

In a study comparing the accuracy of Ga-68 PSMA-11 PET/CT with that of 18F-fluciclovine (a PET radiotracer) PET/CT in detecting BCR after RP in 50 patients, Ga-68 PSMA-11 had a significantly higher detection rate than 18F-fluciclovine (56% vs. 26%, respectively; $p = 0.0026$).[70] Detection rates were significantly higher for Ga-68 PSMA-11 compared with 18F-fluciclovine in the pelvic lymph nodes (30% vs. 8%, respectively; $p = 0.0034$) and in extrapelvic lesions (16% vs. 0%, respectively; $p = 0.0078$). Among the 15 patients in whom lesions were verified by histopathology/biopsy, both 18F-fluciclovine and Ga-68 PSMA-11 had PPVs of 100%. Another retrospective analysis of 37 patients with relapsed PCa showed a significantly higher lesion detection rate with Ga-68 PSMA-11 PET/CT versus standard 18F-fluoromethylcholine PET/CT, especially in patients with low PSA levels.[85]

Finally, in a pilot study of 14 patients with BCR after RP, 43% of the patients had positive PET scans, including 36% with positive Ga-68 PSMA-11 scans and 29% with positive 18F-PSMA-1007 scans.[86] No additional lesions were identified in the prostate fossa by 18F-PSMA-1007 in comparison to Ga-68 PSMA-11. In a study of 102 patients with BCR, 18F-PSMA-1007 was found to have a significantly higher incidence of PSMA-expressing lesions of benign origin than Ga-68 PSMA-11 (245 vs. 52, respectively).[87] Furthermore, the maximum standardized uptake value of these benign lesions was significantly higher ($p < 0.0001$) for 18F-PSMA-1007, indicating a potentially higher source of false positives with this agent than with Ga-68 PSMA-11.

Effect of Ga-68 PSMA-11 PET On the Management of BCR

Ten studies (n = 1697) reported a change in clinical management with Ga-68 PSMA-11 imaging in 16% to 75% of patients with BCR.[71,73,81,82,88-93] In a study of 294 patients, a change in clinical management occurred in 68% of patients, and Ga-68 PSMA-11 PET/CT affected this change in 86% of these patients.[73] Treatment modifications guided by Ga-68 PSMA-11 PET/CT were considered effective in 89% of patients; modifications not guided by Ga-68 PSMA-11 PET/CT were considered effective in 61% of patients ($p < 0.001$). Among patients with BCR following primary curative PCa treatment, delayed imaging with Ga-68 PSMA-11 PET/CT generally led to significantly better uptake and improved contrast, ultimately leading to a change in clinical management for 16% of patients.[91] Moreover, in a study of high-risk patients with PCa, primary staging with Ga-68 PSMA-11 PET/CT reduced BCR versus conventional imaging

techniques (HR = 0.58; p=0.004).[91] Another multicenter prospective trial from 15 countries in 1004 patients with PCa with BCR demonstrated that Ga-68 PSMA-11 PET/CT positivity correlated with Gleason score and PSA level at time of PET scan, PSA doubling time, and radiotherapy as primary treatment. Moreover, treatment modification occurred in 57% of PCa patients with BCR based on the outcomes of Ga-68 PSMA-11 PET/CT imaging.[88]

Safety Profile of Ga-68 PSMA-11

Ga-68 PSMA-11 is a well-tolerated imaging agent. Five studies (n = 880) reported on the safety of Ga-68 PSMA-11 and found no patients experienced serious adverse events, 18 patients reported experiencing mild adverse events (dizziness, nausea, constipation, diarrhea, headache), and one patient reported a fall after imaging that he attributed to furosemide injection, although there were no associated vital sign changes.[12,26,60,72,76] Hofman and colleagues[37] also reported a substantially lower radiation exposure with Ga-68 PSMA-11 PET/CT (8.4 mSv) compared with conventional imaging (combination of CT and bone scan) (19.2 mSv; $p < 0.001$).

Health Economics and Outcomes Research

The cost-effectiveness of Ga-68 PSMA-11 in comparison with conventional imaging has been examined by multiple groups showing that Ga-68 PSMA-11 reduced overall costs because of its increased accuracy in staging, which can obviate the need for unnecessary and costly therapies. In an exploratory analysis evaluating 30 patients over 10 years in Australia, a strategy using Ga-68 PSMA-11 PET/MRI had an average cost of $39,426 and produced an average of 7.48 years of survival, whereas a strategy involving conventional imaging (bone scan and MRI) had an average cost of $44,667 and produced an average of 7.41 years of survival.[94] When the duration of the model was reduced to 5 years, the use of Ga-68 PSMA-11 PET/MRI resulted in cost savings of $3,278 and 0.018 more life-years than conventional imaging. In a cost-effectiveness analysis of the proPSMA study, Ga-68 PSMA-11 PET/CT was found to have a lower estimated cost per scan than the combination of CT and bone scan ($886 vs $1040, respectively).[95] In an intention-to-treat analysis evaluating 83 patients with BCR after RP with or without previous radiotherapy, the percentage of patients receiving appropriate curative radiotherapy instead of palliative ADT was 100% with Ga-68 PSMA-11 PET/CT, 74% with C-11 choline PET/CT, and 33% with CT. A retrospective analysis of 244 patients undergoing PSMA PET/CT for recurrent PCa showed that imaging with Ga-68 PSMA-11 was cost-effective compared with 18F-PSMA-1007.[96] Outcomes research data are yet to be reported from studies in the United States.

18F-PSMA PET/CT

Although Ga-68 PSMA-11 is mainly used for PET imaging of PCa, other 18F ligands are increasingly becoming available. The US FDA recently approved another PSMA-targeted drug, piflufolastat F-18, for imaging of PCa.[97] Similar results were observed with the two agents in other studies in patients with recurrent PCa.[92,98,99] In a head-to-head comparison in 16 patients with intermediate/high-risk PCa, Ga-68 PSMA-11 and 18F-PSMA-1007 PET/CT showed similar performance in identifying dominant prostate lesions.[100] Another study comparing the 18F-PSMA-1007 PET/CT with Ga-68 PSMA-11 PET/CT in 40 treatment-naïve intermediate/high-risk PCa patients showed comparable detection of primary and metastatic lesions.[101]

However, defluorination of 18F radiotracers may influence the accuracy of lesion detection in bones due to unspecified bone uptake,[102] which can alter the choice of treatment and subsequently affect the quality of life of patients.[103] Several recent studies have highlighted that 18F radiotracers are likely to lead to misdiagnosis of bone lesions, with one study reporting nearly 6 times more unspecified bone uptake seen on 18F-PSMA-1007 than with Ga-68 PSMA-11 PET imaging.[87,96,104-109] A retrospective analysis of data from 10 patients with PCa who underwent PET-guided biopsy to confirm observations of indeterminate bone lesions on 18F-PSMA-1007 PET/CT imaging demonstrated that 91% (10/11) of the bone lesions were not metastatic and showed no signs of PSMA expression.[110]

Another study of 243 patients with high-risk or recurrent PCa reported 98 of 267 bone lesions (37%) in 48 (20%) patients with 18F-DCFPyL PET/CT imaging were indeterminate. Of these indeterminate bone lesions, 37 of 98 (38%) were confirmed benign, 42 of 98 (43%) were malignant, and 19 of 98 (19%) remained equivocal at the lesion level. At the patient level, 24 of 48 (50%) had a benign lesion, 11 of 48 (23%) had a malignant lesion, and 13 of 48 (27%) had equivocal findings.[103]

A retrospective matched-pair comparison of 18F-rhPSMA-7 with 68-Ga PSMA-11 PET/CT in patients with primary or recurrent PCa showed a higher incidence of benign tumors among PSMA-positive lesions reported with18F-rhPSMA-7 versus 68-Ga PSMA-11 (67% [379/566] vs 35% [100/289]).[111]

In addition, a study of 283 patients who had 68-Ga PSMA-11 PET and 409 patients who had 18F-PSMA-1007 PET due to BCR showed that 18F-PSMA-1007 PET resulted in a significantly higher rate of nonspecific bone uptake compared with 68-Ga PSMA-11 PET ($p < 0.001$); however, the rate of bone metastases was not significantly different.[109]

The updated joint European Association of Nuclear Medicine (EANM) and Society of Nuclear Medicine and Molecular Imaging

Table 3. Key Ga-68 PSMA-11 imaging guidelines and recommendations*

GUIDELINE	RECOMMENDATION
NCCN Guidelines Version 1.2023[114]	Conventional imaging is no longer a necessary prerequisite to PSMA PET for primary staging or BCR. PSMA PET/CT or PSMA PET/MRI can serve as an equally effective, if not more effective, front-line imaging tool.
SNMMI, ACNM, ACP, ASCO, AUA, ANZSM, EANM Appropriate Use Criteria[115]	**Primary staging:** - Patients with suspected PCa (eg high/increasing PSA levels, abnormal digital rectal examination results): to evaluate for targeted biopsy and detection of intraprostatic tumor (Score 3: PSMA use is rarely appropriate) - Patients with very low, low, and favorable intermediate-risk PCa (Score 2: PSMA use is rarely appropriate) - Newly diagnosed unfavorable intermediate, high-risk, or very high-risk PCa (Score 8: PSMA use is appropriate) - Newly diagnosed unfavorable intermediate, high-risk, or very high-risk PCa with negative/equivocal or oligometastatic disease on conventional imaging (Score 8: PSMA use is appropriate) - Newly diagnosed PCa with widespread metastatic disease on conventional imaging (Score 4: PSMA use may be appropriate) **BCR:** - PSA level persistence or PSA increase from undetectable level after RP (Score 9: PSMA use is appropriate) - PSA increase above nadir after definitive radiotherapy (Score 9: PSMA use is appropriate) - PSA increase after focal therapy of the primary tumor (Score 5: PSMA use may be appropriate)
EANM Standardized Reporting Guidelines v1.0 for PSMA PET[116]	Primary staging: PSMA PET is a suitable replacement for conventional imaging in patients with high risk of nodal involvement; patients at lower risk should be spared by PSMA PET BCR: Perform PSMA PET in any case of proven BCR
Joint EANM and SNMMI Procedure Guideline for Prostate Cancer Imaging: version 1.0[123]	Primary staging: In patients with high-risk disease (Gleason score >7, PSA level >20 ng/mL, clinical stage T2c–3a), Ga-68 PSMA PET/CT can replace abdominopelvic CT for detection of lymph node metastases for local tumor delineation, pelvic MRI cannot be replaced BCR: Ga-68 PSMA PET/CT use is recommended for patients with low PSA level (0.2–10 ng/mL) to identify the site of recurrence and potentially guide salvage therapy
Joint EANM and SNMMI Procedure Guideline for Prostate Cancer Imaging: version 2.0[112]	PSMA-ligand PET should be combined with multiparametric MRI for biopsy guidance

*Note that this table is not comprehensive of all available guidelines.
Abbreviations: ACNM, American College of Nuclear Medicine; ACP, American College of Physicians; ASCO, American Society of Clinical Oncology; AUA, American Urological Association; ANZSM, Australia and New Zealand Society of Nuclear Medicine; BCR, biochemical recurrence; CT, computed tomography; EANM, European Association of Nuclear Medicine; MRI, magnetic resonance imaging; NCCN, National Comprehensive Cancer Network; PCa, prostate cancer; PET, positron emission tomography; PSA, prostate-specific antigen; PSMA, prostate-specific membrane antigen; RP, radical prostatectomy; SNMMI, Society of Nuclear Medicine and Molecular Imaging.

(SNMMI) procedure guidelines for PCa imaging also note non-specific bone uptake with 18F-rhPSMA-7.3.[112] 18F PET imaging may also lead to higher interobserver variability, as demonstrated by a retrospective study of 584 patients with newly diagnosed PCa. Significantly increased interobserver variability was observed with 18F-PSMA-1007 for bone metastases versus 18F-DCFPyL and Ga-68 PSMA-11 ($p = 0.001$ and $p = 0.03$, respectively), and for overall agreement and locoregional lymph node metastases versus 18F-DCFPyL ($p < 0.001$ and $p = 0.01$, respectively).[113]

Guidelines for PSMA imaging

The updated National Comprehensive Cancer Network guidelines now include guidance regarding the use of Ga-68 PSMA-11.[114] The guidelines state that, because of the increased sensitivity and specificity of PSMA PET tracers for detecting micrometastatic disease at initial staging and in cases of BCR, conventional imaging is no longer considered a necessary prerequisite to PSMA PET, and PSMA PET/CT or PSMA PET/MRI can serve as an equally effective or more effective first-line imaging tool for these patients.[114] The updated joint EANM and SNMMI procedure guidelines for PCa imaging also include the use of Ga-68 PSMA-11 PET/CT and recommend combining PSMA-PET/CT with multiparametric MRI for guiding biopsy for confirmation of PCa.[112] Recently,the Society of Nuclear Medicine and Molecular Imaging, American College of Nuclear Medicine, American Urological Association, Australia and New Zealand Society of Nuclear Medicine, American Society of Clinical Oncology, EANM, and the American College of Physicians worked collaboratively to develop appropriate use criteria for PSMA PET imaging (Table 3).[115] In addition, the EANM criteria, PROMISE criteria, and PSMA-RADS have also been published to streamline the interpretation of PSMA PET imaging.[116]

Discussion

Ga-68 PSMA-11 PET/CT is effective in the initial staging and detection of PCa BCR and has advantages over MRI in the initial local staging of PCa, mainly detection of extraprostatic disease in initial staging and BCR and at low PSA levels (≤0.5 ng/mL); potential for leading to a change in radiotherapy target planning[84]; and cost-effectiveness while reducing the amount of radiation exposure to the patient.[94] Bone lesions are easier to interpret on Ga-68 PSMA-11 compared to 18F-based radiotracer imaging.[87,104,111,112] Ga-68

PSMA-11 is well tolerated, further supporting its potential as the imaging agent of choice in PCa.

Ga-68 PSMA-11 has also been used for confirming primary or recurrent PCa in several studies, demonstrating its diagnostic value in clinical practice. Ga-68 PSMA-11 PET/CT was used in combination with MRI to triage patients for biopsy during initial diagnosis and improved NPV for ruling out clinically significant PCa, thereby reducing the number of unnecessary biopsies.[117] In addition, Ga-68 PSMA-11 PET/CT was useful for guiding metastasis-directed radiotherapy in patients with oligometastatic PCa recurrence, delaying the need for ADT and potentially prolonging BCR-free survival.[118]

In a study of patients with metastatic castration-resistant PCa, Ga-68 PSMA-11 PET provided reliable parameters that could be used to predict response to systemic therapies.[119] 68-Ga PSMA-11 was also used for confirmation of metastatic castration-resistant PCa and identification of appropriate patients for PSMA-based radioligand therapy in the phase 3 VISION trial,[120] and is approved in the US for patient selection for PSMA-directed radioligand therapy. Finally, Ga-68 PSMA-11 PET/CT may also be useful in determining appropriate candidates for RP, as the technique has high PPV and specificity for identifying lymph node metastases and local recurrence.[121]

The main limitation of this review is the heterogeneity of the included studies (varying sample sizes, patients being grouped by differing PSA ranges). Variations in reported diagnostic accuracy parameters were seen as anticipated given differences in patient characteristics (eg, PSA, lesion sizes) and study designs. Also, additional studies are needed to determine the effects of Ga-68 PSMA-11 on cost.

In summary, Ga-68 PSMA-11 PET has a favorable safety profile that affords high accuracy for PCa initial staging and the detection of PCa BCR. Although more studies are needed, its use frequently leads to changes in treatment that may positively affect patient outcomes. With increased access, the use of Ga-68 PSMA-11 is expected to expand and include additional applications.

References

1) Sung H, Ferlay J, RL Siegel, et al. Global cancer statistics 2020: GLOBOCAN estimates of incidence and mortality worldwide for 36 cancers in 185 countries. CA Cancer J Clin. 2021;71(3):209-249.

2) Siegel RL, KD Miller, NS Wagle, et al. Cancer statistics, 2023. CA Cancer J Clin. 2023;73(1):17-48.

3) Siegel DA, ME O'Neil, TB Richards, et al. Prostate cancer incidence and survival, by stage and race/ethnicity - United States, 2001-2017. MMWR Morb Mortal Wkly Rep. 2020;69(41):1473-1480.

4) Lowrance WT, RH Breau, R Chou, et al. Advanced Prostate Cancer: AUA/ASTRO/SUO Guideline PART I. J Urol. 2021;205(1):14-21.

5) Atan A and Ö Güzel, How should prostate specific antigen be interpreted? Turk J Urol. 2013;39(3):188-93.

6) Venkatesan AM, E Mudairu-Dawodu, C Duran, et al. Detecting recurrent prostate Cancer using multiparametric MRI, influence of PSA and Gleason grade. Cancer Imaging. 2021;21(1):3.

7) Dess RT, TM Morgan, PL Nguyen, et al. Adjuvant Versus Early Salvage Radiation Therapy Following Radical Prostatectomy for Men with Localized Prostate Cancer. Curr Urol Rep. 2017;18(7):55.

8) Barakzai MA, Prostatic Adenocarcinoma: A Grading from Gleason to the New Grade-Group System: A Historical and Critical Review. Asian Pac J Cancer Prev. 2019;20(3):661-666.

9) Borley N and MR Feneley, Prostate cancer: diagnosis and staging. Asian J Androl. 2009;11(1):74-80.

10) Spratt DE, DJ McHugh, MJ Morris, et al. Management of Biochemically Recurrent Prostate Cancer: Ensuring the Right Treatment of the Right Patient at the Right Time. Am Soc Clin Oncol Educ Book. 2018;38:355-362.

11) Broderick JM, NCCN Guidelines add PSMA-PET imaging modalities for prostate cancer. Urology Times. 2021.

12) Hicks RM, JP Simko, AC Westphalen, et al. Diagnostic Accuracy of (68)Ga-PSMA-11 PET/MRI Compared with Multiparametric MRI in the Detection of Prostate Cancer. Radiology. 2018;289(3):730-737.

13) Banerjee SR and MG Pomper, Clinical applications of Gallium-68. Appl Radiat Isot. 2013;76:2-13.

14) Carlucci G, R Ippisch, R Slavik, et al. (68) Ga-PSMA-11 NDA Approval: A Novel and Successful Academic Partnership. J Nucl Med. 2021;62(2):149-155.

15) Telix Pharmaceuticals Limited, FDA Approves Telix's Prostate Cancer Imaging Product, Illuccix®. 2021, Telix Pharmaceuticals Limited: Melbourne, AustraliaIndianapolis, IN.

16) Sonni I, M Eiber, WP Fendler, et al. Impact of (68)Ga-PSMA-11 PET/CT on Staging and Management of Prostate Cancer Patients in Various Clinical Settings: A Prospective Single-Center Study. J Nucl Med. 2020;61(8):1153-1160.

17) Al-Bayati M, J Grueneisen, S Lütje, et al. Integrated 68Gallium Labelled Prostate-Specific Membrane Antigen-11 Positron Emission Tomography/Magnetic Resonance Imaging Enhances Discriminatory Power of Multi-Parametric Prostate Magnetic Resonance Imaging. Urol Int. 2018;100(2):164-171.

18) Basha MAA, MAG Hamed, O Hussein, et al. (68)Ga-PSMA-11 PET/CT in newly diagnosed prostate cancer: diagnostic sensitivity and interobserver agreement. Abdom Radiol (NY). 2019;44(7):2545-2556.

19) Berger I, C Annabattula, J Lewis, et al. (68) Ga-PSMA PET/CT vs. mpMRI for locoregional prostate cancer staging: correlation with final histopathology. Prostate Cancer Prostatic Dis. 2018;21(2):204-211.

20) Budäus L, SR Leyh-Bannurah, G Salomon, et al. Initial Experience of (68)Ga-PSMA PET/CT Imaging in High-risk Prostate Cancer Patients Prior to Radical Prostatectomy. Eur Urol. 2016;69(3):393-6.

21) Chen M, X Qiu, Q Zhang, et al. PSMA uptake on [68Ga]-PSMA-11-PET/CT positively correlates with prostate cancer aggressiveness. Q J Nucl Med Mol Imaging. 2022;66(1):67-73.

22) Chen M, Q Zhang, C Zhang, et al. Comparison of (68)Ga-prostate-specific membrane antigen (PSMA) positron emission tomography/computed tomography (PET/CT) and multi-parametric magnetic resonance imaging (MRI) in the evaluation of tumor extension of primary prostate cancer. Transl Androl Urol. 2020;9(2):382-390.

23) Demirci E, L Kabasakal, OE Şahin, et al. Can SUVmax values of Ga-68-PSMA PET/CT scan predict the clinically significant prostate cancer? Nucl Med Commun. 2019;40(1):86-91.

24) Donato P, A Morton, J Yaxley, et al. (68) Ga-PSMA PET/CT better characterises localised prostate cancer after MRI and transperineal prostate biopsy: Is (68)Ga-PSMA PET/CT guided biopsy the future? Eur J Nucl Med Mol Imaging. 2020;47(8):1843-1851.

25) Donato P, MJ Roberts, A Morton, et al. Improved specificity with (68)Ga PSMA PET/CT to detect clinically significant lesions "invisible" on multiparametric MRI of the prostate: a single institution comparative analysis with radical prostatectomy histology. Eur J Nucl Med Mol Imaging. 2019;46(1):20-30.

26) El Hajj A, B Yacoub, M Mansour, et al. Diagnostic performance of Gallium-68 prostate-specific membrane antigen positron emission tomography-computed tomography in intermediate and high risk prostate cancer. Medicine (Baltimore). 2019;98(44):e17491.

27) Fendler WP, DF Schmidt, V Wenter, et al. 68Ga-PSMA PET/CT Detects the Location and Extent of Primary Prostate Cancer. J Nucl Med. 2016;57(11):1720-1725.

28) 2Fendler WP, J Calais, M Allen-Auerbach, et al. (68)Ga-PSMA-11 PET/CT Interobserver Agreement for Prostate Cancer Assessments: An International Multicenter Prospective Study. J Nucl Med. 2017;58(10):1617-1623.

29) Ferraro DA, UJ Muehlematter, HI Garcia Schüler, et al. (68)Ga-PSMA-11 PET has the potential to improve patient selection for extended pelvic lymph node dissection in intermediate to high-risk prostate cancer. Eur J Nucl Med Mol Imaging. 2020;47(1):147-159.

30) Gao J, C Zhang, Q Zhang, et al. Diagnostic performance of (68)Ga-PSMA PET/CT for identification of aggressive cribriform morphology in prostate cancer with whole-mount sections. Eur J Nucl Med Mol Imaging. 2019;46(7):1531-1541.

31) Gupta M, PS Choudhury, D Hazarika, et al. A Comparative Study of (68)Gallium-Prostate Specific Membrane Antigen Positron Emission Tomography-Computed Tomography and Magnetic Resonance Imaging for Lymph Node Staging in High Risk Prostate Cancer Patients: An Initial Experience. World J Nucl Med. 2017;16(3):186-191.

32) Gupta M, PS Choudhury, S Rawal, et al. Initial risk stratification and staging in prostate cancer with prostatic-specific membrane antigen positron emission tomography/computed tomography: A first-stop-shop. World J Nucl Med. 2018;17(4):261-269.

33) Herlemann A, V Wenter, A Kretschmer, et al. (68)Ga-PSMA Positron Emission Tomography/Computed Tomography Provides Accurate Staging of Lymph Node Regions Prior to Lymph Node Dissection in Patients with Prostate Cancer. Eur Urol. 2016;70(4):553-557.

34) Hinsenveld FJ, EMK Wit, PJ van Leeuwen, et al. Prostate-Specific Membrane Antigen PET/CT Combined with Sentinel Node Biopsy for Primary Lymph Node Staging in Prostate Cancer. J Nucl Med. 2020;61(4):540-545.

35) Hirmas N, A Al-Ibraheem, K Herrmann, et al. [(68)Ga]PSMA PET/CT Improves Initial Staging and Management Plan of Patients with High-Risk Prostate Cancer. Mol Imaging Biol. 2019;21(3):574-581.

36) 3Hoffmann MA, M Miederer, HJ Wieler, et al. Diagnostic performance of (68)Gallium-PSMA-11 PET/CT to detect significant prostate cancer and comparison with (18)FEC PET/CT. Oncotarget. 2017;8(67):111073-111083.

37) 3Hofman MS, N Lawrentschuk, RJ Francis, et al. Prostate-specific membrane antigen PET-CT in patients with high-risk prostate cancer before curative-intent surgery or radiotherapy (proPSMA): a prospective, randomised, multicentre study. Lancet. 2020;395(10231):1208-1216.

38) Jena A, R Taneja, S Taneja, et al. Improving Diagnosis of Primary Prostate Cancer With Combined (68)Ga-Prostate-Specific Membrane Antigen-HBED-CC Simultaneous PET and Multiparametric MRI and Clinical Parameters. AJR Am J Roentgenol. 2018;211(6):1246-1253.

39) 3Kalapara AA, T Nzenza, HYC Pan, et al. Detection and localisation of primary prostate cancer using (68) gallium prostate-specific membrane antigen positron emission tomography/computed tomography compared with multiparametric magnetic resonance imaging and radical prostatectomy specimen pathology. BJU Int. 2020;126(1):83-90.

40) Kopp J, D Kopp, E Bernhardt, et al. (68) Ga-PSMA PET/CT based primary staging and histological correlation after extended pelvic lymph node dissection at radical prostatectomy. World J Urol. 2020;38(12):3085-3090.

41) Liu C, T Liu, Z Zhang, et al. (68)Ga-PSMA PET/CT Combined with PET/Ultrasound-Guided Prostate Biopsy Can Diagnose Clinically Significant Prostate Cancer in Men with Previous Negative Biopsy Results. J Nucl Med. 2020;61(9):1314-1319.

42) Lopci E, G Lughezzani, A Castello, et al. Prospective Evaluation of (68)Ga-labeled Prostate-specific Membrane Antigen Ligand Positron Emission Tomography/Computed Tomography in Primary Prostate Cancer Diagnosis. Eur Urol Focus. 2021;7(4):764-771.

43) Lopci E, A Saita, M Lazzeri, et al. (68)Ga-PSMA Positron Emission Tomography/Computerized Tomography for Primary Diagnosis of Prostate Cancer in Men with Contraindications to or Negative Multiparametric Magnetic Resonance Imaging: A Prospective Observational Study. J Urol. 2018;200(1):95-103.

44) Maurer T, JE Gschwend, I Rauscher, et al. Diagnostic Efficacy of (68)Gallium-PSMA Positron Emission Tomography Compared to Conventional Imaging for Lymph Node Staging of 130 Consecutive Patients with Intermediate to High Risk Prostate Cancer. J Urol. 2016;195(5):1436-1443.

45) Muehlematter UJ, IA Burger, AS Becker, et al. Diagnostic Accuracy of Multiparametric MRI versus (68)Ga-PSMA-11 PET/MRI for Extracapsular Extension and Seminal Vesicle Invasion in Patients with Prostate Cancer. Radiology. 2019;293(2):350-358.

46) Nandurkar R, P van Leeuwen, P Stricker, et al. (68)Ga-HBEDD PSMA-11 PET/CT staging prior to radical prostatectomy in prostate cancer patients: Diagnostic and predictive value for the biochemical response to surgery. Br J Radiol. 2019;92(1095):20180667.

47) Öbek C, T Doğanca, E Demirci, et al. The accuracy of (68)Ga-PSMA PET/CT in primary lymph node staging in high-risk prostate cancer. Eur J Nucl Med Mol Imaging. 2017;44(11):1806-1812.

48) Pallavi UN, S Gogoi, P Thakral, et al. Incremental value of Ga-68 prostate-specific membrane antigen-11 positron-emission tomography/computed tomography scan for preoperative risk stratification of prostate cancer. Indian J Nucl Med. 2020;35(2):93-99.

49) Park SY, C Zacharias, C Harrison, et al. Gallium 68 PSMA-11 PET/MR Imaging in Patients with Intermediate- or High-Risk Prostate Cancer. Radiology. 2018;288(2):495-505.

50) Petersen LJ, JB Nielsen, NC Langkilde, et al. (68)Ga-PSMA PET/CT compared with MRI/CT and diffusion-weighted MRI for primary lymph node staging prior to definitive radiotherapy in prostate cancer: a prospective diagnostic test accuracy study. World J Urol. 2020;38(4):939-948.

51) Rahbar K, M Weckesser, S Huss, et al. Correlation of Intraprostatic Tumor Extent with ^{68}Ga-PSMA Distribution in Patients with Prostate Cancer. J Nucl Med. 2016;57(4):563-7.

52) Rahman LA, D Rutagengwa, P Lin, et al. High negative predictive value of 68Ga PSMA PET-CT for local lymph node metastases in high risk primary prostate cancer with histopathological correlation. Cancer Imaging. 2019;19(1):86.

53) Sahlmann CO, B Meller, C Bouter, et al. Biphasic ^{68}Ga-PSMA-HBED-CC-PET/CT in patients with recurrent and high-risk prostate carcinoma. Eur J Nucl Med Mol Imaging. 2016;43(5):898-905.

54) Thalgott M, C Düwel, I Rauscher, et al. One-stop-shop whole-body (68)Ga-PSMA-11 PET/MRI compared with clinical nomograms for preoperative T and n staging of high-risk prostate cancer. J Nucl Med. 2018;59(12):1850-1856.

55) 5\Tulsyan S, CJ Das, M Tripathi, et al. Comparison of 68Ga-PSMA PET/CT and multiparametric MRI for staging of high-risk prostate cancer68Ga-PSMA PET and MRI in prostate cancer. Nucl Med Commun. 2017;38(12):1094-1102.

56) \van Leeuwen PJ, L Emmett, B Ho, et al. Prospective evaluation of 68Gallium-prostate-specific membrane antigen positron emission tomography/computed tomography for preoperative lymph node staging in prostate cancer. BJU Int. 2017;119(2):209-215.

57) \van Leeuwen PJ, M Donswijk, R Nandurkar, et al. Gallium-68-prostate-specific membrane antigen ((68) Ga-PSMA) positron emission tomography (PET)/computed tomography (CT) predicts complete biochemical response from radical prostatectomy and lymph node dissection in intermediate- and high-risk prostate cancer. BJU Int. 2019;124(1):62-68.

58) \von Klot CJ, AS Merseburger, A Böker, et al. (68)Ga-PSMA PET/CT imaging predicting intraprostatic tumor extent, extracapsular extension and seminal vesicle invasion prior to radical prostatectomy in patients with prostate cancer. Nucl Med Mol Imaging. 2017;51(4):314-322.

59) Yilmaz B, R Turkay, Y Colakoglu, et al. Comparison of preoperative locoregional Ga-68 PSMA-11 PET-CT and mp-MRI results with postoperative histopathology of prostate cancer. Prostate. 2019;79(9):1007-1017.

60) Zang S, G Shao, C Cui, et al. 68Ga-PSMA-11 PET/CT for prostate cancer staging and risk stratification in Chinese patients. Oncotarget. 2017;8(7):12247-12258.

61) Zhang Q, S Zang, C Zhang, et al. Comparison of (68)Ga-PSMA-11 PET-CT with mpMRI for preoperative lymph node staging in patients with intermediate to high-risk prostate cancer. J Transl Med. 2017;15(1):230.

62) Zhang J, S Shao, P Wu, et al. Diagnostic performance of (68)Ga-PSMA PET/CT in the detection of prostate cancer prior to initial biopsy: comparison with cancer-predicting nomograms. Eur J Nucl Med Mol Imaging. 2019;46(4):908-920.

63) Hope TA, M Eiber, WR Armstrong, et al. Diagnostic accuracy of 68Ga-PSMA-11 pet for pelvic nodal metastasis detection prior to radical prostatectomy and pelvic lymph node dissection: A multicenter prospective phase 3 imaging trial. JAMA Oncol. 2021;7(11):1635-1642.

64) Yaxley JW, S Raveenthiran, FX Nouhaud, et al. Outcomes of primary lymph node staging of intermediate and high risk prostate cancer with (68)Ga-PSMA positron emission tomography/computerized tomography compared to histological correlation of pelvic lymph node pathology. J Urol. 2019;201(4):815-820.

65) Klingenberg S, J Fredsøe, KD Sørensen, et al. Recurrence rate after radical prostatectomy following primary staging of high-risk prostate cancer with (68)Ga-PSMA PET/CT. Acta Oncol. 2022;61(10):1289-1294.

66) Zou S, S Song, J Zhou, et al. Time point-independent tumor positivity of (68)Ga-PSMA-PET/CT pre- and post-biopsy in high-risk prostate cancer. Ann Nucl Med. 2022;36(6):523-532.

67) Petersen LJ and HD Zacho, PSMA PET for primary lymph node staging of intermediate and high-risk prostate cancer: an expedited systematic review. Cancer Imaging. 2020;20(1):10.

68) Wong HS, J Leung, D Bartholomeusz, et al. Comparative study between (68) Ga-prostate-specific membrane antigen positron emission tomography and conventional imaging in the initial staging of prostate cancer. J Med Imaging Radiat Oncol. 2018;62(6):816-822.

69) Abufaraj M, B Grubmüller, M Zeitlinger, et al. Prospective evaluation of the performance of [(68)Ga]Ga-PSMA-11 PET/CT(MRI) for lymph node staging in patients undergoing superextended salvage lymph node dissection after radical prostatectomy. Eur J Nucl Med Mol Imaging. 2019;46(10):2169-2177.

70) Calais J, F Ceci, M Eiber, et al. (18)F-fluciclovine PET-CT and (68)Ga-PSMA-11 PET-CT in patients with early biochemical recurrence after prostatectomy: a prospective, single-centre, single-arm, comparative imaging trial. Lancet Oncol. 2019;20(9):1286-1294.

71) Emmett L, U Metser, G Bauman, et al. Prospective, multisite, international comparison of (18)F-Fluoromethylcholine PET/CT, multiparametric MRI, and (68)Ga-HBED-CC PSMA-11 PET/CT in men with high-risk features and biochemical failure after radical prostatectomy: Clinical performance and patient outcomes. J Nucl Med. 2019;60(6):794-800.

72) Fendler WP, J Calais, M Eiber, et al. Assessment of 68Ga-PSMA-11 PET accuracy in localizing recurrent prostate cancer: A prospective single-arm clinical trial. JAMA Oncol. 2019;5(6):856-863.

73) Fourquet A, L Lahmi, T Rusu, et al. Restaging the biochemical recurrence of prostate cancer with [(68)Ga]Ga-PSMA-11 PET/CT: Diagnostic performance and impact on patient disease management. Cancers (Basel). 2021;13(7).

74) Hamed MAG, MAA Basha, H Ahmed, et al. (68)Ga-PSMA PET/CT in patients with rising prostatic-specific antigen after definitive treatment of prostate cancer: Detection efficacy and diagnostic accuracy. Acad Radiol. 2019;26(4):450-460.

75) Jilg CA, V Drendel, HC Rischke, et al. Diagnostic Accuracy of Ga-68-HBED-CC-PSMA-Ligand-PET/CT before Salvage Lymph Node Dissection for Recurrent Prostate Cancer. Theranostics. 2017;7(6):1770-1780.

76) Lawhn-Heath C, RR Flavell, SC Behr, et al. Single-center prospective evaluation of (68) Ga-PSMA-11 PET in biochemical recurrence of prostate cancer. AJR Am J Roentgenol. 2019;213(2):266-274.

77) Mandel P, D Tilki, FK Chun, et al. Accuracy of (68)ga-prostate-specific membrane antigen positron emission tomography for the detection of lymph node metastases before salvage lymphadenectomy. Eur Urol Focus. 2020;6(1):71-73.

78) Pfister D, D Porres, A Heidenreich, et al. Detection of recurrent prostate cancer lesions before salvage lymphadenectomy is more accurate with (68)Ga-PSMA-HBED-CC than with (18)F-Fluoroethylcholine PET/CT. Eur J Nucl Med Mol Imaging. 2016;43(8):1410-7.

79) Radzina M, M Tirane, L Roznere, et al. Accuracy of (68)Ga-PSMA-11 PET/CT and multiparametric MRI for the detection of local tumor and lymph node metastases in early biochemical recurrence of prostate cancer. Am J Nucl Med Mol Imaging. 2020;10(2):106-118.

80) Rauscher I, T Maurer, AJ Beer, et al. Value of 68Ga-PSMA HBED-CC PET for the Assessment of Lymph Node Metastases in Prostate Cancer Patients with Biochemical Recurrence: Comparison with Histopathology After Salvage Lymphadenectomy. J Nucl Med. 2016;57(11):1713-1719.

81) Zacho HD, JB Nielsen, K Dettmann, et al. 68Ga-PSMA PET/CT in patients with biochemical recurrence of prostate cancer: A prospective, 2-center study. Clin Nucl Med. 2018;43(8):579-585.

82) Grubmüller B, P Baltzer, D D'Andrea, et al. (68)Ga-PSMA 11 ligand PET imaging in patients with biochemical recurrence after radical prostatectomy - diagnostic performance and impact on therapeutic decision-making. Eur J Nucl Med Mol Imaging. 2018;45(2):235-242.

83) Afshar-Oromieh A, E Avtzi, FL Giesel, et al. The diagnostic value of PET/CT imaging with the (68)Ga-labelled PSMA ligand HBED-CC in the diagnosis of recurrent prostate cancer. Eur J Nucl Med Mol Imaging. 2015;42(2):197-209.

84) Kranzbühler B, J Müller, AS Becker, et al. Detection Rate and Localization of Prostate Cancer Recurrence Using (68)Ga-PSMA-11 PET/MRI in Patients with Low PSA Values ≤ 0.5 ng/mL J Nucl Med. 2020;61(2):194-201.

85) Afshar-Oromieh A, CM Zechmann, A Malcher, et al. Comparison of PET imaging with a (68)Ga-labelled PSMA ligand and (18) F-choline-based PET/CT for the diagnosis of recurrent prostate cancer. Eur J Nucl Med Mol Imaging. 2014;41(1):11-20.

86) Sheehan-Dare G, J Ende, A Amin, et al. Pilot trial comparing the performance of 68Ga-PSMA-11 PET/CT to 18F-PSMA-1007 PET/CT in the detection of prostate cancer recurrence in men with rising PSA following radical prostatectomy. Journal of Nuclear Medicine. 2021;62(supplement 1):1323-1323.

87) Rauscher I, M Krönke, M König, et al. Matched-Pair Comparison of (68)Ga-PSMA-11 PET/CT and (18)F-PSMA-1007 PET/CT: Frequency of Pitfalls and Detection Efficacy in Biochemical Recurrence After Radical Prostatectomy. J Nucl Med. 2020;61(1):51-57.

88) Cerci JJ, S Fanti, EE Lobato, et al. Diagnostic performance and clinical impact of (68)Ga-PSMA-11 PET/CT imaging in early relapsed prostate cancer after radical therapy: A prospective multicenter study (IAEA-PSMA Study). J Nucl Med. 2022;63(2):240-247.

89) Deandreis D, A Guarneri, F Ceci, et al. (68)Ga-PSMA-11 PET/CT in recurrent hormone-sensitive prostate cancer (HSPC): a prospective single-centre study in patients eligible for salvage therapy. Eur J Nucl Med Mol Imaging. 2020;47(12):2804-2815.

90) Farolfi A, F Ceci, P Castellucci, et al. (68) Ga-PSMA-11 PET/CT in prostate cancer patients with biochemical recurrence after radical prostatectomy and PSA <0.5 ng/ml. Efficacy and impact on treatment strategy. Eur J Nucl Med Mol Imaging. 2019;46(1):11-19.

91) Kunikowska J, K Pełka, O Tayara, et al. Ga-68-PSMA-11 PET/CT in patients with biochemical recurrence of prostate cancer after primary treatment with curative intent-impact of delayed imaging. J Clin Med. 2022;11(12).

92) Morigi JJ, PD Stricker, PJ van Leeuwen, et al. Prospective comparison of 18F-fluoromethylcholine Versus 68Ga-PSMA PET/CT in prostate cancer patients who have rising PSA after curative treatment and are being considered for targeted therapy. J Nucl Med. 2015;56(8):1185-90.

93) Rousseau C, M Le Thiec, L Ferrer, et al. Preliminary results of a (68) Ga-PSMA PET/CT prospective study in prostate cancer patients with occult recurrence: Diagnostic performance and impact on therapeutic decision-making. Prostate. 2019;79(13):1514-1522.

94) Gordon LG, TM Elliott, A Joshi, et al. Exploratory cost-effectiveness analysis of (68) Gallium-PSMA PET/MRI-based imaging in patients with biochemical recurrence of prostate cancer. Clin Exp Metastasis. 2020;37(2):305-312.

95) de Feria Cardet RE, MS Hofman, T Segard, et al. Is prostate-specific membrane antigen positron emission tomography/computed tomography imaging cost-effective in prostate cancer: An analysis informed by the proPSMA trial. Eur Urol. 2021;79(3):413-418.

96) Alberts I, C Mingels, HD Zacho, et al. Comparing the clinical performance and cost efficacy of [68Ga]Ga-PSMA-11 and [18}F]PSMA-1007 in the diagnosis of recurrent prostate cancer: a Markov chain decision analysis. Eur J Nucl Med Mol Imaging. 2022;49(12):4252-4261.

97) Keam SJ, Piflufolastat F 18: Diagnostic first approval. Mol Diagn Ther. 2021;25(5):647-656.

98) Paymani Z, T Rohringer, R Vali, et al. Diagnostic performance of [(18)F]fluorocholine and [(68)Ga]Ga-PSMA PET/CT in prostate cancer: A comparative study. J Clin Med. 2020;9(7).

99) Calais J, WP Fendler, K Herrmann, et al. Comparison of (68)Ga-PSMA-11 and (18)F-Fluciclovine PET/CT in a case series of 10 patients with prostate cancer recurrence. J Nucl Med. 2018;59(5):789-794.

100) Kuten J, I Fahoum, Z Savin, et al. Head-to-head comparison of (68)Ga-PSMA-11 with (18)F-PSMA-1007 PET/CT in staging prostate cancer using histopathology and immunohistochemical analysis as a reference standard. J Nucl Med. 2020;61(4):527-532.

101) Chandekar KR, H Singh, R Kumar, et al. Comparison of 18 F-PSMA-1007 PET/CT With 68 Ga-PSMA-11 PET/CT for Initial Staging in Intermediate- and High-Risk Prostate Cancer. Clin Nucl Med. 2023;48(1):e1-e8.

102) Lütje S, GM Franssen, K Herrmann, et al. In vitro and in vivo characterization of an (18)F-AlF-labeled PSMA ligand for imaging of PSMA-expressing xenografts. J Nucl Med. 2019;60(7):1017-1022.

103) Phelps TE, SA Harmon, E Mena, et al. Predicting Outcomes of Indeterminate Bone Lesions on (18)F-DCFPyL PSMA PET/CT Scans in the Setting of High-Risk Primary or Recurrent Prostate Cancer. J Nucl Med. 2022.

104) Grünig H, A Maurer, Y Thali, et al. Focal unspecific bone uptake on [(18)F]-PSMA-1007 PET: a multicenter retrospective evaluation of the distribution, frequency, and quantitative parameters of a potential pitfall in prostate cancer imaging. Eur J Nucl Med Mol Imaging. 2021;48(13):4483-4494.

105) Wondergem M, FM van der Zant, WAM Broos, et al. Matched-pair comparison of (18)F-DCFPyL PET/CT and (18)F-PSMA-1007 PET/CT in 240 prostate cancer patients: Interreader agreement and lesion detection rate of suspected lesions. J Nucl Med. 2021;62(10):1422-1429.

106) Hoberück S, S Löck, A Borkowetz, et al. Intraindividual comparison of [(68) Ga]-Ga-PSMA-11 and [(18)F]-F-PSMA-1007 in prostate cancer patients: a retrospective single-center analysis. EJNMMI Res. 2021;11(1):109.

107) Hammes J, M Hohberg, P Täger, et al. Uptake in non-affected bone tissue does not differ between [18F]-DCFPyL and [68Ga]-HBED-CC PSMA PET/CT. PLoS One. 2018;13(12):e0209613.

108) Byrne M, N Ranasinha, C Mercader, et al. Fluorine-18 (18F) prostate-specific membrane antigen (PSMA) positron emission tomography (PET) and the diagnosis and staging of primary prostate cancer (PCa). in AUA 2022. 2022. New Orleans, LA: May 13-16, 2022.

109) Seifert R, T Telli, M Opitz, et al. Unspecific (18)F-PSMA-1007 bone uptake evaluated through PSMA-11 PET, bone scanning, and MRI triple validation in patients with biochemical recurrence of prostate cancer. J Nucl Med. 2023;64(5):738-743.

110) Vollnberg B, I Alberts, V Genitsch, et al. Assessment of malignancy and PSMA expression of uncertain bone foci in [(18)F]PSMA-1007 PET/CT for prostate cancer-a single-centre experience of PET-guided biopsies. Eur J Nucl Med Mol Imaging. 2022;49(11):3910-3916.

111) Kroenke M, L Mirzoyan, T Horn, et al. Matched-pair comparison of (68)Ga-PSMA-11 and (18)F-rhPSMA-7 PET/CT in patients with primary and biochemical recurrence of prostate cancer: Frequency of non-tumor-related uptake and tumor positivity. J Nucl Med. 2021;62(8):1082-1088.

112) Fendler WP, M Eiber, M Beheshti, et al. PSMA PET/CT: joint EANM procedure guideline/SNMMI procedure standard for prostate cancer imaging 2.0. Eur J Nucl Med Mol Imaging. 2023.

113) Hagens MJ, DE Oprea-Lager, AN Vis, et al. Reproducibility of PSMA PET/CT Imaging for Primary Staging of Treatment-Naïve Prostate Cancer Patients Depends on the Applied Radiotracer: A Retrospective Study. J Nucl Med. 2022;63(10):1531-1536.

114) National Comprehensive Cancer Network. NCCN Clinical Practice Guidelines in Oncology. Prostate Cancer. Version 1.2023.Available from: https://www.nccn.org/professionals/physician_gls/pdf/prostate.pdf 2022.[cited 2023 09/16/2022]

115) Jadvar H, J Calais, S Fanti, et al. Appropriate use criteria for prostate-specific membrane antigen PET imaging. J Nucl Med. 2022;63(1):59-68.

116) Ceci F, DE Oprea-Lager, L Emmett, et al. E-PSMA: the EANM standardized reporting guidelines v1.0 for PSMA-PET. Eur J Nucl Med Mol Imaging. 2021;48(5):1626-1638.

117) Emmett L, J Buteau, N Papa, et al. The additive diagnostic value of prostate-specific membrane antigen positron emission tomography computed tomography to multiparametric magnetic resonance imaging triage in the diagnosis of prostate cancer (PRIMARY): A prospective multicentre study. Eur Urol. 2021;80(6):682-689.

118) Artigas C, P Flamen, F Charlier, et al. (68) Ga-PSMA PET/CT-based metastasis-directed radiotherapy for oligometastatic prostate cancer recurrence after radical prostatectomy. World J Urol. 2019;37(8):1535-1542.

119) Grubmüller B, S Rasul, P Baltzer, et al. Response assessment using [(68) Ga]Ga-PSMA ligand PET in patients undergoing systemic therapy for metastatic castration-resistant prostate cancer. Prostate. 2020;80(1):74-82.

120) 1Sartor O, J de Bono, KN Chi, et al. Lutetium-177-PSMA-617 for metastatic castration-resistant prostate cancer. N Engl J Med. 2021.

121) Pfister D, F Haidl, T Nestler, et al. (68) Ga-PSMA-PET/CT helps to select patients for salvage radical prostatectomy with local recurrence after primary radiotherapy for prostate cancer. BJU Int. 2020;126(6):679-683.

122) Abghari-Gerst M, WR Armstrong, K Nguyen, et al. A Comprehensive Assessment of (68) Ga-PSMA-11 PET in Biochemically Recurrent Prostate Cancer: Results from a Prospective Multicenter Study on 2,005 Patients. J Nucl Med. 2022;63(4):567-572.

123) Fendler WP, M Eiber, M Beheshti, et al. (68)Ga-PSMA PET/CT: Joint EANM and SNMMI procedure guideline for prostate cancer imaging: version 1.0. Eur J Nucl Med Mol Imaging. 2017;44(6):1014-1024

Revolutionizing Brain MRI Acquisition

Akshay Pai, PhD; Silvia Ingala, MD, PhD

Magnetic resonance imaging has seen significant strides in automation, with innovative solutions such as autoadaptive protocoling leading the way. These technologies are reshaping brain MRI protocols, offering unparalleled precision and expediting the diagnostic process.

The Evolution of MRI Protocols

Traditionally, MRI protocoling has been largely a manual operation, requiring radiologists to meticulously configure imaging for each patient based on clinical indications. This process, while effective, can be time consuming and prone to human error.[1,2] In response to these challenges, the industry has made a paradigm shift towards automation, aiming to streamline workflows, improve consistency, and ultimately deliver better patient outcomes.[3]

Affiliations: Dr Pai is co-founder of and chief technology officer at Cerebriu A/S, Kobenhvn, Denmark. Dr Ingala is a postdoctoral researcher at Copenhagen University Hospital Rigshospitalet, Department of Radiology in Kobenhavn, Denmark, and a medical consultant to Cerbriu A/S.

Advances in Protocol Optimization

Emerging artificial intelligence (AI)-based solutions have the potential to play a significant role in automating of brain MRI protocols. These technologies utilize AI and machine learning algorithms to sift through extensive datasets and derive imaging protocols customized to the individual characteristics of each patient. By analyzing a few initial sequences such as FLAIR, DWI, and others (eg, T2*, GRE, SWI), these systems can recommend the most suitable scanning sequences based on preliminary detection of conditions like tumors (for contrast) or infarctions (for vascular imaging).

This approach not only refines the personalization of patient care but also converts protocol configuration from a manual and time-consuming task to one that can be completed in approximately one minute.

Coupled with preliminary automation of protocoling based on patient history, such tools can enable radiologists to redirect their focus to higher-order tasks such as interpreting imaging results. This enhances overall efficiency and minimizes the likelihood of human error associated with manual protocol selection.[4]

The automated protocol, moreover, contributes to the standardization of imaging practices across healthcare institutions. Consistent, reproducible protocols are crucial for longitudinal studies, research collaboration, and ensuring that medical professionals can compare results with confidence.

Smart Alerts: Real-time Quality and Triage

Automation can also introduce another feature: real-time alerts for quality assurance. This disease triage mechanism monitors the ongoing MRI scan, continuously analyzing image data for potential artifacts and critical findings. The automatic alert system can then instantly notify radiologists and technologists of deviations from expected image quality or abnormal conditions in the brain.

This feedback can aid in swiftly identifying and addressing technical or patient-related hurdles, diminishing the likelihood of needing additional scans and curtailing the duration of scanning procedures. This not only boosts patient comfort and satisfaction but also maximizes the efficiency of scanner usage.[5] Consequently, it facilitates enhanced throughput and superior allocation of

Overview of Automation in MRI.

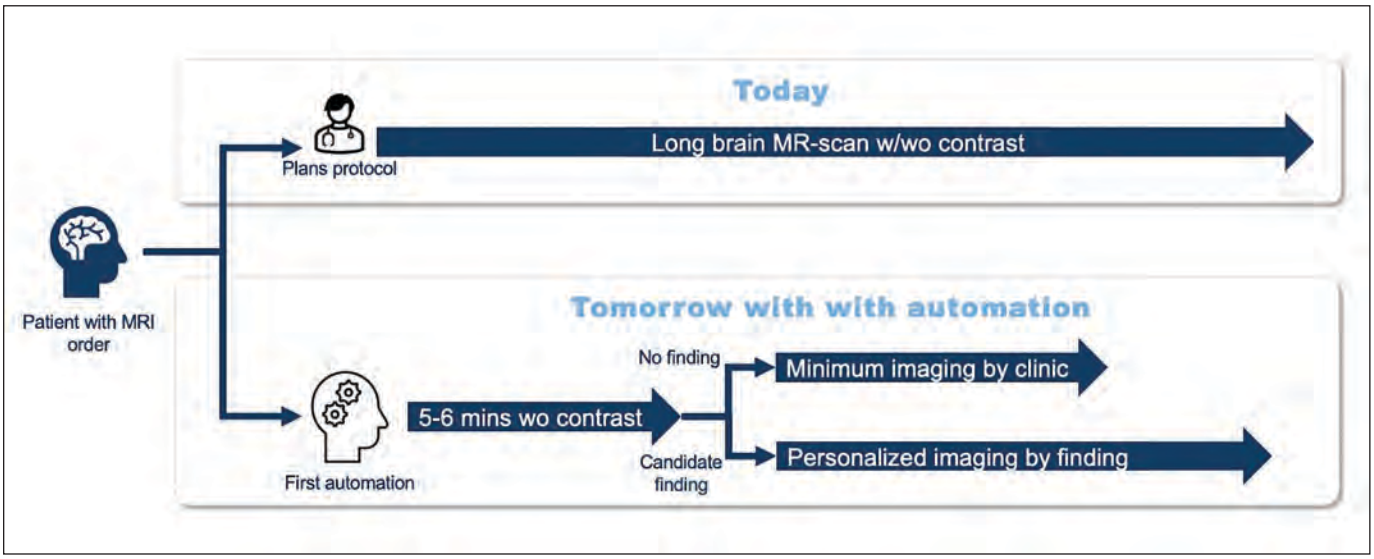

resources in busy imaging environments. One recent independent study, for example, confirmed the AI-based system's effectiveness in detecting acute ischemic lesions on brain MRI, which can be crucial to accelerating patient treatment.[6]

Clinical Impact and Future Perspectives

Automated brain MRI protocoling, along with adaptive protocoling and alerting during scanning, holds tremendous promise, especially in neuroimaging, where protocoling can be quite intensive. The increased efficiency, standardization, and real-time quality assurance contribute to a more seamless and reliable diagnostic process and ultimately benefits healthcare professionals and their patients.

As they continue to evolve, the potential exists to integrate these solutions with electronic health records and other clinical information systems. This integration could foster a more comprehensive patient-centric approach, where imaging protocols are not only optimized based on preliminary imaging data but also informed by a patient's more complete medical history and clinical, laboratory, pathology and other data, rather than simply relying on the information accompanying the imaging request. This holistic approach could lead to even more personalized and precise imaging protocols, potentially further enhancing diagnostic accuracy.

By harnessing the power of AI and machine learning, protocoling technologies hold promise for streamlining workflows, enhancing efficiency, and improving the overall quality of neuroimaging. As healthcare embraces digital transformation, innovations like these will be pivotal to ensuring the best possible care of patients. The future holds exciting possibilities, promising a new era of precision and reliability in brain MRI protocols.

References

1) Schemmel A, Lee M, Hanley T, et al. Radiology workflow disruptors: a detailed analysis. *J Am Coll Radiol.* 2016;13:1210-1214.

2) Ginat D T, Uppuluri P, Christoforidis G, Katzman G, Lee S-K. Identification of neuroradiology MRI protocol errors via a quality-driven categorization approach. *J Am Coll Radiol.* 2016; 13: 545-548.

3) Dodoo MS, Duszak R,. Hughes D R. Trends in the utilization of medical imaging from 2003 to 2011: clinical encounters offer a complementary patient-centered focus. *J Am Coll Radiol.* 2013;10: 507-512.

4) Denck J, Haas O, Guehring J, Maier A, Rothgang E. Automated protocoling for MRI exams-challenges and solutions. *J Digit Imaging.* 2022; 35(5):1293-1302.

5) Rao K, Perry S, Hagedorn J, Carter K, Balkenende B, Policeni B. Impact of a reading room coordinator on efficiency of on-call radiology residents. *J Am Coll Radiol.* 2023 Sep 29:S1546-1440 (23)00729-9.

6) Krag CH, Müller FC, Gandrup KL, et al. Diagnostic test accuracy study of a commercially available deep learning algorithm for ischemic lesion detection on brain MRIs in suspected stroke patients from a non-comprehensive stroke center. *Eur J Radiol.* 2023; 168:111126.

Cyberattacks: Not a Matter of If, but When

Kerri Reeves

Kerri Reeves is a contributing editor based in Ambler, PA.

Cyberattacks have become commonplace in healthcare. In fact, 88% of surveyed healthcare organizations experienced at least one cyberattack in the past year.[1] While 44 million Americans were affected by health information breaches in 2022, the number skyrocketed to 106 million last year, impacting one in three people.[2] In the past four years, the Office of Civil Rights (OCR) has seen a 239% increase in large breaches involving hacking and a 278% increase in ransomware attacks.[3] These occur every 11 seconds, and a data breach, on average, costs $9.23 million.[4]

For cybercriminals involved in identity theft or fraud, personal health information (PHI) is big business. Stolen health records sell up to ten times or more than credit card numbers.[5] Recent targets include Shields Health Care Group, a Massachusetts-based medical imaging service provider that had 2.3 million patient records exposed by a cybercriminal,[6] and California-based Regal Medical Group, a victim of a ransomware attack that compromised the PHI of 3.3 million patients.[7]

"It's a big problem," says Christoph Wald, MD, PhD, MBA, professor and chair of the Department of Radiology at UMass Chan-Lahey in Burlington, Massachusetts. Dr Wald warns that owing to the widespread nature of vulnerabilities, "Sooner or later, you will find yourself in the situation [of an attack]."

Comprehensive cybersecurity—protection of equipment, networks, and systems from digital attacks—is necessary in today's healthcare climate to maintain quality services and safety of patient data. It is particularly important in radiology, where legacy imaging systems remain prevalent. A department's oldest imaging assets may be based on obsolete operating systems and often cannot be equipped with modern cybersecurity protection software.

"From a radiologist's perspective, you're always managing [up to] 20 years of legacy technology in your department," says Dr Wald, adding that without regular security patches, vulnerabilities will persist, putting entire organizations at risk.

Potentially Severe Consequences of Cyberattacks

For radiology, which is operationally dependent on resources connected through local and wide-area networks, an attack's impact can be extensive. Image output, creation, transport, review, interpretation, dictation, and report distribution are digital and rely largely on integration with health information systems, radiology information systems (RIS), electronic health records (EHR), and picture archiving and communication systems (PACS).

"Radiology is the first digital specialty. We are completely and 100% dependent on these systems and networks," Dr Wald says. "When we get attacked, the whole chain of imaging care may break down immediately—with potentially immediate effects on patient care depending on the clinical setting."

Numerous financial, logistical, and patient care consequences may result when operations are compromised. The University of Vermont Health Network (UVMHN) in Burlington, Vermont, was targeted by a major cyberattack in 2020. Kristen DeStigter, MD, chair of the Department of Radiology and chief of Health Care Service at the system, says that impact was significant.

"This was complete devastation," says Dr DeStigter, who revealed that their entire infrastructure,

Christoph Wald, MD, PhD, MBA

Radiology is the first digital specialty. We are completely and 100% dependent on these systems and networks.

including more than 5,000 end-user devices across 1,300 servers, were affected by malware.

She said the attack occurred after an employee opened a seemingly ordinary email attachment on their laptop at a coffee shop. Ten days later, when connecting to the health system's network, a Trojan virus hidden within that attachment infiltrated the network, allowing malicious actors to deploy additional malware to probe other parts of the network. Soon, ransomware reached a virtual server and began encrypting all virtual hard disks, resulting in a widespread system outage. While the network's EHR was not impacted, it was shut down proactively.

While medical imaging technology and associated integrated networks have vastly improved care for patients, the seamless connectivity can make entire health systems vulnerable to security breaches and subsequent complications. Patients may need to be rerouted to neighboring institutions, experiencing compromises or delays in imaging care. Further, in-hospital mortality goes up 20 to 35% for patients admitted during a ransomware attack.[8]

UVMHN experienced 39 days of downtime in outpatient imaging, resulting in "serious financial consequences," says Dr DeStigter, citing losses of more than $63 million. Fortunately, there were no untoward patient outcomes.

Other cyber targets have become defendants in class action lawsuits resulting from the exposure of PHI,[9] which can also result in penalties running into the millions of dollars levied under the Health Insurance Portability and Accountability Act (HIPAA). Banner Health, for example, was penalized $1.25 million for HIPAA violations discovered after a massive data breach.[10]

In November, North Carolina-based US Radiology, which has operations in New York State, agreed to pay a $450,000 fine following a ransomware attack that exposed PHI of nearly 200,000 patients after the company failed to remediate a vulnerability.[11] New York Attorney General Letitia James said that patients "deserve confidence," stating "In the face of increasing cyberattacks and more sophisticated scams to steal private data, I urge all companies to make necessary upgrades and security fixes to their computer hardware and systems."[11]

Preparedness and Protection

In establishing a cybersecurity strategy, radiology leaders must prioritize protective measures to limit vulnerabilities across their organizations and preparedness for attacks. Indeed, they must be ready to switch to analog mode at a moment's notice.

"My biggest piece of advice is to be prepared. Treat your preparation like a mass casualty drill," Dr DeStigter says. "The downtime workflow should be well established and practiced multiple times."

She says UVMHN kept eight workstations operational with 24/7 radiology coverage. They had no computers, PACS, RIS, connected workstations, dictation, email, pagers, or Internet except for patient Wi-Fi systems.

"Our entire system went into a 'downtime procedure' we had never practiced," says Dr DeStigter, adding that the department had to quickly buy paper, printers, pens, and other supplies.

Most radiology departments simply are not prepared for suspension of digital operations, Dr Wald says.

"When it happens, it's going to be a mess, so it's important to have some building blocks of functioning," he observes, referring to ensuring the availability of and accessibility to paper forms,

filing systems, processes, and modality-specific working groups.

Steps to Ensure Secure Systems

From a hardware and software standpoint, the American College of Radiology (ACR) recommends that the information technology departments of healthcare facilities, including radiology, be sure to:[4]

- regularly update and patch operating systems on imaging and other equipment;
- encrypt data on physical media and data in transit;
- manage security software, including authentication and passwords;
- tightly control data access on a need-to-know basis;
- establish secure configurations of networks;
- perform regular equipment audits to ensure procedures are followed;
- perform penetration testing and regular vulnerability assessments; and
- consider end-point protection in the form of individual firewalls to protect especially critical equipment.

"Everyone has a piece of the responsibility to defend our devices," Dr Wald says, adding that radiology leaders should stress cybersecurity awareness as the foundation of department-wide policies and behaviors.

While securing technology to reduce vulnerabilities is important, humans—who are constantly creating, interacting with, and sharing data—are the vital link in cybersecurity.

"If you had to pick one thing to do [for cybersecurity], the human side is the most effective bang for the buck," he says, citing a statistic that 90% of cyber incidents are related to human behavior, including clicking on phishing emails, using weak passwords, or failing to update software.

Dr Wald says educating employees about not clicking on unfamiliar links or opening attachments in suspicious emails, only using organization-approved USB drives; not downloading information from untrusted websites; and safeguarding laptops from unauthorized access is vitally important. All employees should be aware of cyberthreats, common entry points, and potential consequences. They should also have a safe and simple way to speak up and report anything out of the ordinary.

Unfortunately, none of these measures is fool proof.

"Protection will not result in the absence of an event however small or big, so being prepared at least to the point that you have some concept of what you're going to do if you go down [is important]," says Dr Wald, advising that one person in the department should be tasked with ensuring cybersecurity and preparedness as part of daily operations.

Know the Drill

Mapping out an imaging enterprise's information ecosystem so radiology managers understand which functions are performed in-house and which ones are managed by external IT vendors is also beneficial. By establishing how various systems are

connected, radiology leaders can determine how to stay operational when "the lights go out," as well as who to contact about specific concerns, Dr Wald says, which enables continuity of patient care and instills department-wide confidence.

Conducting simulated cyberattack drills is also a good idea; they help employees learn how to recognize potentially threatening emails and respond to suspicious events, as well as to identify areas for improvement. Connecting radiology with other departments enables the entire facility to share information and resolve complications.

Radiology department leaders should also work with their equipment vendors to maintain security of legacy systems. If a vendor-run program isn't available, IT and cybersecurity companies are available to help implement measures such as isolating a resource from the rest of the network with firewalls, Dr Wald explains.

The Cybersecurity and Infrastructure Security Agency, the Department of Health and Human Services, and the Health Sector Coordinating Council Cybersecurity Working Group all offer providers tools, resources, training, and information.[12] In addition, the ACR's IT Commission Cybersecurity Work Group hosts a cybersecurity resource page with helpful how-tos, primers, videos, links to government resources and chat forums, as well as recommendations for recovery strategies.[4]

At UVMHN, site of the most significant healthcare cyberattack of 2020, Dr DeStigter recalls the impact on the organization's finances, employee morale, and patient care.

"It took seven months for us to come back fully in radiology," she says, noting that some 300 employees were furloughed or reassigned because of the attack. She also recalls the disappointment of oncology patients whose prior studies were rendered unavailable to help assess whether their treatments were working.

"We thought we were secure. No hospital is secure," says Dr DeStigter, who urges collaboration and investment in cybersecurity measures to safeguard patient data and maintain the uninterrupted provision of medical imaging services.

"Hospital administrators and their IT department should ensure radiology is prioritized and well-protected," she concludes.

References and Resources

1) Olsen E. 88% of healthcare organizations experienced a cyberattack in past year, report finds. Healthcare Dive. Published Oct. 11, 2023. Accessed Jan 30, 2024. https://www.healthcaredive.com/news/88-percent-healthcare-organizations-report-cyberattack-ponemon-institute/696358/.

2) Southwick R. Healthcare cyberattacks have affected more than 100 million people in 2023. Chief Healthcare Executive. Published Dec 18, 2023. Accessed Jan 30, 2024. https://www.chiefhealthcareexecutive.com/view/health-data-cyberattacks-have-affected-more-than-100-million-people-in-2023.

3) HHS' Office for Civil Rights Settles Ransomware Cyber-Attack Investigation. U.S. Department of Health and Human Services. Released October 31, 2023. Accessed Jan 30, 2024. https://www.hhs.gov/about/news/2023/10/31/hhs-office-civil-rights-settles-ransomware-cyber-attack-investigation.html.

4) Welcome to the Cybersecurity Resource Hub. American College of Radiology. Accessed via Jan 30, 2024. https://www.acr.org/Practice-Management-Quality-Informatics/Informatics/Cybersecurity-Resources

5) Riggi J. A high-level guide for hospital and health system senior leaders. AHA Center for Health Innovation. Accessed via Jan 30, 2024. https://www.aha.org/center/cybersecurity-and-risk-advisory-services/importance-cybersecurity-protecting-patient-safety.

6) Petkauskas V. US medical provider hack impacts 2.3m+ victims. Cybernews. Published Nov 15, 2023. Accessed Jan 30, 2024. https://cybernews.com/news/shields-health-care-group-data-breach/

7) Diaz N. 11 lawsuits filed against California medical group over ransomware attack that affected 3 million patients. Beckers Hospital Review. Published March 15, 2023. Accessed via Jan 30, 2024. https://www.beckershospitalreview.com/cybersecurity/11-lawsuits-filed-against-california-medical-group-over-ransomware-attack-that-affected-3-million-patients.html.

8) Levi R. Ransomware attacks against hospitals put patients' lives at risk, researchers say. National Public Radio Oct 20, 2023. Accessed Jan 30, 2024. https://www.npr.org/2023/10/20/1207367397/ransomware-attacks-against-hospitals-put-patients-lives-at-risk-researchers-say#:~:text=HANNAH%20NEPRASH%3A%20During%20a%20ransomware,at%20the%20University%20of%20Minnesota.

9) The Top 15 Healthcare Industry Cyber Attacks of the Past Decade. Arctic Wolf. Published Aug 22, 2023. Accessed Jan 30, 2024. https://arcticwolf.com/resources/blog/top-healthcare-industry-cyberattacks/

10) Davis J. Banner Health pays $1.25M penalty over HIPAA failures from 2016 breach. SC Media. Published Feb 2, 2023. Accessed Jan 30, 2024. https://www.scmagazine.com/analysis/banner-health-pays-1-25m-penalty-over-hipaa-failures-from-2016-breach.

11) Greig J. NY AG issues $450k penalty to US Radiology after unpatched bug led to ransomware attack. The Record. Published Nov 8, 2023. Accessed Jan 30, 2024. https://therecord.media/new-york-attorney-general-fines-radiology-firm-after-ransomware-attack.

12) Healthcare and Public Health Cybersecurity. Cybersecurity and Infrastructure Security Agency. Accessed Jan 30, 2024. https://www.cisa.gov/topics/cybersecurity-best-practices/healthcare#:~:text=Together%2C%20CISA%20brings%20technical%20expertise,issues%20in%20HPH%20every%20day.

Limy Bile Syndrome

Gary G. Ghahremani, MD

Case Summary

An adult with cirrhosis due to hepatitis C infection was referred for abdominal imaging.

Computed tomography (CT) revealed a large, radiopaque gallbladder containing numerous calculi. A nodular liver and ascites were also present. Magnetic resonance imaging (MRI) showed cholelithiasis and an enhancing lesion of the right hepatic lobe consistent with hepatocellular carcinoma.

Imaging Findings

Precontrast CT showed a distended gallbladder measuring 10.2 cm in length and 4 cm in diameter, filled with markedly radiopaque content (184 HU). The gallbladder contained many small calculi and its neck was blocked by a 1.2 cm impacted stone. A cirrhotic liver and massive ascites were also visible (Figure 1). Ultrasonography of the gallbladder redemonstrated the cholelithiasis, but there was no pain or tenderness on palpation (Murphy sign) to indicate cholecystitis (Figure 2). MRI obtained 4 months later showed the abnormal gallbladder and ascites, as well as a 1.6 cm enhancing lesion in segment 8 of the right hepatic lobe that represented a hepatocellular carcinoma (Figure 3). This tumor was treated twice with transarterial embolization (TACE) prior to liver transplantation.

Affiliation: Department of Radiology, University of California-San Diego Medical Center, San Diego, California.

Diagnosis

Limy bile syndrome.

The differential diagnosis includes gallbladder opacification by contrast material following oral cholecystography or endoscopic retrograde cholangiography, vicarious excretion due to renal or hepatic failure, and porcelain gallbladder.

Discussion

Limy bile syndrome (LBS), also known as milk-of-calcium gallbladder, is a rare idiopathic condition usually recognized by its distinct radiological features.[1-3] The condition is characterized by dense opacification of the gallbladder, and seldom the bile ducts, with a creamy solution of calcium salts in the form of carbonate, oxalate, phosphate, or bilirubinate. The underlying pathogenesis is believed to be abnormal metabolism of calcium and low pH of excreted bile.[4] In most of the reported cases the gallbladder had been obstructed by an impacted stone in its neck or cystic duct. Limy bile syndrome can be associated with hyperparathyroidism, chronic cholecystitis, gallstone-induced pancreatitis and, in very rare instances, gallbladder cancer or cholangiocarcinoma.[5,6]

This entity is usually diagnosed in patients older than 40 years, with a 3:1 female-to-male ratio.[4] Only a few cases have been reported in pediatric patients.[7] Most patients with LBS are asymptomatic; the condition is detected incidentally on imaging studies performed for unrelated abdominal disorders.[1,8] However, some patients present with right subcostal pain, fever, and jaundice resulting from concurrent cholecystitis or biliary obstruction by gallstones.[1,6]

The typical finding on abdominal radiography and CT is that of a densely radiopaque gallbladder filled with a highly viscous substance, intraluminal calculi, and often obstructed by an impacted gallstone in its neck or cystic duct. Sonography and MRI can demonstrate cholelithiasis and associated ascites

Figure 1. Noncontrast CT of the abdomen. (A) Axial image of the upper abdomen reveals a distended gallbladder with highly radiopaque content and numerous calculi. Ascites and splenomegaly due to liver cirrhosis are visible. (B) This section demonstrates the 1.2 cm obstructing stone (arrow) in the neck of the gallbladder.

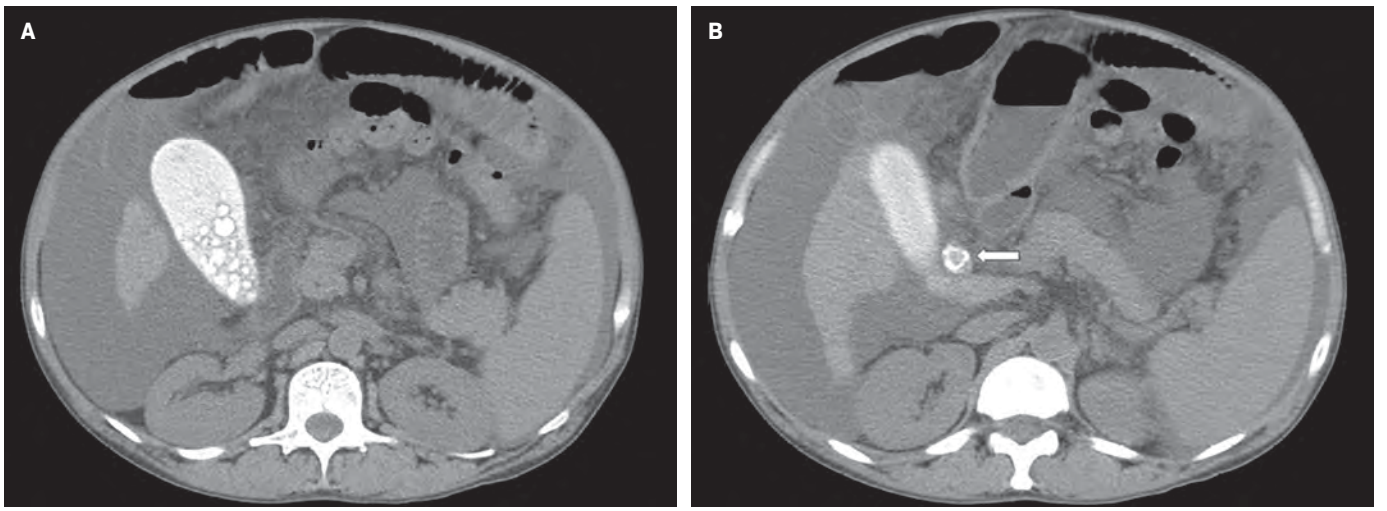

Figure 2. A sonogram of the gallbladder in sagittal section demonstrates its normal wall thickness and many retained calculi within its lumen.

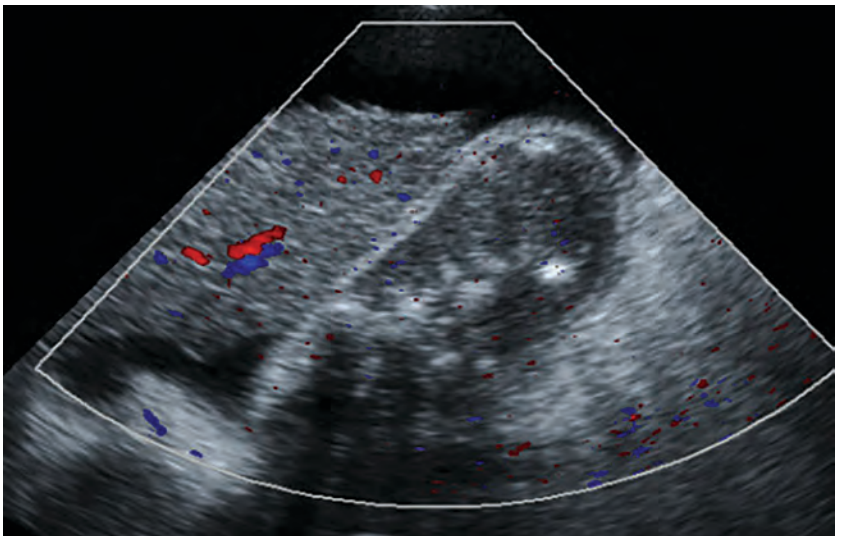

Figure 3. Axial (A) T1 and (B) T2 MRI of the upper abdomen show the enlarged gallbladder with its very viscous content and cholelithiasis (arrows). Note the large amounts of intraperitoneal fluid and cirrhotic liver.

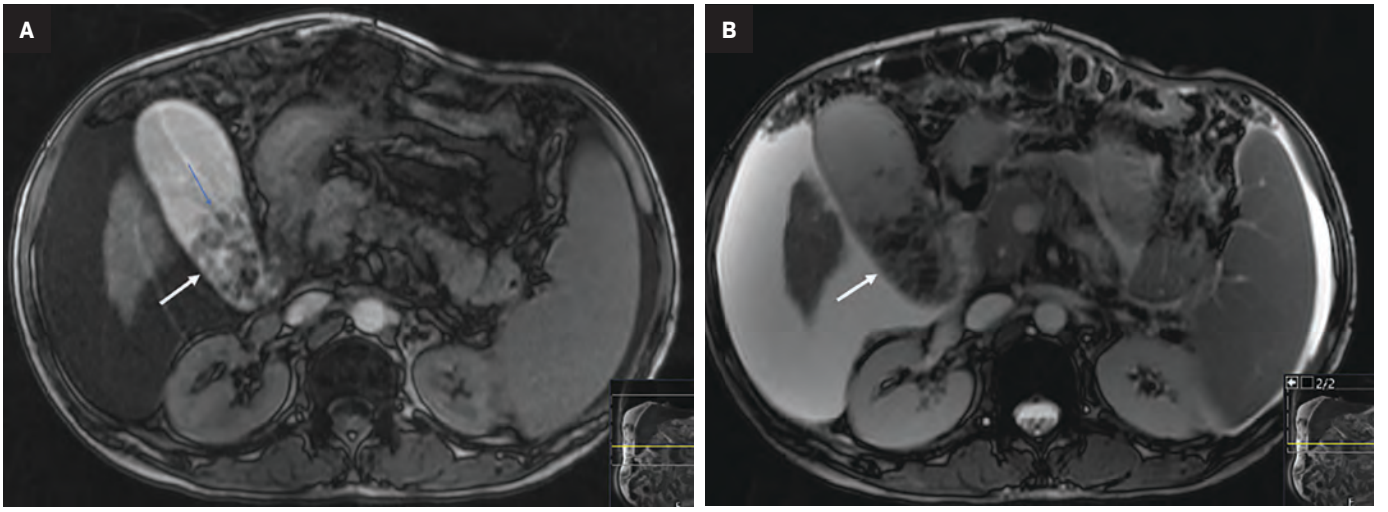

or pathological processes of the liver as in this case.[1-4]

The recommended treatment is cholecystectomy.[1,6] This operation is usually performed electively, to prevent future complications. Spontaneous resolution through discharge of abnormal gallbladder content into the duodenum has been reported in a few isolated instances.[8-10]

Conclusion

Abdominal radiography and cross-sectional imaging modalities play a crucial role in the diagnosis of limy bile syndrome and evaluation of its associated pathological processes. This case report highlights the unique clinical and imaging features that help in the recognition and management of this rare entity.

References

1) Ballas KD, Alatsakis MB, Rafailidis SF, et al. Limy bile syndrome: review of seven cases. *ANZ J Surg* 2005; 75(9): 787-789. doi: 10.1111

2) Mazzie JP, Gold BM, Bartolomeo R, Katz DS. Milk of calcium in the common bile duct: CT identification. *AJR* 2002; 179(3); 804-805. doi: 10.2214.

3) Indiran V. Milk of calcium bile. *Abdom Radiol* 2016; 41: 1869-1870. doi: 10.1007

4) Rahate NP, Muacevic A, Adler JR. Limy bile syndrome: a report of a rare case. *Cereus.* 2022; 14(7): e27473. doi: 10.7759

5) Takatori Y, Yamauchi K, Negoro Y, et al. Limy bile syndrome complicated with primary hyperparathyroidism. *Intern Med.* 2003; 42(1): 44-47. doi: 10.2169

6) Almuhsin AM, Altaweel A, Abouleid A. Endoscopic management of limy bile syndrome presenting with obstructive jaundice. *BMJ Case Rep* 2019; 12(9): e231798. doi: 10.1136

7) Higashidate N, Fukahori S, Saikusa N, et al. Asymptomatic limy bile gallstone in a 6-year-old boy. *J Pediatr Surg Case Rep.* 2022; 85: e102429.

8) Arif SH, Mohammed AA. Limy bile (milk of calcium bile) associated with gallstones discovered incidentally during laparoscopic cholecystectomy. *Int J Surg Case Rep.* 2019; 61:127-129. doi:10.1016

9) Levy I, Lantsberg I, Khoda J. Spontaneous disappearance of limy bile: a cause of acute pancreatitis? *J Clin Gastroenterol.*1994; 18(3): 220-221. doi: 10.1097

10) Itoh H. Management of limy bile syndrome: no therapy, laparotomy or endoscopic treatment? *Intern Med* 2003; 42(1);1-2.

Arrested Pneumatization of the Left Central Skull Base

Vijay Radhakrishnan; Dhiraj Rajkumar, MD; Sanjay Radhakrishnan

Case Summary

An adult with a history of headache and obstructive sleep apnea presented to their primary care provider with nasal congestion. The patient had no other relevant medical history of chronic illness. The patient also had no history of smoking and was not on blood thinners.

Imaging Findings

Maxillofacial CT scan (Figure 1) revealed a nonexpansile lesion involving the left central skull base. Further examination revealed internal curvilinear calcifications with well-defined sclerotic margins.

Diagnosis

Arrested pneumatization of the left central skull base

Discussion

Arrested pneumatization (AP) is a commonly misdiagnosed condition that occurs in the early stages of fetal development and continues through childhood and puberty.[1] Sinus development diverges from the typical developmental pattern.[2] Arrested pneumatization results from the failure of pneumatization before respiratory mucosa can extend into locations of early fatty marrow conversion.[2] This uncommon developmental variant typically occurs near the sphenoid sinus in the central skull base. The etiology for this maldevelopment is currently unknown, and diagnosis is usually incidental on imaging for another condition. Some potential factors that may contribute to this entity include bone composition and vascularization, although further research is necessary.[1]

Preoperative diagnosis with CT and MRI is key to avoiding unnecessary surgery and/or other treatment of AP, which is widely considered a normal variant in fetal development that requires no additional treatment. A specific set of four criteria must be met for confident diagnosis: 1) the lesion must be located at a site of normal pneumatization or accessory sphenoid sinus pneumatization; 2) the lesion should have thin, well-defined sclerotic margins; 3) the lesion must be nonexpansile; and 4) internal curvilinear calcifications must be present.[2-4]

Detailed inspection of images, coupled with awareness of the entity, can aid in making the diagnosis.[1] Mistaking this entity can contribute to unnecessary surgeries and/or follow-up examinations. Possible differential considerations include but are not limited to ossifying fibroma, bone metastases, and chondrosarcoma.[2]

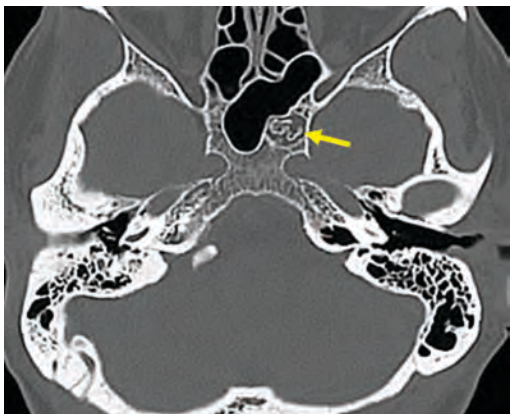

Figure 1. Maxillofacial CT scan reveals a nonexpansile lesion approximately 1 cm in diameter involving the left half of the basisphenoid/ventral clivus. The lesion has internal curvilinear calcifications with well-defined sclerotic margins. All criteria for the diagnosis of arrested pneumatization are met.

Conclusion

Arrested pneumatization is a developmental variant with a poorly understood etiology. Radiologists should be familiar with the key features of AP on CT and MRI in order to make an accurate diagnosis.

References

1) Park S-H, Hwang J-H. Arrested pneumatization of the sphenoid sinus in the skull base. *Brain Tumor Research and Treatment*. 2021; 9 (1):40-43. doi:10.14791/btrt.2021.9.e2

2) Welker KM, DeLone DR, Lane JI, Gilbertson JR. Arrested pneumatization of the skull base: Imaging characteristics. *Am J Roentgenol.* 2008;190 (6):1691-1696. doi:10.2214/ajr.07.3131

3) Duignan M, Wood A. Arrested pneumatization of the skull base: An under-recognized skull base anomaly. *ANZ J Surg.*. 2020; 91(1-2). doi:10.1111/ans.16118

4) Jalali E, Tadinada A. Arrested pneumatization of the sphenoid sinus mimicking intraosseous lesions of the skull base. *Imaging Sci Dentistry*. 2015; 45 (1):67-72. doi:10.5624/isd.2015.45.1.67

Affiliations: University of Texas Rio Grande Valley (Mr Vijay and Sanjay Radhakrishnan); Michael E. Debakey VA Medical Center, Department of Radiology (Dr Rajkumar)

Aortoenteric Fistula Following Aortobifemoral Grafting

Param Patel, BS; George Weck, MD; Steven Lee, MD; Bret Coughlin, MD; Prasanta Karak, MD

Case Summary

An adult with diabetes presented to the emergency department with a 3-week history of right-sided abdominal and right lower extremity pain. The patient was 2 years status postaortobifemoral (type) bypass graft.

Imaging Findings

Initial noncontrast CT (Figure 1) demonstrated an aortoiliac bypass graft abutting the second portion of the duodenum without an intervening fat plane. There were several locules of gas in the proximal right iliac limb of the bypass graft concerning for abnormal fistulous communication between the duodenum and the graft. Contrast-enhanced CT corroborated this finding and further demonstrated complete occlusive thrombus of the right iliac limb of the bypass graft. Subsequent positron emission tomography (PET)/CT (Figure 2) demonstrated fluorodeoxyglucose avidity of the entire aortoiliac bypass graft, raising strong suspicion for an infected bypass graft. Following CT angiography, an upper endoscopy confirmed the suspected diagnosis of aortoenteric fistula (AEF, Figure 3.).

Diagnosis

Aortoenteric fistula

Affiliations: University of Connecticut School of Medicine (Mr.Patel); Department of Radiology, Hartford Hospital (Drs Weck, Lee, Coughlin, Karak).

Discussion

Primary AEFs can be caused by abdominal aortic aneurysms, which have mass effect upon gastrointestinal (GI) structures and can erode into the bowel in the presence of inflammation. Primary AEFs have an incidence of 0.04-0.07%, and are typically associated with septic aortitis, cancer, and autoimmune diseases.[1] Secondary AEFs usually result from aortic prosthetic graft erosion after open repair and affect the third portion of the duodenum because of this portion's retroperitoneal fixation and proximity to the aorta. The overall incidence of secondary AEFs is 0.36-1.6%, and they are rarely observed after endovascular aneurysm repair.[2]

Aortoenteric fistulae typically present with minor "herald" GI bleeding followed by catastrophic life-threatening hemorrhage, making early diagnosis and treatment crucial for improved clinical outcomes.[3] In addition to recurrent septicemia from enteric pathogens and abdominal pain, some patients may present with a pulsatile abdominal mass that indicates an aneurysm.[4] Management of AEFs involves surgical intervention, including repair or excision of the affected aortic segment, as well as GI reconstruction if necessary. Although no imaging modality provides high sensitivity and specificity to diagnose AEFs, CT is the preferred for emergency evaluation, owing to its speed and availability. The accuracy of CT in diagnosing AEFs varies widely, with sensitivity ranging from 40% to 90% and specificity ranging from 33% to 100%.[5]

The development of secondary aortoenteric fistula involves various mechanisms, including bacterial contamination of a prosthetic graft leading to infection, anastomotic failure, and peri-graft infection.[3] Other factors contributing to secondary AEF pathogenesis include bowel damage, ischemia, mechanical injury, inflammation, and erosion. Pseudoaneurysms or perigraft abscesses can compress or invade the intestinal lumen, while mechanical erosion of the intestinal wall can be caused by graft-induced inflammation and infection. In this case, the placement of the graft near the small bowel may have resulted in repetitive microtrauma from pulsatile motion, leading to bacterial seeding and graft infection and ultimately resulting in aortic graft thrombosis. The breakdown of the graft wall resulted in the formation of a fistulous connection.

The cardinal manifestations of secondary AEF primarily consist of GI bleeding and severe hemorrhagic shock.[6] Frequently, patients with AEF may experience graft infection, which can manifest with fever and sepsis. Our patient had right lower extremity pain secondary to aortoiliac occlusive disease stemming from the thrombosed graft. This thrombus can be protective against active arterial extravasation into the GI tract.

This patient exhibited marked leukocytosis without fever, raising concerns of possible graft infection,

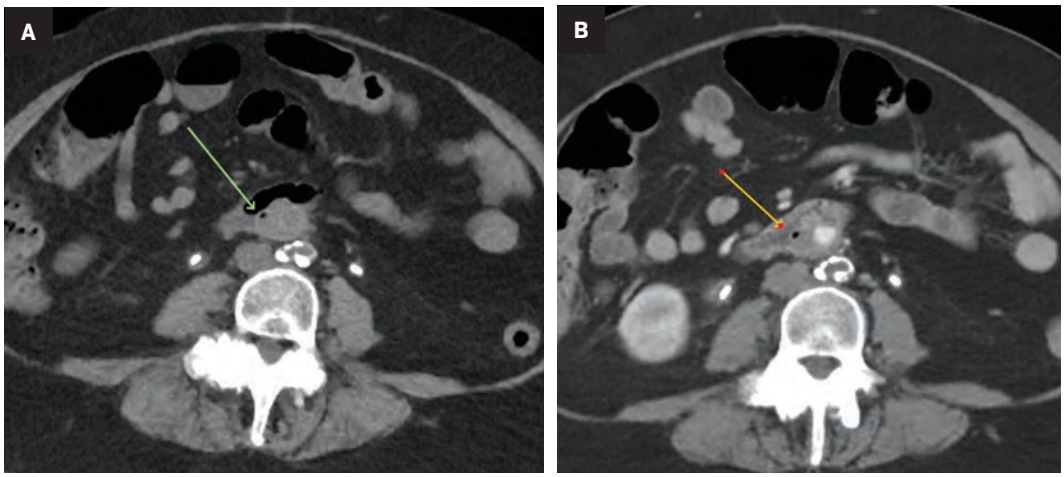

Figure 1. (A) Axial view of a noncontrast CT demonstrates loss of fat plane between the third portion of the duodenum and the aortoiliac bypass graft. The identification of a locule of gas (arrow) adjacent to the aortoiliac bypass graft, which cannot be definitively delineated as being extraluminal, raises a strong suspicion for an aortoenteric fistulous connection. (B) Axial CTA view of the abdomen demonstrates occlusive thrombus at the origin of the right limb of the aortoiliac bypass graft (arrow). There is a persistent antidependent locule of gas within the graft with no active arterial extravasation.

Figure 2 . Coronal PET/CT coronal view demonstrates patchy FDG uptake throughout the entire aortoiliac bypass graft tracking into both groins, suggestive of infection/ inflammation.

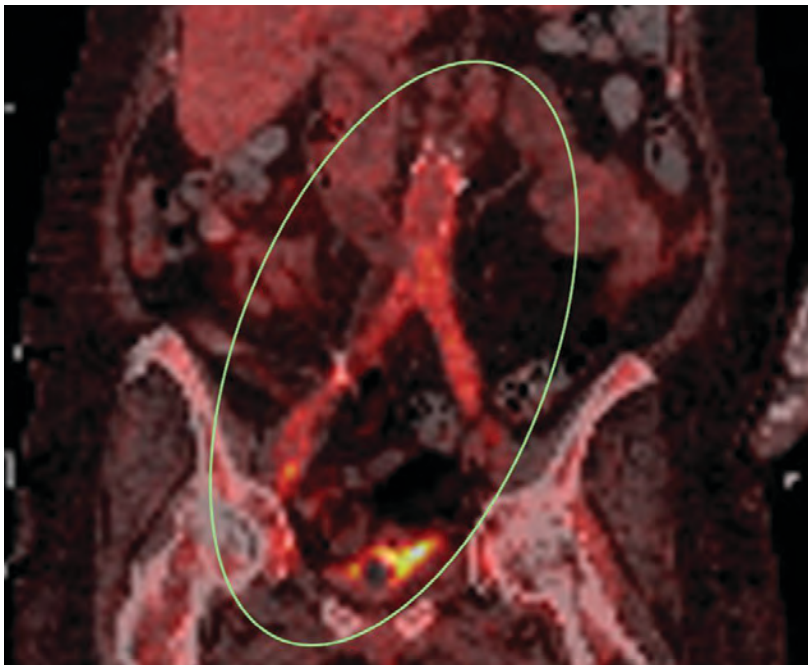

a suspicion that was confirmed by the PET scan findings. PET scanning can help determine the extent of infection in a graft, which can help guide the extent of graft explant. The surgical approaches in these cases may be open or endovascular and should be individualized for each patient.

Conclusion

Secondary AEF is a rare and life-threatening complication of abdominal aortic aneurysm repair. Diagnosis of secondary AEF can be challenging and relies on a high index of clinical suspicion in patients with prior aortic intervention. Distinctive CT findings associated with AEF include ectopic gas within the aortic wall, thickening of the local bowel near the aorta, and rupture of the aortic wall. This case highlights the importance of recognizing the potential for mechanical factors to contribute to the development of secondary aortoenteric fistula.

Figure 3. Upper gastrointestinal endoscopy reveals the vascular graft (yellow) within the lumen of the third part of the duodenum.

References

1) Voorhoeve R, Moll FL, de Letter JA, Bast TJ, Wester JP, Slee PH. Primary aortoenteric fistula: report of eight new cases and review of the literature. *Ann Vasc Surg*. 1996;10(1):40-48. doi:10.1007/BF02002340

2) Busuttil SJ, Goldstone J. Diagnosis and management of aortoenteric fistulas. *Semin Vasc Surg*. 2001;14(4):302-311. doi:10.1053/svas.2001.27888

3) Simon T, Feller E. Diverse presentation of secondary aortoenteric fistulae. *Case Rep Med*. 2011;2011:406730. doi:10.1155/2011/406730

4) Bergqvist D, Björck M. Secondary arterio-enteric fistulation--a systematic literature analysis. *Eur J Vasc Endovasc Surg*. 2009;37(1):31-42. doi:10.1016/j.ejvs.2008.09.023

5) Hughes FM, Kavanagh D, Barry M, Owens A, MacErlaine DP, Malone DE. Aortoenteric fistula: a diagnostic dilemma *Abdom Imaging*. 2007;32(3):398-402. doi:10.1007/s00261-006-9062-7

6) Bíró G, Szabó G, Fehérvári M, Münch Z, Szeberin Z, Acsády G. Late outcome following open surgical management of secondary aortoenteric fistula. *Langenbecks Arch Surg*. 2011;396(8):1221-1229. doi:10.1007/s00423-011-0807-6

"No nation is greater than another. The difference is people and the leaders."

—Benjamin Suulola

Learning in Unlikely Places

C. Douglas Phillips, MD

Dr Phillips is a Professor of Radiology, Director of Head and Neck Imaging, at Weill Cornell Medical College, NewYork-Presbyterian Hospital, New York, NY. He is a member of the *Applied Radiology* Editorial Advisory Board.

A huge benefit of academia is being able to work hard for less money. No. Did he say that? Of course not. Jeez, that was unhinged. What I MEANT to say is that a huge benefit of academia is being able to make friends and develop colleagues among a large group of national and international radiologists who share your interests and specialty.

My wife and I have been really lucky to travel and see some pretty incredible practices and hospitals and meet some amazingly bright and driven radiologists from all around the world. A recent visit that I feel obligated to talk about is our trip to Tallinn and Tartu, Estonia. (Yes, by all means, consult a map if you need to.)

We visited for two reasons—to lecture at the 2022 Baltic Congress of Radiology meeting, and to lecture to residents and trainees at the University of Tartu Hospital.

In all honesty, we approached this with a fair amount of trepidation: What would we see? What would the lecture halls be like? How advanced would this medical culture be? You know how we 'muricans can be—hard to imagine that anyone does things as well as we do. The superiority thing is almost always there, and even though we've already been to many European countries that do everything we do, only maybe a good bit better, it still lives there in my brain. So, what might Estonia show us?

These are amazing people. They are resilient. Left by the Soviet Union in 1991 (after nearly a half-century of occupation) with not much of worth, they turned every bit of hard luck and crumbling infrastructure into something magnificent. The hospitals are good—very good. Their equipment may be a little less in number, but absolutely of top quality. Good cars, great roads, well-lit streets, wonderful shops and restaurants.

We saw robots delivering take-out on the street, the wheeled beasts occasionally waiting at a corner for the light to change before charging on down the street to drop off a pizza. The meeting was at a renovated Soviet-era power plant, now chic and elegant with state-of-the-art functionality while maintaining a retro feel. It was populated with artisan shops and work areas.

Wonderful food was everywhere, and most importantly, so were wonderful people. Folks who have seen a little different history than we have and appreciate where they are and know exactly where they are going. And the training staff in radiology are caring, bright, and driven. We enjoyed our time immensely and yes, we would happily go back.

It sure made me reflect on things. Odd times here in the US. Some have decided to revisit some isolationist attitudes that maybe haven't worked so well before. Polarization levels are high. Getting out and around is a good way to kill those thoughts. We had the opportunity to meet, work with, teach, and learn from some amazing people. I'd like to stay engaged with these folks. I think I learned as much as I could ever teach.

Keep doing that good work. Broaden your horizons. Mahalo.

AppliedRadiology®

The Journal of Practical Medical Imaging and Management

UPDATE YOUR SUBSCRIPTION

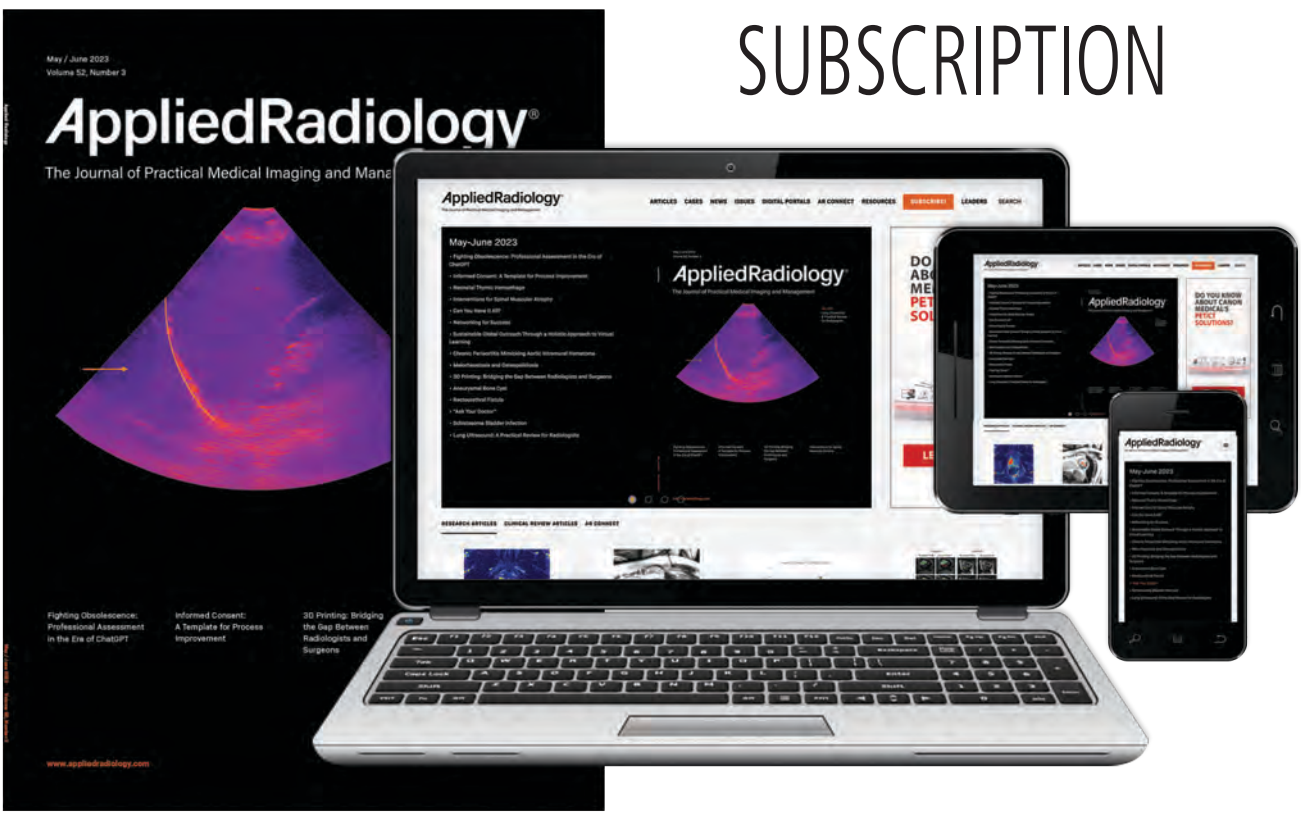

Since 1972, *Applied Radiology* has brought physician-authored clinical review articles to the radiology community.

Applied Radiology content includes clinical review articles, radiological cases, and specialty columns such as Eye on AI and the ever-popular Wet Read by C. Douglas Phillips, MD, FACR.

Now you can have it all your way (FREE) without missing a single issue.

Please take a moment to update your subscription preferences.

appliedradiology.com/#subscribe

CT Suite | MR Suite | Injectors and Digital Solutions

SmartInject
SOLUTIONS FROM BRACCO

Point-of-care imaging solutions that help promote patient safety and streamline workflow

NEXO®
Contrast management system

Advance patient care with smart injectors and digital solutions from Bracco.

Learn more at **SmartInject.com**

Bracco Diagnostics Inc.
259 Prospect Plains Road, Building H
Monroe Township, NJ 08831 USA

Phone: 609-514-2200
Toll Free: 1-877-272-2269 (U.S. only)
Fax: 609-514-2446

BRACCO
LIFE FROM INSIDE

Committed to Science,
Committed **to You.**™